JAERI-M
9819

A THROUGH CALCULATION OF 1,100 MWe PWR LARGE BREAK LOCA BY THYDE-P

(SAMPLE CALCULATION RUN 20)

November 1981

Takasi SHIMIZU and Yoshiro ASAHI

日本原子力研究所
Japan Atomic Energy Research Institute

この報告書は，日本原子力研究所がJAERI-Mレポートとして，不定期に刊行している研究報告書です．入手，複製などのお問合わせは，日本原子力研究所技術情報部（茨城県那珂郡東海村）あて，お申しこしください．

JAERI-M reports, issued irregularly, describe the results of research works carried out in JAERI. Inquiries about the availability of reports and their reproduction should be addressed to Division of Technical Information, Japan Atomic Energy Research Institute, Tokai-mura, Naka-gun, Ibaraki-ken, Japan.

JAERI-M 9819

A Through Calculation of 1,100 MWe PWR Large Break LOCA by THYDE-P

(Sample Calculation Run 20)

Takasi SHIMIZU and Yoshiro ASAHI

Division of Reactor Safety Evaluation,
Tokai Research Establishment, JAERI

(Received November 5, 1981)

THYDE-P is a code to analyze loss-of-coolant accidents (LOCA's) of the pressurized water reactor (PWR). In this report, the calculated results of THYDE-P sample calculation Run 20 is presented, which is a through BE (best estimated model) calculation of LOCA for a comercial 1,100 MWe class PWR plant.

Keywords: LOCA, PWR, THYDE-P Code, Code Verification, Through Calculation, Best Estimated Model

JAERI-M 9819

THYDE－P コードによる1,100 MWe PWR 大破断事故の一貫計算 （サンプル計算 Run 20）

日本原子力研究所東海研究所安全解析部

志水　孝司・朝日　義郎

（1981年11月5日受理）

THYDE－Pコードは，加圧水型原子炉の冷却材喪失事故を解析するコードである。本報告書には，サンプル計算20の計算結果が載せてある。サンプル計算20は1,100 MWeクラスの商用加圧水型原子力発電プラントのBE（最適予測）計算による冷却材喪失事故の一貫計算である。

Contents

1. Introduction 1

2. Code Modifications 2

2.1 Mass Equation 2
2.2 Flow Model 2
2.3 Implicit Solution of Fuel Rod Temperature 3
2.4 Improvement of CHF and Heat Transfer Correlations .. 3

3. Main Assumptions and Conditions for Run 20 4

3.1 Run 20 Plant Representation 4
3.2 CHF Correlations 7
3.3 Heat Transfer Correlations 7
3.4 Critical Flow 8
3.5 Relaxation Parameters 8
3.6 Drift Flux Model 9

4. Calculated Results 17

4.1 Overall Description 17
4.2 Fuel and Core 17
4.3 Downcomer and Lower plenum 18
4.4 Break 19
4.5 Pressurizer 19
4.6 Pumped Injection 19
4.7 Accumulator 19
4.8 Steam Generator 20
4.9 Pump 20
4.10 Diference due to Drift Velocity 20

5. Concluding Remarks 47

Acknowledgments 47

References 47

Appendix A 48

目　　次

1. 序 …… 1
2. コード修正 …… 2
2.1 質量方程式 …… 2
2.2 流動モデル …… 2
2.3 燃料棒温度の陰的解法 …… 3
2.4 CHF および熱伝達相関式の改良 …… 3
3. Run 20 の主要な仮定と条件 …… 4
3.1 Run 20 におけるプラント表現 …… 4
3.2 CHF 相関式 …… 7
3.3 熱伝達相関式 …… 7
3.4 臨界流 …… 8
3.5 緩和パラメータ …… 8
3.6 ドリフトフラックス …… 9
4. 計算結果 …… 17
4.1 全体的記述 …… 17
4.2 燃料と炉心 …… 17
4.3 ダウンカマーと下部プレナム …… 18
4.4 破断口 …… 19
4.5 加圧器 …… 19
4.6 ポンプ注入 …… 19
4.7 蓄圧器注入 …… 19
4.8 蒸気発生器 …… 20
4.9 ポンプ …… 20
4.10 ドリフト速度の違いによる …… 20
5. 結　　論 …… 47
謝　　辞 …… 47
参考文献 …… 47

付録A　Run 20 の入力データ …… 48

List of Figures

3-1 Nodalization
3-2 Steady State Pressure Distribution
3-3 Relative Velocity
4-1-1 Pressure in Core
4-2-1 Average Channel Surface Temperature
4-2-2 Average Channel Surface Temperature
4-2-3 Hot Channel Surface Temperature
4-2-4 Hot Channel Surface Temperature
4-2-5 Average Channel Center Temperature
4-2-6 Hot Channel Center Temperature
4-2-7 Heat Transfer Coefficient at Average Channel
4-2-8 Heat Transfer Coefficient at Average Channel
4-2-9 Core Inlet Flow
4-2-10 Core Inlet Flow
4-2-11 Core Outlet Flow
4-2-12 Core Outlet Flow
4-2-13 Heat Generation in Fuel
4-2-14 Gap Pressure
4-2-15 Heat Transfer Coefficient at Gap
4-2-16 Quality at Average Channel
4-2-17 Enthalpy at Core Inlet
4-2-18 Enthalpy at Core Outlet
4-2-19 Core Cross Flow
4-3-1 Flow in Downcomer
4-3-2 Flow in Lower Plenum
4-3-3 Quality in Downcomer
4-3-4 Quality in Lower Plenum
4-4-1 Break Flow
4-4-2 Enthalpy at Break Point
4-4-3 Quality at Break Point
4-4-4 Pressure at Break Point
4-5-1 Pressurizer Surge Flow
4-5-2 Pressure in Pressurizer Duct
4-5-3 Flow in Intact Loop Hot Leg
4-5-4 Water Level in Pressurizer
4-6-1 Flow in Pumped Injection Duct
4-6-2 Pressure in Pumped Injection Duct
4-6-3 Enthalpy in Pumped Injection Duct
4-7-1 Pressure in Accumulator Duct
4-7-2 Flow in Accumulator Duct
4-7-3 Enthalpy in Accumulator Duct
4-7-4 Enthalpy in ECC Injection Point
4-8-1 Steam Generator Feed Water
4-8-2 Heat Transfer Coefficient in Intact Loop S.G.
4-8-3 Heat Transfer Coefficient in Broken Loop S.G.
4-8-4 Heat Flow in Steam Generator
4-8-5 Pressure in S.G. Secondary System

4-9-1 Pump Speed
4-9-2 Pump Head
4-10-1 Average Channel Surface Temperature
4-10-2 Average Channel Surface Temperature
4-10-3 Heat Transfer Coefficient in Average Channel
4-10-4 Heat Transfer Coefficient in Average Channel

List of Table

3-1 Node Geometrical Data
3-2 Loss Coefficient
3-3 Heat Transfer Correlations
3-4 Heat Transfer Correlations in Mode-4
4-1 Chronology of Events

1. Introduction

THYDE-P[1] is a computer code to analyze the transient thermal hydraulic response of a PWR plant to a postulated LOCA loss of coolant accident).

The present status of THYDE-P may be considered to be at the stage of verification, so that what is needed at present for THYDE-P development may be to conduct a systematic study by sample calculations.

Thus far, sample calculations 10[2], 30[3] and 40[4] have been reported. In these calculations, a large break in the cold leg is assumed to occur. Run 10 is calculated for a typical 4-loop comercial PWR, while Runs 30 and 40 for LOFT.

In this report, sample calculation Run 20 by the latest version (SV02L03) for a typical 4-loop PWR plant will be presented, which is characterized by

(1) BE calculation,
(2) two core channels calculation with single cross flow area,
(3) discharge coefficient 0.6,
(4) through calculation to end of reflooding,
(5) locked rotor of centrifugal pumps,
(6) ECC water enthalpy 30kcal/kg,
(7) same heat transfer correlations in reflooding as in blowdown, and
(8) double ended guilotine break at the cold leg

The geometrical plant data are almost identical with those used in RELAP4/MOD5 sample problem[5].

2. Code Modifications

The detail of the THYDE-P code was described in Ref.(1), part of which, however, had been revised since its publication. Among those, main items were;

(1) solution technique at low pressure,
(2) flow model at low pressure,
(3) implicit solution of fuel rod temperature, and
(4) improvement of CHF and heat transfer correlations.

2.1 Mass Equation

In Run 10 calculation, the mass and energy conservation equations were used in the form of

$$\dot{h} = \frac{1}{\rho h}\left\{G_A h_A - G_E h_E - h(G_A - G_E) + I_A - I_E + Q\right\} \quad \text{--- (1)}$$

$$\left\{1 + \frac{1}{\rho}\frac{\partial \rho}{\partial h}(h-h_A)\right\}G_A - \left\{1 + \frac{1}{\rho}\frac{\partial \rho}{\partial h}(h-h_E)\right\}G_E - \frac{1}{\rho}\frac{\partial \rho}{\partial h}(I_A - I_E + Q) - L\frac{\partial \rho}{\partial h}\frac{dp}{dt} \quad \text{--- (2)}$$

where

$$I = x\rho_{fs}u_{gj}(h_{gs} - h_{fs})$$

They were obtained from

$$L\frac{\partial \rho}{\partial t} = G_A - G_E \quad \text{--- (3)}$$

and

$$L\frac{\partial \rho h}{\partial t} = G_A h_A - G_E h_E + I_A - I_E + Q \quad \text{--- (4)}$$

with the help of

$$d\rho = \frac{\partial \rho}{\partial h}dh + \frac{\partial \rho}{\partial p}dp \quad \text{--- (5)}$$

Since it was found in the course of sample calculation Run 10 that relationship(5) broke down at low pressure and low quality, it was decided to implement Eq. (3) instead of Eq. (2) in THYDE-P so that mass is strictly conserved.

2.2 Flow Model

When low enthalpy ECC water was injected into primary loop, depressurization of the system caused by a rapid condensation took place and the calculations by the homogeneous equilibrium models failed. In the refill-reflood phase of a large break LOCA analysis for a comercial PWR plant, the enthalpy of ECC water was 30kcal/kg, whereas the coolant enthalpy was about 500～600 kcal/kg, so that the situation was beyond equilibrium model.

In the present calculation, a non-equilibrium model for

density calculation was introduced to cover this non-equilibrium phenomenon by means of a relaxation equation;

$$\frac{d\rho}{dt} = \frac{\rho - \rho^*}{\tau} \quad \text{--- (6)}$$

ρ ; equilibrium density
ρ^* ; non-equilibrium densiyt
τ ; delay parameter

2.3 Implicit Solution of Fuel Rod Temperature

The heat conduction equation within a fuel rod was given by

$$\rho C_p \frac{\partial T}{\partial t} = \frac{1}{r}\frac{\partial}{\partial r}(kr\frac{\partial T}{\partial r}) + \frac{\partial}{\partial z}(k\frac{\partial T}{\partial z}) + Q \quad \text{--- (7)}$$

Radial mesh width was the order of 10^{-3} m, while axial mesh width was the order of 1 m. So the equation was simplified ignoring the second term of the right hand side which was originally included in the equation, and was solved using a fully linear implicit method. By this improvement coupled with other implicit techniques for various parameters, calculations go ahead with a larger time step width.

2.4 Improvement of CHF and Heat Transfer Correlations

In the present version, various types of correlations for CHF and heat transfer were included in THYDE-P code, and the user can select appropriate correlations.

Presently available CHF correlations are;

(1) Biasi correlation
(2) GE correlation
(3) B&W-2, Bernett, Modified Bernett correlation
(4) Modified Zuber correlation

and available heat transfer correlations are;

for nucleate boiling condition
(1) Jens-Lottes correlation
(2) Thom correlation

for post-CHF forced convection condition
(1) Groenevelt correlation and,
(2) Dougall-Rhosenow correlation

for post-CHF pool condition
(1) Berenson correlation
(2) Modified Bromley correlation
(3) Bromley-Pomeranz correlation

3. Main Asumptions and Conditions for Run 20

3.1 Run 20 Plant Representation

An overall description of the specified 4-loop 1,100MWe PWR is given in section 2 of Ref. (2).

The input data used in the present calculation are listed in Appendix A. In the following, the main inputs and assumptions for Run 20 are shown.

(1) The specific enthalpy of ECC water in pumped injection and accumulator injection were assumed to be 30 kcal/kg.

(2) The nodalization of the present calculation is shown in Fig.3-1.

Nodes from 23 to 28 represent average core channel and a hot core channel was nodalized into nodes from 29 to 34. Node 36 was added for a cross flow simulation. The lower plenum and the upper plenum were expressed by a single node (node 22 and node 37, respectively), and the downcomer was simulated also by a single node (node 21). The upperhead was simulated by linkage node 38. The steam generator and the accumulator were modeled as special nodes and were nodalized into nodes 46,47 and nodes 41,42, respectively.

(3) The double-ended break were assumed to occur at junction 8 at 0.01 sec after the calculation started. The pressure at the break was assumed to drop to the containment pressure exponentially with a time constant 0.4 sec.

(4) In the steady state adjustment, THYDE-P requires initial mass flux and enthalpy at one point of the primary loop. They were selected to be

$$G = 9.0 \times 10^3 \quad kg/m^2.sec$$
$$h = 360 \ kcal/kg$$

at point A of normal node 1.

The geometrical data and loss coefficients for each node are shown in Table 3-1 and Table 3-2. Fig.3-2 shows the distribution of node average pressure in the primary loop which was obtained following the procedure described in section 4 of Ref. (2).

(5) Steam generator was modeled by the following data.

secondary system pressure	62atm
U-tube pitch	3.0×10^{-2} m
number of U-tubes of one unit	3265
specific enthalpy of feedwater	222 kcal/kg
feedwater mass flow rate	474.0 kg/sec
subcooled water level	4.0 m
void fraction of saturated region	0.95

initial heat flux

node no.	heat flux(kcal/m².sec)
14	65.65
15	49.24
16	41.03

The feedwater was cut off at 0.4 sec after LOCA initiated. In the present calculation, a relief valve could not be simulated.

(6) The core was divided radially into two regions, i.e. average channel region and hot channel region. The hot channel simulated the most hottest assembly in the core, and its hot channel factor was assumed to be 1.30. Input data for the core nodes were;

reactor themal power 3,479 MWt
initial heat flux and number of fuel rods

	hot channel region		average channel region	
	node no.	heat flux (kcal/m².sec)	node no.	heat flux (kcal/m².sec)
initial heat flux	29	non-heated	23	non-heated
	30	203.0	24	156.0
	31	304.0	25	234.0
	32	304.0	26	234.0
	33	203.0	27	156.0
	34	non-heated	28	non-heated
number of rods	200		39170	

fuel length	3.66 m
plenum gas volume	1.235×10^{-5} m
clad outer diameter	1.0732×10^{-2} m
clad thickness	6.187×10^{-4} m
pellet diameter	9.3146×10^{-3} m
fuel rod pitch	1.42×10^{-2} m

(The last four values are those at a full power operating condition)

(7) Input data for the pressurizer were;

cross-sectional area	3.58 m²
height	15.56 m
subcooled water level	9.0 m
void fraction of saturated region	0.99
stand pipe length	0.1 m

(8) ECC water was assumed to be injected into mixing junction 28 in the intact loop, and into mixing junction 34 in the broken loop. Input data for ECC were;

Accumulator

initial water volume	23.3 m^3
initial nitrogen volume	10.0 m^3
specific enthalpy of water	30 kcal/kg
initial pressure	44 atm

Pumped injection

specific enthalpy of water	30 kcal/kg
mass flow rate	220 kg/sec

for each loop.

Pumped injection was initiated after the break took place with a delay time of 25 sec.

(9) No structual heat source or sink was assumed.

(10) No paticular model for the container was provided except the temporary behavior of the container pressure which was an input function of time, i.e.;

time(sec)	0.0	7.5	15.0	30.0	1000.0
pressure(atm)	1.0	2.7	4.0	4.0	4.0

(11) Reverse flow at the break point occurred when the pressure in the primary loop became below the containment pressure. The quality for this reverse flow was set to 0.001. The loss coefficient at the break point for a reverse flow was 20.0, so that the total amount of reverse flow turned out to be small compared with ECC water injected.

(12) Because the flow area at the pump node was small compared with the other nodes, the pressure in the broken loop pump node dropped very rapidly in the early stage of blowdown. To avoid this unrealystically great pressure drop, the momentum flux term was omitted from the momentum equation only in the pump node.

(13) Core bypass area was nodalized into a single node, so condensation at this node became so large in reflooding stage that flow tended to go into the bybass region rather than into the core nodes. To prevent this flow pattern, the loss coefficient of bypass node was increased gradually from 47.9 to 150.0 after 60.0 sec.

(14) Loss coefficient of node 10 for a reverse flow was increased gradually from 0.1 to 10.0 to account for a form loss at the connection between the downcomer and the pipe after 21 sec.

3.2 CHF Correlations

In the present calculation, in the same way as RELAP-4 code[6], B&W-2, Bernett, and Modified Bernett correlations were used as follows;

p	>1500	B&W-2 correlation
1500> p	>1300	Iterpolation between B&W-2 and Bernett
1300> p	>1000	Bernett correlation
1000> p	>725	Interpolation between Bernett and Modified Bernett
725> p		Modified Bernett

in pool condition i.e. $G<G_{min}$, CHF was calculated by

$$\phi = (\phi_{CHF} - \phi_{min})G/G_{min} + \phi_{min}$$

ϕ_{min} ; 67.9 kcal/m^2.sec (90000 Btu/ft^2.hr)
G_{min} ; 271.2 kg/m^2.sec (20000 lbm/ft^2.hr)
ϕ_{CHF} ; CHF value at $G=G_{min}$

3.3 Heat Transfer Correlations

The heat transfer correlations used in the present calculation were summarized in Table 3-3 and Table 3-4. In the post CHF calculation, heat transfer correlations which assume film boiling conditions are likely to be underestimated compared with experimental data at low qualities. So transition boiling are assumed if quality becomes smaller than a threshold value in the following way.

(1) Forced convection transition boiling

$$h^{tr} = (h_0^{tr} - h_c^{tr})\left(\frac{x}{x_T}\right)^2 + 2(h_c^{tr} - h_0^{tr})\frac{x}{x_T} + h_0^{tr}$$

h^{tr} ; H.T.C. in transition boiling
h_o^{tr} ; H.T.C. by Mode 4 at x=0.0
h_c^{tr} ; H.T.C. by Mode 4 at x=x
x ; quality
x_T ; threshold quality (=0.5)

(2) Pool transition boiling

$$h^{tr} = \phi_{CHF}/(T_W - T_B)$$

h^{tr} ; H.T.C. in transition boiling
ϕ_{CHF} ; CHF value at present condition
T_W ; wall temperature
T_B ; bulk temperature
x_T ; threshold quality (=0.1)

3.4 Critical Flow

Zaloudeck equation and Moody table are implemented for a subcooled condition and a saturated condition respectively. At the region, $0.0<x<0.02$, critical flows calculated by these two models are connected smoothly. The discharge coefficient for Moody model was 0.6.

3.5 Relaxation Parameters

In the THYDE-P the relaxation models are implemented to avoid discontinuity or rapid change which may be brought about by various mode transitions.

(1) In order to ensure smooth variation in enthalpy with the flow direction change, we introduce parameters for each node such that

$$\frac{d\eta_i}{dt} = \frac{S - \eta_i}{\tau_1} \quad \text{--- (8)} \qquad (\eta_i = A \text{ or } E)$$

where S 1 when $G < 0$
0 when $G \geq 0$
τ_1 delay parameter (=0.05 sec)

Eq. (8) is calculated using a linear implicit method.

(2) To ensure continuous transition of the heat transfer coefficient with mode changes, h^{tr} is smoothed by

$$\frac{dh^{tr}}{dt} = \frac{h_c^{tr} - h^{tr}}{\tau_2} \quad \text{--- (9)}$$

where h^{tr} ; effective H.T.C.
h_c^{tr} ; H.T.C. calculated by correlations
τ_2 ; delay parameter (=0.08 sec)

Eq. (9) is calculated using a linear implicit method.

(3) As shown in Section 2.2, to avoid a rapid depressurization caused by a condensation, coolant density change is moderated as follows;

$$\frac{d\rho^*}{dt} = \frac{\rho - \rho^*}{\tau}$$

Since there is no theoretical basis to determine τ until now, we have no choice but to set the values empirically in the way that τ is proportional to node volume.
In the present calculation, τ was set as follows;

after 8 sec

1.0 sec	for nodes 8,9,19,20 and nodes 41,44
0.08 sec	for other nodes
1.0 sec	for mixing junctions 28 and 34
0.08 sec	for other mixing junctions

after 21 sec

1.0 sec	for nodes 23 and 29
2.0 sec	for nodes 24 28 and nodes 30 34
4.0 sec	for nodes 17 20 and nodes 41 44
6.0 sec	for nodes 5 7 and node 9
10.0 sec	for nodes 10,22 and 35
12.0 sec	for node 8
20.0 sec	for node 21 (downcomer node)
0.1 sec	for other nodes
4.0 sec	for mixing junctions from 28 to 34
0.1 sec	for other mixing junctions

3.6 Drift Flux Model

In the THYDE-P code, the relative velocity between gas and liquid is given by

$$u_{rel} = \frac{u_{gj}}{1-\alpha} \qquad \text{--- (10)}$$

where U_{gj} is the drift velocity,

$$u_{gj} = u_{gj}^{0} S_{\alpha}^{2} = 1.41\left[\frac{9\sigma(\rho_{fs}-\rho_{gs})}{\rho_{fs}^{2}}\right]^{1/4} S_{\alpha}^{2} \qquad \text{--- (11)}$$

and S_{α} is chosen to be of the form

$$S_{\alpha} = 1 - e^{-\frac{1-\alpha}{1-\alpha_c}} \qquad \text{--- (12)}$$

so as to avoid that U_{rel} becomes unrealistically great as α approaches unity.

As the energy equation is the form of (1) in section 2.1, the term 'I' plays an important role, when flow becomes stagnant i.e. G = 0. On the other hand, in the RELAP4 code[6] a vertical slip model is introduced to account for the energy transport effect by two phase flow, using the vertical slip velocity defined only by void fractions as follows;

$$V_{slip} = (10.0 + 4.0\times\Delta\alpha)\,\alpha(1-\alpha)^{(1\,-\,1.25\alpha)} \qquad \text{--- (13)}$$

In the reflooding stage, flow in the core becomes nearly

stagnant and void fractions are great, so the drift flux model becomes important in energy transport calculation and the value of the drift velocity has a great influence on a quenching time.

In the reflooding stage, the system pressure becomes nearly equal to the containment pressure (in the present calculation 4.0 atm), so the drift velocity U_{gj}^{o} has almost the same value anywhere in the system (in the present calculation, about 0.21 m/sec). Plot data in Fig.3-3 are calculated using these values.

As be seen from Eqs. (11) and (12), the relative velocity in a high void region depends greatly on the value of α_c.

In Fig.3-3 U_{rel} for α_c = 0.8, 0.97, 0.99 are shown with V_{slip} clculated by Eq. (13). In the present calculation α_c was set to 0.97, as will be discussed in section 4.10.

Table 3-1 Node Geometrical Data

Node No.	Description	Flow Area A (m^2)	Node Length L (m)	Node Volume V (m^3)
1	Broken loop hot leg	0.4266	5.240	2.235
2	SG inlet plenum	2.8953	1.665	4.821
3	SG U-tube	0.9952	5.000	4.976
4	SG U-tube	0.9952	5.460	5.434
5	SG U-tube	0.9952	10.460	10.410
6	SG outlet plenum	2.8953	1.665	4.821
7	Broken loop cold leg	0.4865	7.340	3.571
8	Pump	0.1917	12.412	2.379
9	Broken loop cold leg	0.3837	2.825	1.084
10	Broken loop cold leg	0.3837	3.130	1.201
11	Intact loop hot leg	1.2798	2.000	2.560
12	Intact loop hot leg	1.2798	3.240	4.147
13	SG inlet plenum	8.6859	1.665	14.462
14	SG U-tube	2.9856	5.460	14.928
15	SG U-tube	2.9856	5.460	16.301
16	SG U-tube	2.9856	10.460	31.229
17	SG outlet plenum	8.6859	1.665	14.462
18	Intact loop cold leg	1.4594	7.340	10.712
19	Pump	0.5750	12.412	7.137
20	Intact loop cold leg	1.1512	5.955	6.855
21	Downcomer	2.7435	7.248	19.885
22	Lower plenum	4.8578	6.075	29.511
23	non-Active core in average	4.3552	0.230	1.002
24	Active core in average	4.3552	0.800	3.484
25	Active core in average	4.3552	0.800	3.484
26	Active core in average	4.3552	0.800	3.484
27	Active core in average	4.3552	0.800	3.484
28	non-Active core in average	4.3552	0.230	1.002
29	non-Active core in hot	0.0222	0.230	5.11-3
30	Active core in hot	0.0222	0.800	1.78-2
31	Active core in hot	0.0222	0.800	1.78-2
32	Active core in hot	0.0222	0.800	1.78-2
33	Active core in hot	0.0222	0.800	1.78-2
34	non-Active core in hot	0.0222	0.230	5.11-3
35	Core bypass	0.2419	3.660	0.885
36	Core cross area	9.079-4	0.100	9.08-5
37	Upper plenum	9.2941	4.341	40.346
38	Upper head	3.8568	3.658	14.108
39	Pressurizer surge line	0.0661	15.00	0.992
40	Pressurizer surge line	0.0661	14.30	0.945
41	Pumped injection duct	0.2192	12.00	2.630
42	Pumped injection duct	0.0731	12.00	0.877
43	Accumulator duct	0.1161	120.00	13.932
44	Accumulator duct	0.0387	120.00	4.644

Table 3-2 Loss Coefficient

Node No.	K	K^{Af}	K^{Ar}	K^{Ef}	K^{Er}
1	0.023	0.043	0.084	0.0	0.0
2	0.021	3.73	1.97	0.0	0.0
3	0.011	0.033	0.048	0.0	0.0
4	0.008	0.0	0.0	0.0	0.0
5	0.017	0.0	0.0	0.033	0.048
6	0.030	0.0	0.0	3.73	1.97
7	0.019	0.042	0.077	0.0	0.0
8	0.303	0.273	0.367	0.203	0.203
9	0.028	0.0	0.0	0.0	0.0
10	0.019	0.0	0.0	0.0	0.0
11	0.024	0.043	0.083	0.0	0.0
12	0.028	0.0	0.0	0.0	0.0
13	0.013	3.73	1.97	0.0	0.0
14	0.025	0.033	0.048	0.0	0.0
15	0.021	0.0	0.0	0.0	0.0
16	0.027	0.0	0.0	0.033	0.048
17	0.029	0.0	0.0	3.73	1.97
18	0.022	0.042	0.077	0.0	0.0
19	0.303	0.273	0.367	0.203	0.203
20	0.011	0.0	0.0	0.0	0.0
21	1.032	0.0	0.0	0.0	0.0
22	1.398	0.0	0.0	0.0	0.0
23	6.416	0.74	0.74	0.0	0.0
24	6.161	0.0	0.0	0.0	0.0
25	6.072	0.0	0.0	0.0	0.0
26	6.218	0.0	0.0	0.0	0.0
27	6.045	0.0	0.0	0.0	0.0
28	6.737	0.0	0.0	0.0	0.0
29	5.295	1.284	2.482	0.0	0.0
30	5.642	0.0	0.0	0.0	0.0
31	5.570	0.0	0.0	0.0	0.0
32	5.574	0.0	0.0	0.0	0.0
33	4.662	0.0	0.0	0.0	0.0
34	6.104	0.76	0.34	0.0	0.0
35	47.857	0.77	0.83	0.87	0.78
36	12.354	0.0	0.0	0.0	0.0
37	2.08-2	0.0	0.0	0.0	0.0
38	5.0	1.491+4	1.491+4	0.0	0.0
39	5.0	0.41	0.87	0.0	0.0
40	5.0	0.0	0.0	0.0	0.0
41	10.0	0.0	0.0	0.0	0.0
42	10.0	0.0	0.0	0.0	0.0
43	10.0	0.109	0.049	0.0	0.0
44	10.0	0.109	0.049	0.0	0.0

Table 3-3 Heat Transfer Correlations

Mode	Conditions		Correlations
	Coolant Condition	Other Conditions	
1	subcooled	$T_w < T_{sat}$	Dittus-Boelter
2	subcooled	$T_w > T_{sat}$	Interpolation between Mode1 and Mode3
3	saturated	$\phi < \phi_{CHF}$	Thom
4	saturated	$\phi > \phi_{CHF}$	(see Table 3.4)
5	superheated	$Re < 3000$	Forced convection
6	superheated	$3000 < Re < 5000$	Interpolation between Mode5 and Mode7
7	superheated	$Re > 5000$	McEligot

Table 3-4 Heat Transfer Correlations in Mode-4

Mode	Conditions	Correlations
4-1	$G > G_{min}$, $x > x_{c1}$	Groenevelt and Dougall-Rhosenow
4-2	$G > G_{min}$, $x < x_{c1}$	Forced convection transition boiling
4-3	$G < G_{min}$, $x > x_{c2}$	Modified Bromley
4-4	$G < G_{min}$, $x < x_{c2}$	Pool transition boiling

T_w ; Wall temperature

G_{min} ; Minimum mass flux (=271.2 kg/m^{2}sec)

x_{c1} ; Threshold quality (=0.5)

x_{c2} ; Threshold quality (=0.1)

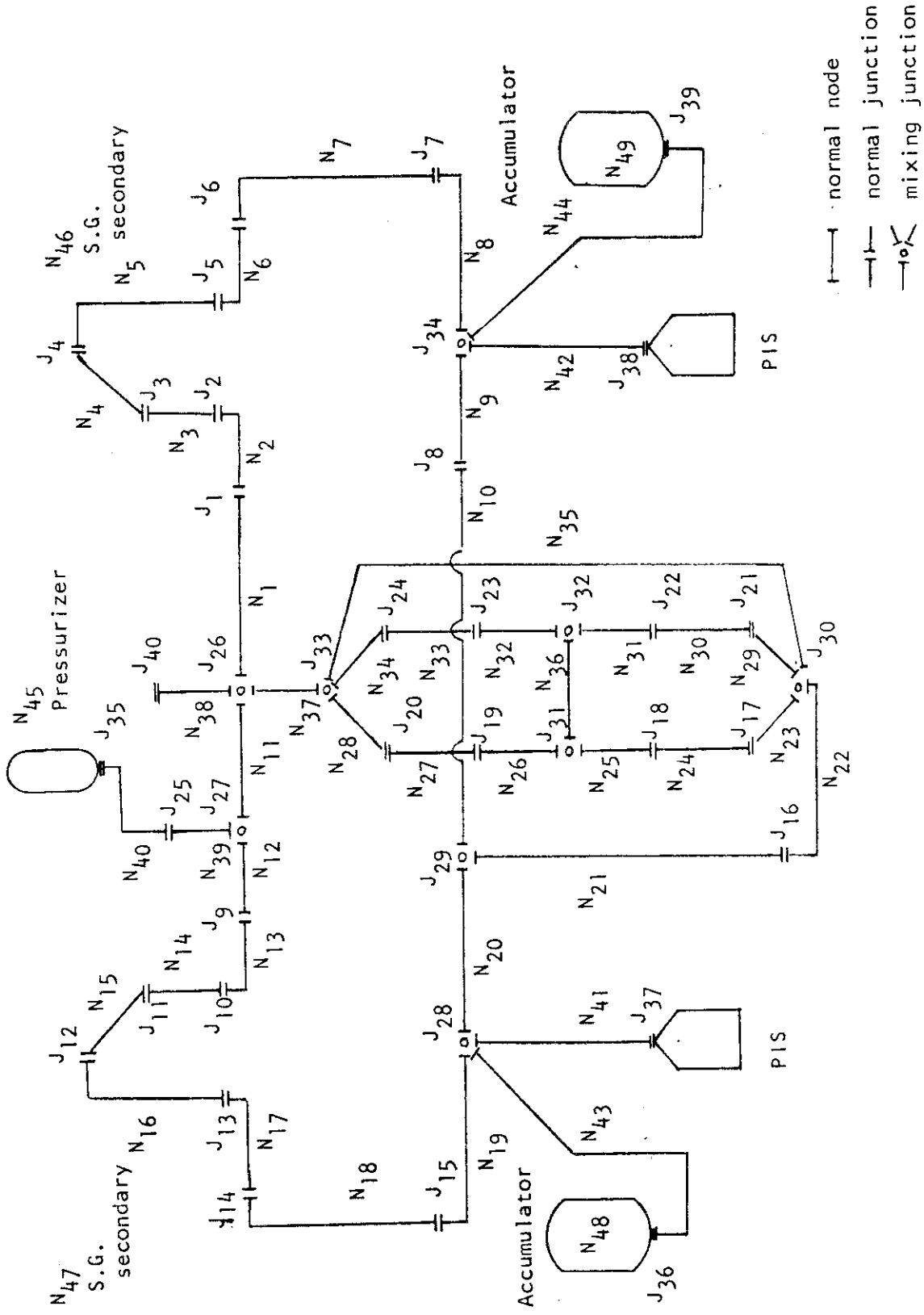

Fig. 3-1 Nodalization for 4-loop PWR

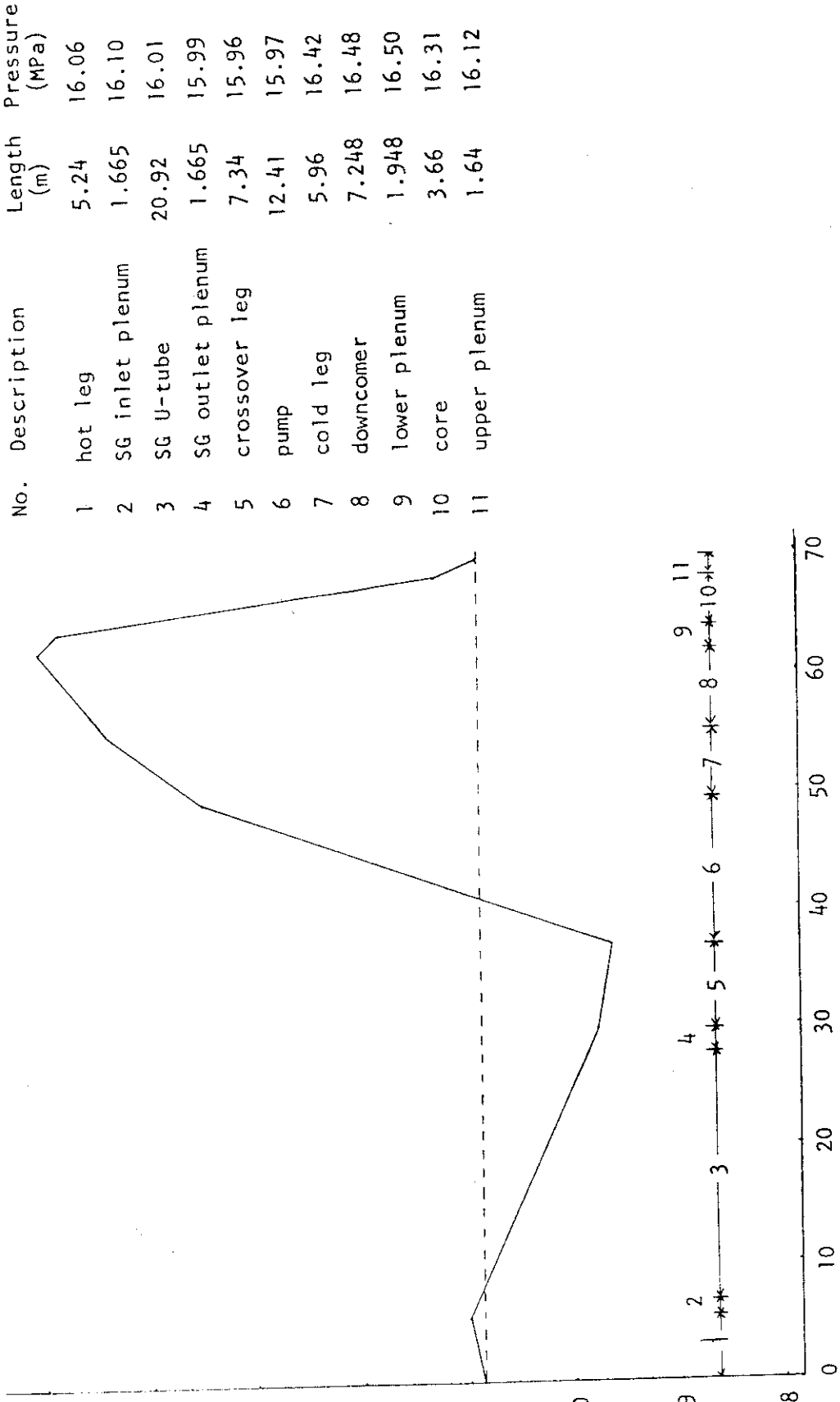

No.	Description	Length (m)	Pressure (MPa)
1	hot leg	5.24	16.06
2	SG inlet plenum	1.665	16.10
3	SG U-tube	20.92	16.01
4	SG outlet plenum	1.665	15.99
5	crossover leg	7.34	15.96
6	pump	12.41	15.97
7	cold leg	5.96	16.42
8	downcomer	7.248	16.48
9	lower plenum	1.948	16.50
10	core	3.66	16.31
11	upper plenum	1.64	16.12

Fig. 3-2 Steady State Pressure Distribution

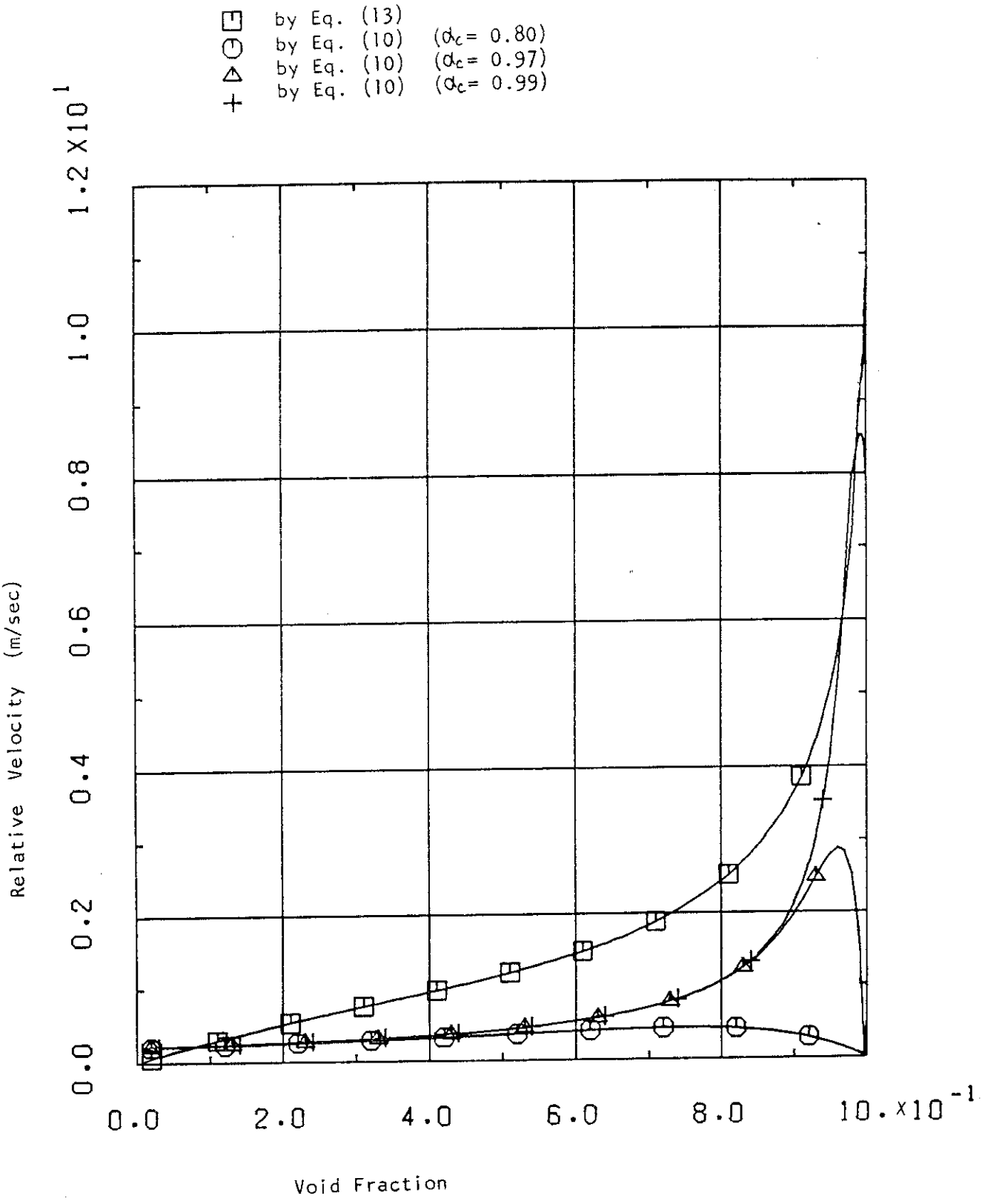

Fig. 3-3 Relative Velocity

4. Calculated Results

In this section, we will show the calculated results of Run 20 along with the discussions on them.

The maximum time step width was set to 32 ms after 20sec, and the total CPU time required for Run 20 by a FACOM M-200 computer was about 1.5 hours.

4.1 Overall Description

The chlonology of events is shown in Table 4-1. If we define the end of blowdown to be the time when the system pressure stops decreasing and the injected ECC water starts to flow down the downcomer, then it was 38 sec after the break occurred. The accumulator in the intact loop started injection at 16 sec and a duct node (node 20) was filled with subcooled water at 25 sec, but almost all of injected ECC water flowed out directly through the break until 38 sec. After ECC water penetrated the downcomer, an upward flow persisted in the heated section of the core by 49 sec which we define to be the time of the start of the reflooding. The accumulator was exhausted at 62 sec, but the P.I. kept injecting low enthalpy water. The driving force of the P.I. together with the static head of water in the downcomer supplied subcooled water to the heated section of the core and eventually quenching took place. After 140 sec all heated nodes in the average channel quenched, so that the average quench velocity was about 3.5 cm/sec.

The system pressure was shown in Fig.4-1-1. At 0.05 sec after the break occurred, the system was depressurized to 14 Mpa and bubbles appeared at the core nodes. After 0.1 sec, the upper plenum and the hot leg region became saturated successively so the system depressurized more gradually to the containment pressure. Except the period of ECC water penetration through the downcomer and the lower plenum, the system pressure was kept constantlly at a little bit above the containment pressure after 45 sec.

4.2 Fuel and Core

In Figs.4-2-1 to 4-2-4, the clad surface temperatures in the average channel and in the hot channel are shown. The fuel center temperatures for two channels are shown in Fig.4-2-5 and in Fig.4-2-6, respectively.

The clad surface temperatures reached the peak temperature after 10 sec, and then they dropped owing to a reverse flow in the core. After 25 sec the core flow became stagnant again so the surface temperature rose gradually till 50 sec when reflooding began. After reflooding started, the surface temperature began to decrease and the lowest part of the heated section of the average core became quenched at 74 sec. After that, the core quenched from lower part to upper part successively and all of the heated section of the average core became quenched by 140 sec. On the other hand, in the hot channel region quenching delayed compared with the average channel.

The period during which film boiling was dominant was rather long after reflooding started (see Figs.4-2-7 and 4-2-8). By taking a node average quality as the arithmetic mean of x_A and x_E instead of the outlet quality, an average quality would decrease more rapidly and as a result, the heat transfer mode would shift to the pool transition mode more earlier.

Fig.4-2-7 and Fig.4-2-8 show the behavior of the heat transfer coefficient in the average channel along with the heat transfer modes designated by

2 ; subcooled boiling
3 ; nucleate boiling
4 ; film boiling
4' ; transition boiling
5 ; forced convection by superheated steam

In Figs.4-2-9 to 4-2-12, the mass flux in the core inlet and in the core outlet are shown. Fig.4-2-13 shows the heat generation rate in fuels. Fig.4-2-14 and Fig.4-2-15 show the behavior of the fuel gap pressure and the heat transfer coefficient in the gap, respectively. The gap pressure was controlled mainly by the temperature in the gas plenum. The heat transfer coefficient in the gap was almost constant during the transient, so the initial value would become an important factor for the calculation of fuel temperatures. Fig.4-2-16 shows qualities in the average channel, which indicates that qualities oscillate around 0.1, because the heat transfer modes change between the film boiling condition and the pool transition boiling condition at the threshold quality of 0.1.

Figs.4-2-17 and 4-2-18 show enthalpies in the core inlet and in the core outlet. Fig.4-2-19 shows a core cross flow. By comparing the core inlet flow with the core outlet flow in the hot channel region, it is seen that a cross flow flattens the flow distributions in the upper region of the core. This fact coincides with our phisical intuition.

4.3 Downcomer and Lower plenum

Figs.4-3-1 and 4-3-2 show the mass flux in the downcomer and in the lower plenum, respectively. Figs.4-3-3 and 4-3-4 show qualities in the downcomer and in the lower plenum.
By 44 sec, G_{21}^{A} started to increase and at 48 sec G_{21}^{E} became positive. After that, the difference between G_{21}^{A} and G_{21}^{E} became small indicating that the downcomer was filled with liquid.

As for the flow in the lower plenum, in the early stage of blowdown from 1 sec to 3 sec the value of $G_{22}^{A} - G_{22}^{E}$ was negative, indicating that flashing occurred in the node, but water flowed out of the system through the downcomer rather than into the core. The reason is supposed to be that the upperhead reached saturation earlier than the lower plenum on account of the high initial enthalpy, and that the water from the upperhead flowed down the core during this period.

From 46 sec till 72 sec, the value of $G_{22}^{A} - G_{22}^{E}$ remained positive and a moderate condensation occurred in the lower plenum. This is because a large delay parameter for the density calculation was used in the downcomer node.

4.4 Break

Fig.4-4-1 shows break flows G^{E}_{10} and G^{A}_{9}. In Fig.4-4-2 enthalpies at the break point are shown. It should be noted that G^{E}_{10} took on a positive value at the initial steady state. As soon as the break occurred, G^{E}_{10} deccelerated and began to reverse its direction. But the other break flow G^{A}_{9} remained mostly positive throughout the LOCA.

From 30 sec till 47 sec, the break flow G^{E}_{10} increased and its enthalpy was below 100 kcal/kg. It shows that the ECC water bypassed over the downcomer to the break during this period. Fig.4-4-4 shows the pressure at the break, P^{E}_{10} and P^{A}_{9}, which indicate that break flows G^{E}_{10} and G^{A}_{9} returned to inertial flows at 26 sec and 30 sec, respectively.

4.5 Pressurizer

At 1.9 sec, region 2 (the lower region of the pressurizer) became saturated. At 22.5 sec, the level of region 2 reached the top of the stand pipe so that the coolant in region 1 started to flow out of the pressurizer. Fig.4-5-1 shows the surge flow G^{A}_{39}, whose rate of change varied at 1.9 sec and 22.5 sec, corresponding to the times when region 2 became saturated and when its level reached the top of the stand pipe. Fig.4-5-2 shows P^{A}_{39} and P^{E}_{40}, the former of which has the same tendency as those in the primary loop, and the latter is pressure in the pressurizer. The difference between P^{E}_{40} and P^{A}_{39} can be regarded as the driving force for the flow in the pressurizer duct. Fig.4-5-3 shows the mass flux in the intact loop hot leg. The surge water from the pressurizer flowed into the core from 10 sec till 25 sec and it cooled the core effectively.

Fig.4-5-4 shows the water level in the pressurizer. At 22.5 sec it vanished. From 76 sec the water level increased to about 3.0 m, but the integrated mass of this flow was about 50 kg and had no effect on core cooling.

4.6 Pumped Injection

Figs.4-6-1,4-6-2 and 4-6-3 show the behavior of the P.I. system. When the P.I. system was actuated at 25 sec, P^{E}_{41} deviated from P^{A}_{41} as shown in Fig.4-6-2, and their difference accounted for the driving force of P.I. flow shown in Fig.4-6-1. Fig.4-6-3 shows h^{E}_{41} which gradually approached to the ECC water enthalpy of 30 kcal/kg after the actuation of P.I.

The mass flow rate in the intact loop P.I. duct was 660 kg/sec, and about one third of it flowed into the core after the termination of the accumulator injection. So the P.I. system played an important role on core cooling.

4.7 Accumulator

The accumulator was actuated at 16 sec and it was terminated at 62 sec with a time constant of 3.0 sec. Fig.4-7-1 shows P^{A}_{43} and P^{E}_{43}. The former is practically the system pressure, while

the latter the pressure of the accumulator. The difference between P^{A}_{43} and P^{E}_{43} is the driving force of the accumulator. Fig.4-7-2 shows G^{E}_{43} . Fig.4-7-3 shows h^{E}_{43} , which started to decrease at 16 sec to 30 kcal/kg and after the termination of the accumulator injection increased due to flow reversal at the injection duct.

Fig.4-7-4 shows entalpies at 19E and 20A, which tend to deviate from each other with the actuation of A.I. and P.I. When A.I. terminated at 62 sec, the quality at 20A increased because of the superheated steam flow through The S.G., but a steady flow to the core continued due to the low enthalpy water from P.I. system.

4.8 Steam Generator

Fig.4-8-1 shows the S.G. feedwater flows in the broken and intact loops. Figs.4-8-2 and 4-8-3 show the heat transfer coefficient between nodes 47 and 14, and between nodes 46 and 3, respectively. Fig.4-8-4 shows the heat inputs to nodes 3 and 14 from the corresponding steam generators, both of which became heat sources to the primary flow at 17 sec. Fig.4-8-5 shows the pressure in the S.G. secondary system. The pressure in the broken loop S.G. reached 8.2 MPa, but a relief flow was not taken into account.

4.9 Pump

Fig.4-9-1 shows the relative pump speed. It was shown that the rotor was locked when the break occurred and pump speed decreased exponentially with a time constant 0.05 sec.

Fig.4-9-2 shows pump heads in each loop.

4.10 Difference due to Drift Velocity

In Fig.4-10-1, the clad surface temperatures calculated on the condition that $\sigma_c = 0.97$ (see Eq. (12) in section 3.6) are shown, and in Fig.4-10-2 the clad surface temperatures for $\sigma_c = 0.8$ are shown. In Figs.4-10-3 and 4-10-4, heat transfer coefficients for each case are shown.

In the case where σ_c was set to 0.97, the lowest part of the heated section in the average channel became quenched at 74 sec, while in the case where σ_c was set to 0.80, the quenching time was delayed. The reason is that when σ_c is set to small value such as 0.80 the drift velocity becomes nealy zero at the quench front where a large amount of bubbles are formed, and energy transfer by rise effect of these bubbles can not be taken into account.

At the quench front, heat from fuel rods is transfered to coolant by forming bubbles, and these bubbles rise faster than liquid. To evaluate a relative velocity between vapour and liquid at the quench front is difficult, though, in the present calculation this velocity was limited to about 2.5 m/sec (when $\sigma_c = 0.97$) as the maximum velocity.

Table 4-1 Chronology of Events Table

Time (sec)	Events
0.01	Break took place and pump was tripped.
0.221	Upperhead became saturated.
0.40	SG feed water was tripped.
1.40	Lower plenum became saturated.
16.0	Accumulator in intact loop started injection.
22.5	Pressurizer water level reached stand pipe.
25.01	Pumped injection started.
38.0	ECC water penetrated the downcomer. (start of refill)
47.0	Bypass ended.
49.0	Subcooled water reached the bottom of core. (start of reflood)
74.0	Bottom core node in average channel quenched.
140.0	All nodes in average channel quenched.

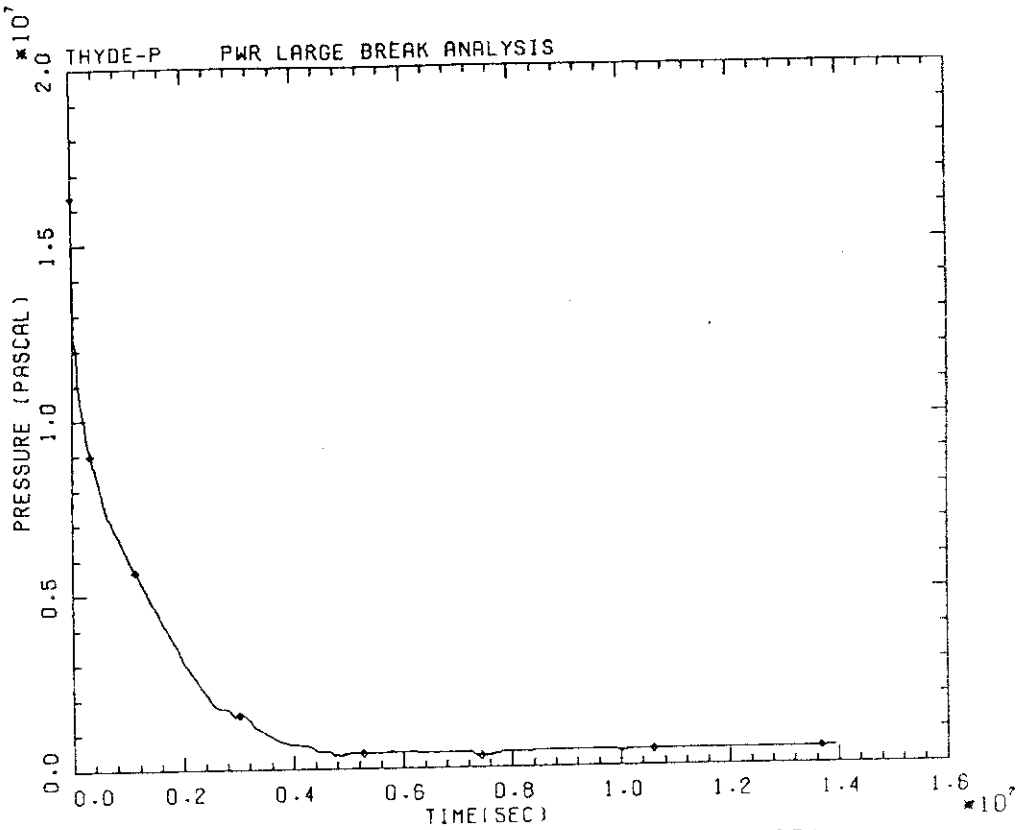

FIG. 4-1-1 PRESSURE IN CORE (NODE 25)

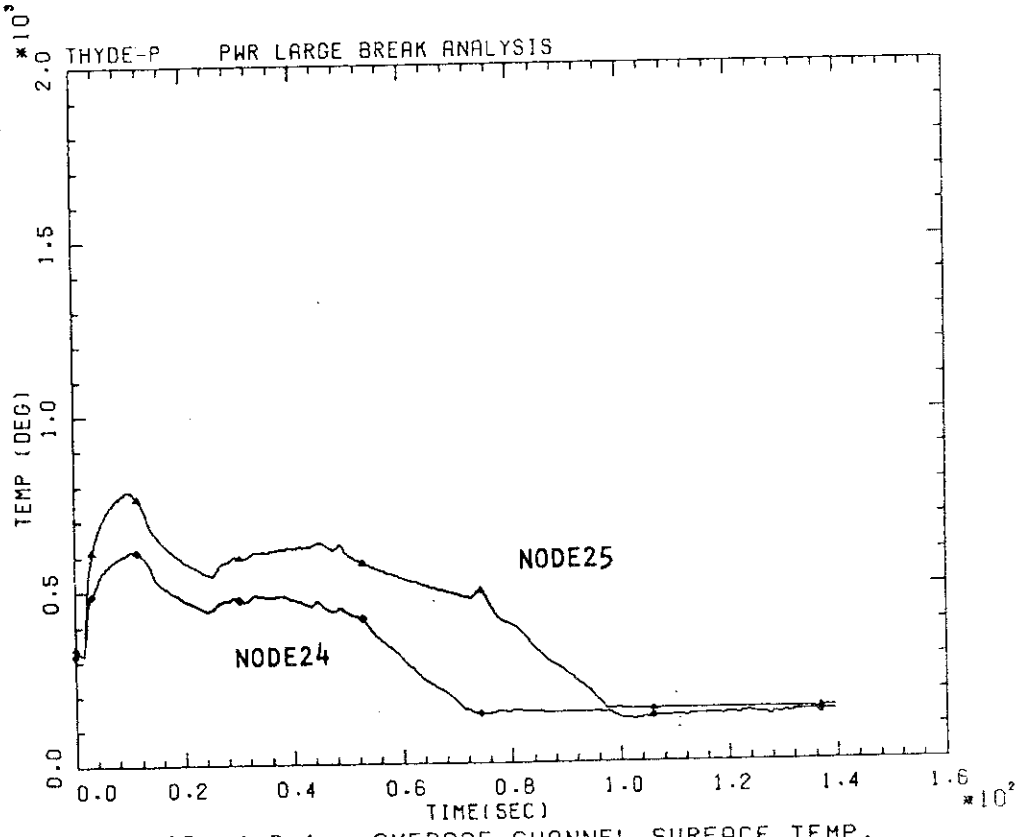

FIG. 4-2-1 AVERAGE CHANNEL SURFACE TEMP.

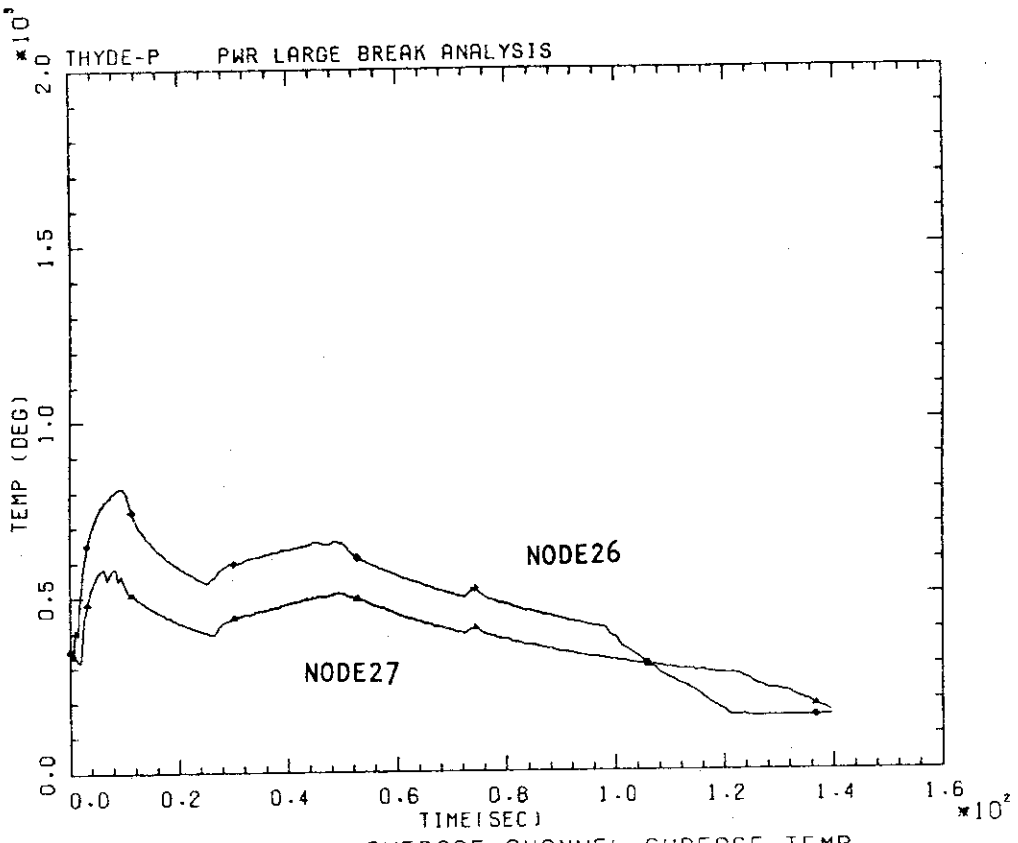

FIG. 4-2-2 AVERAGE CHANNEL SURFACE TEMP.

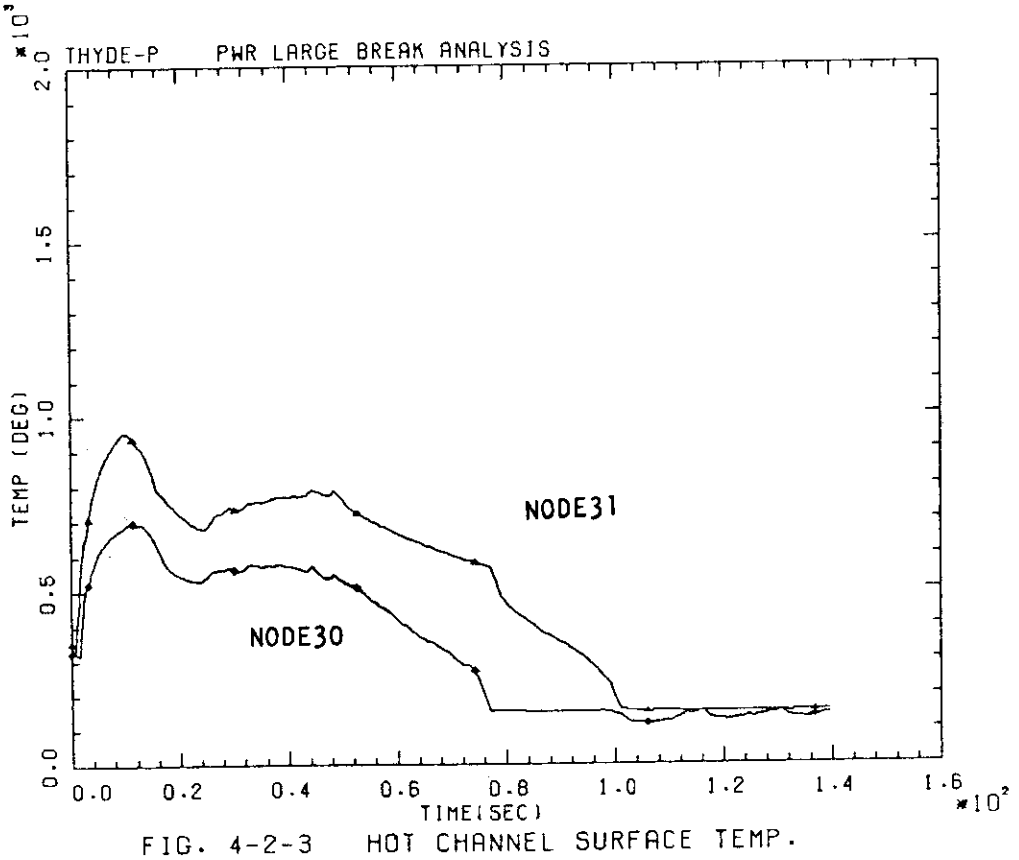

FIG. 4-2-3 HOT CHANNEL SURFACE TEMP.

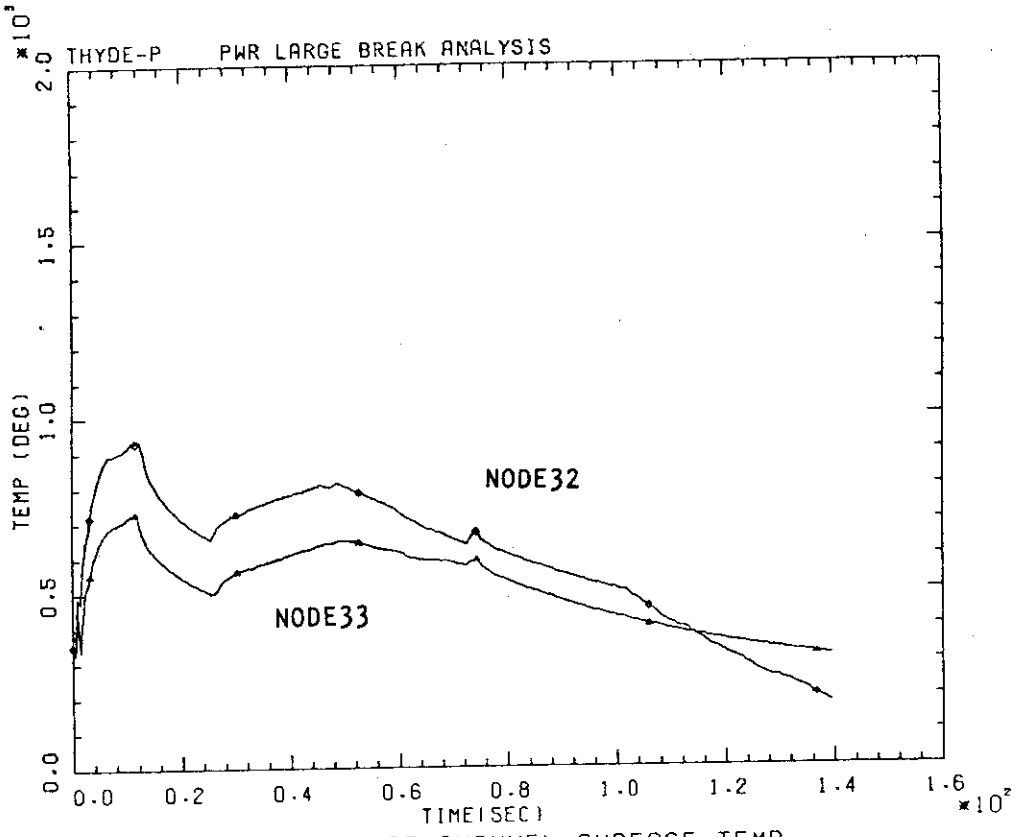

FIG. 4-2-4 HOT CHANNEL SURFACE TEMP.

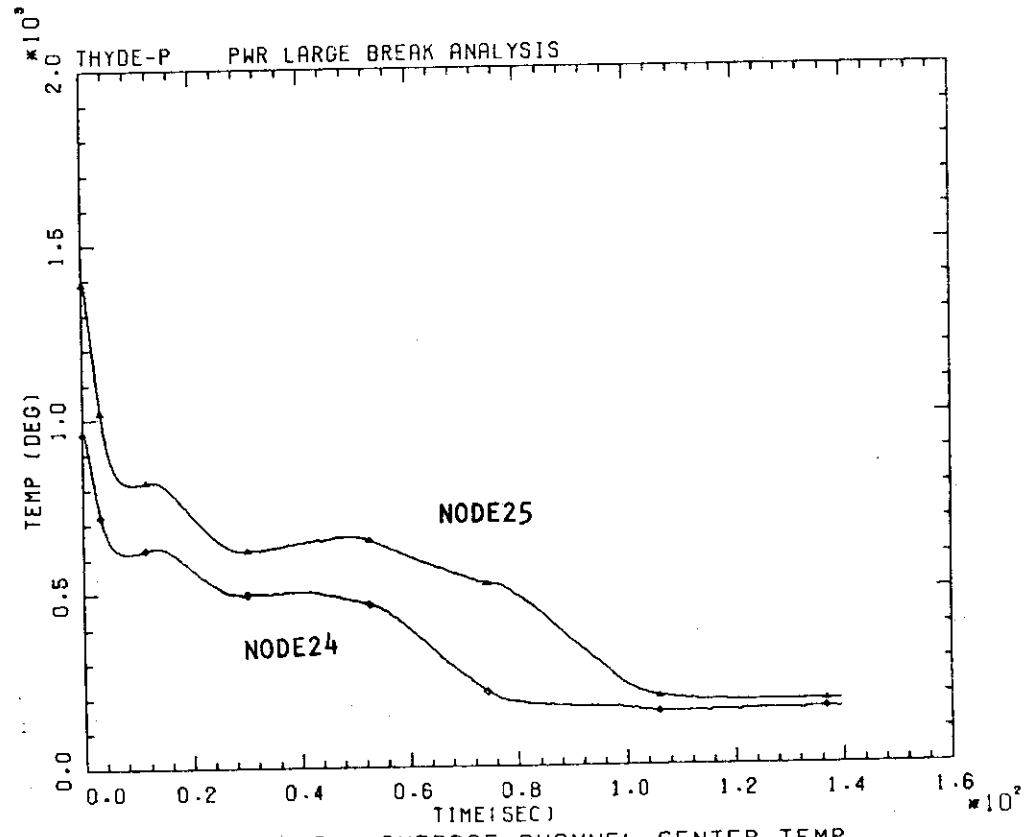

FIG. 4-2-5 AVERAGE CHANNEL CENTER TEMP.

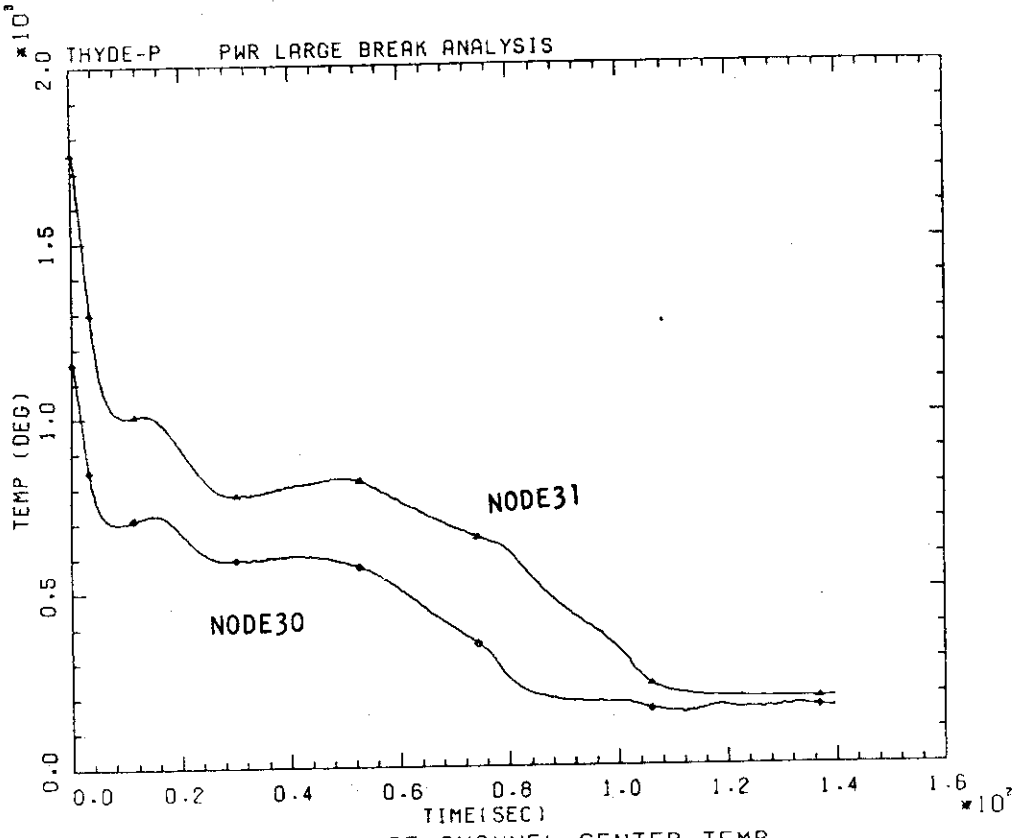

FIG. 4-2-6 HOT CHANNEL CENTER TEMP.

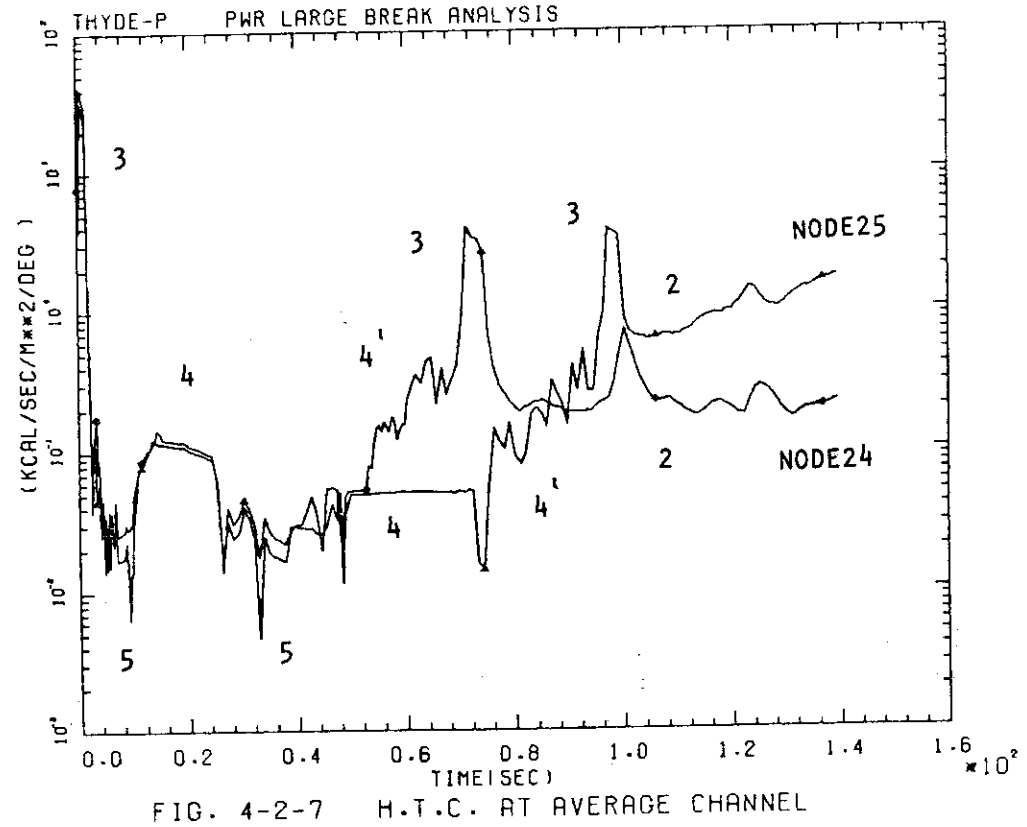

FIG. 4-2-7 H.T.C. AT AVERAGE CHANNEL

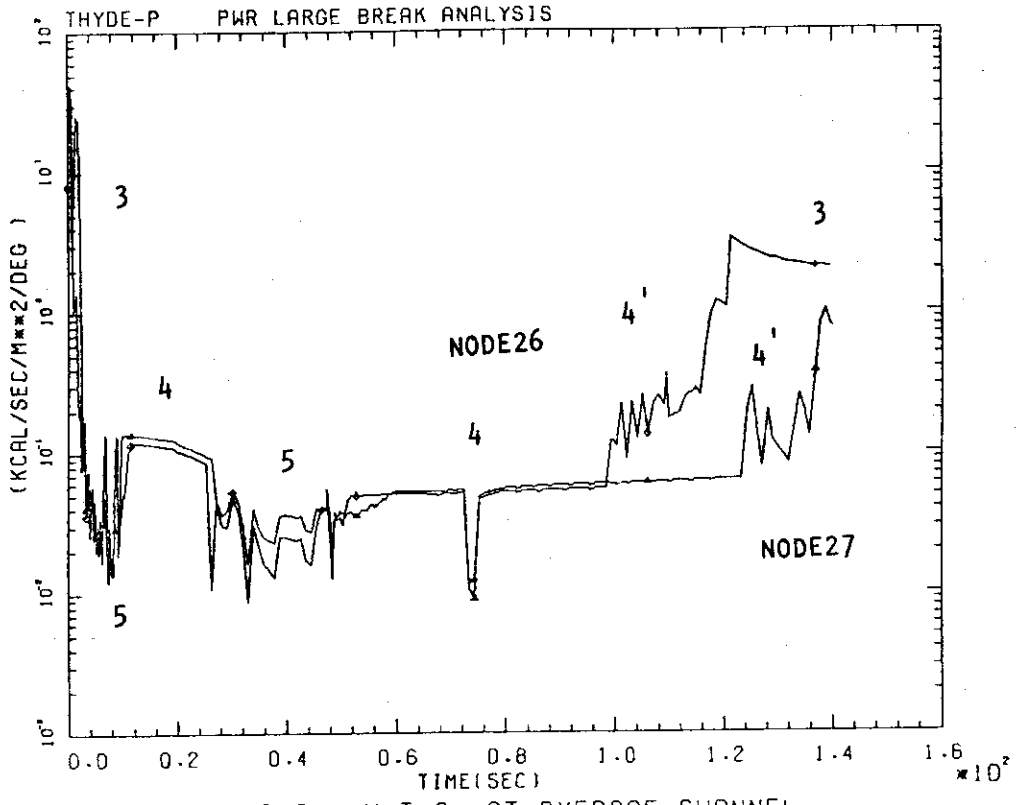

FIG. 4-2-8 H.T.C. AT AVERAGE CHANNEL

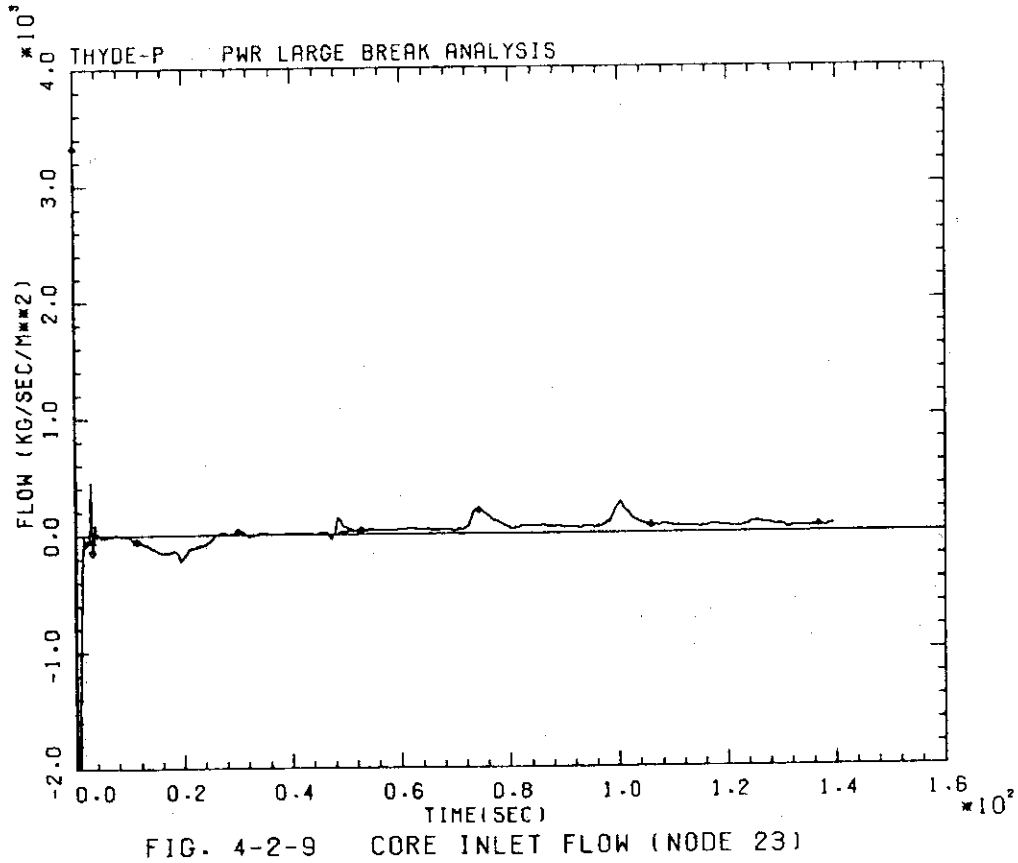

FIG. 4-2-9 CORE INLET FLOW (NODE 23)

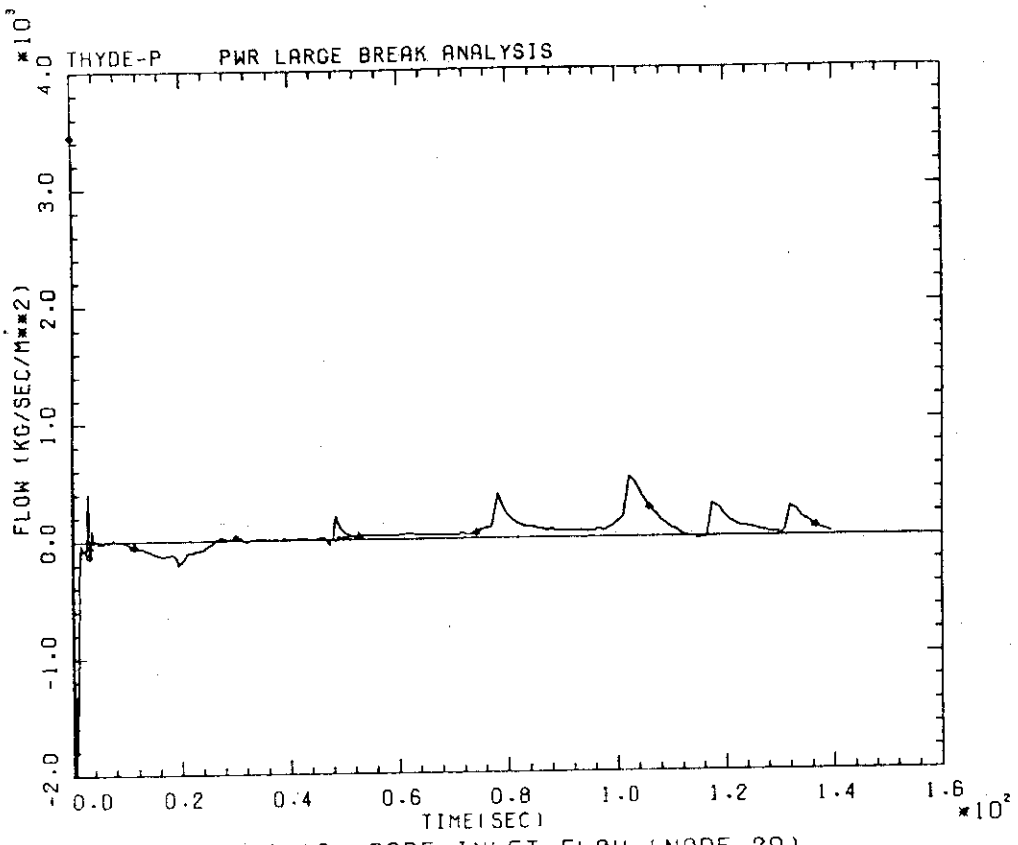

FIG. 4-2-10 CORE INLET FLOW (NODE 29)

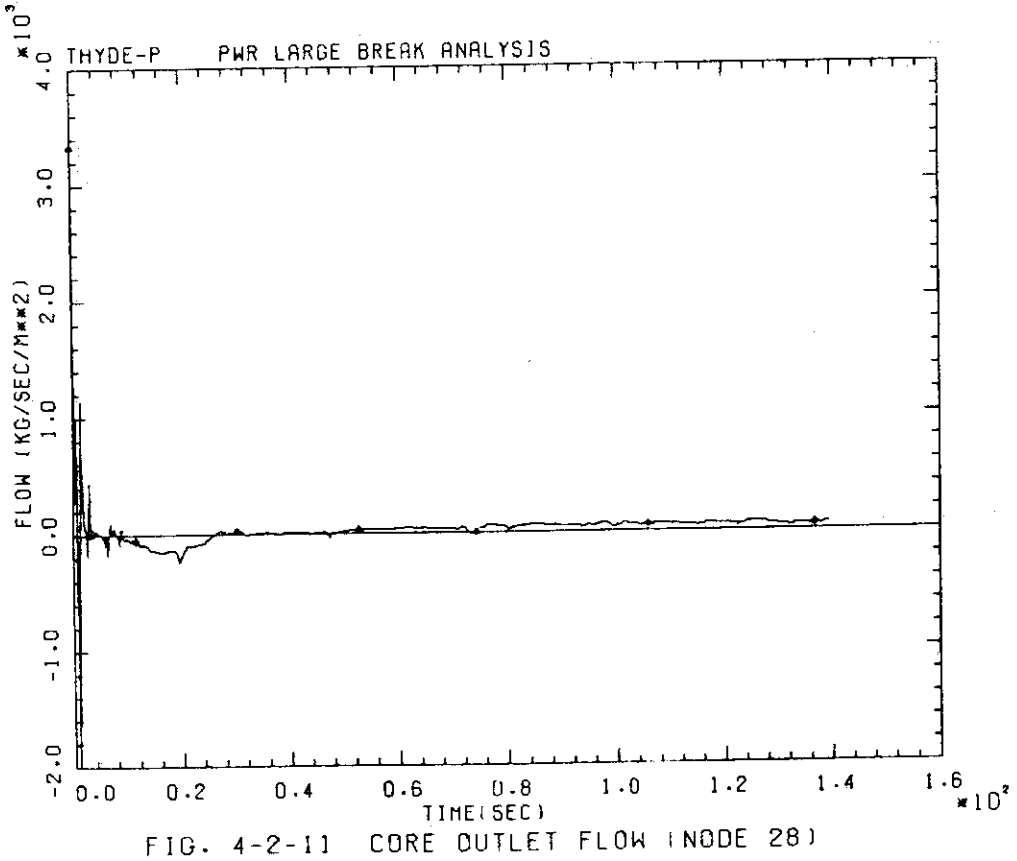

FIG. 4-2-11 CORE OUTLET FLOW (NODE 28)

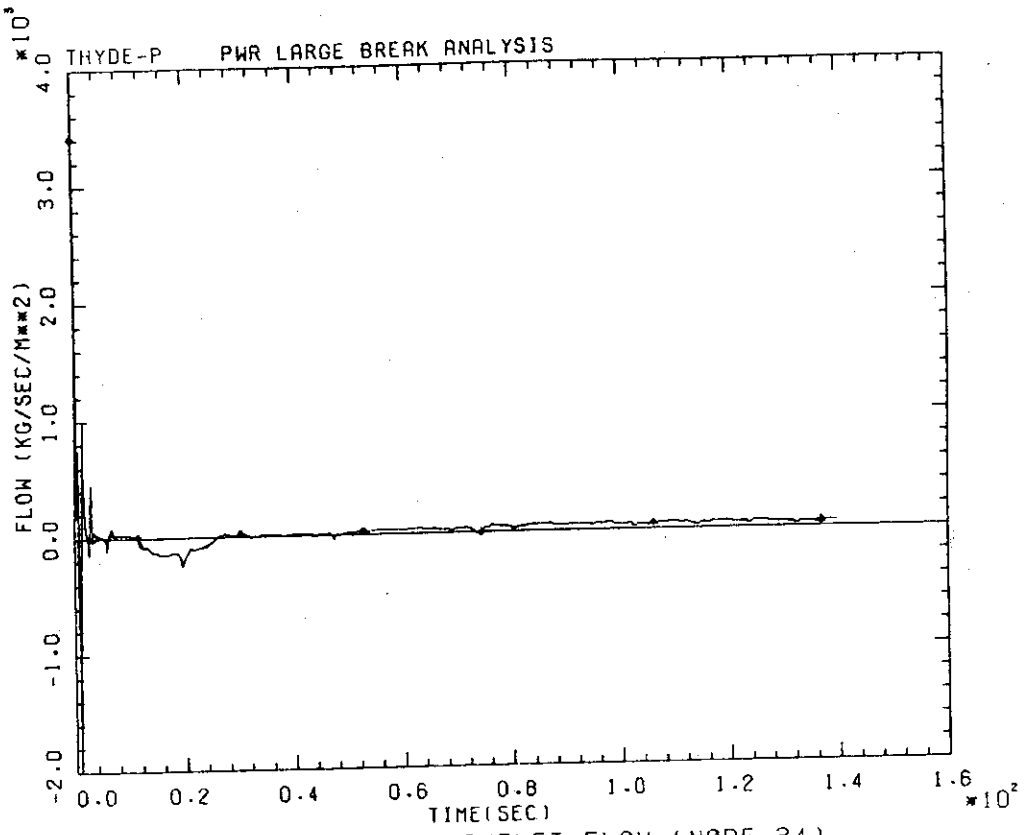

FIG. 4-2-12 CORE OUTLET FLOW (NODE 34)

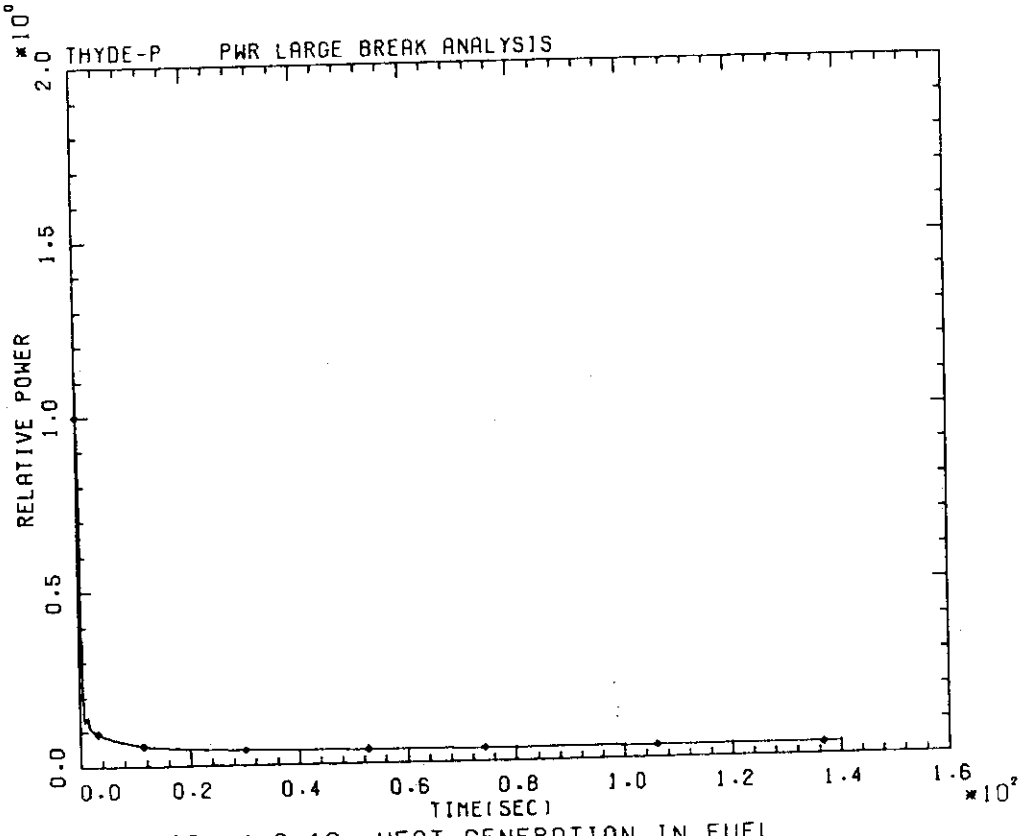

FIG. 4-2-13 HEAT GENERATION IN FUEL

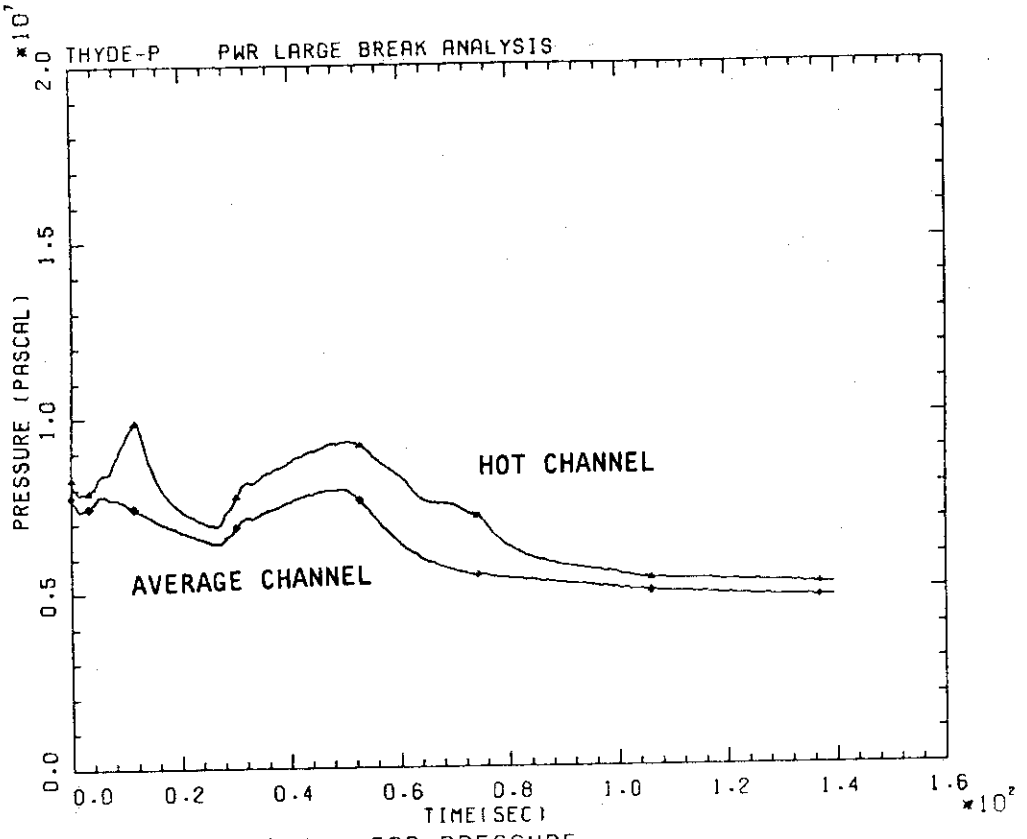

FIG. 4-2-14 GAP PRESSURE

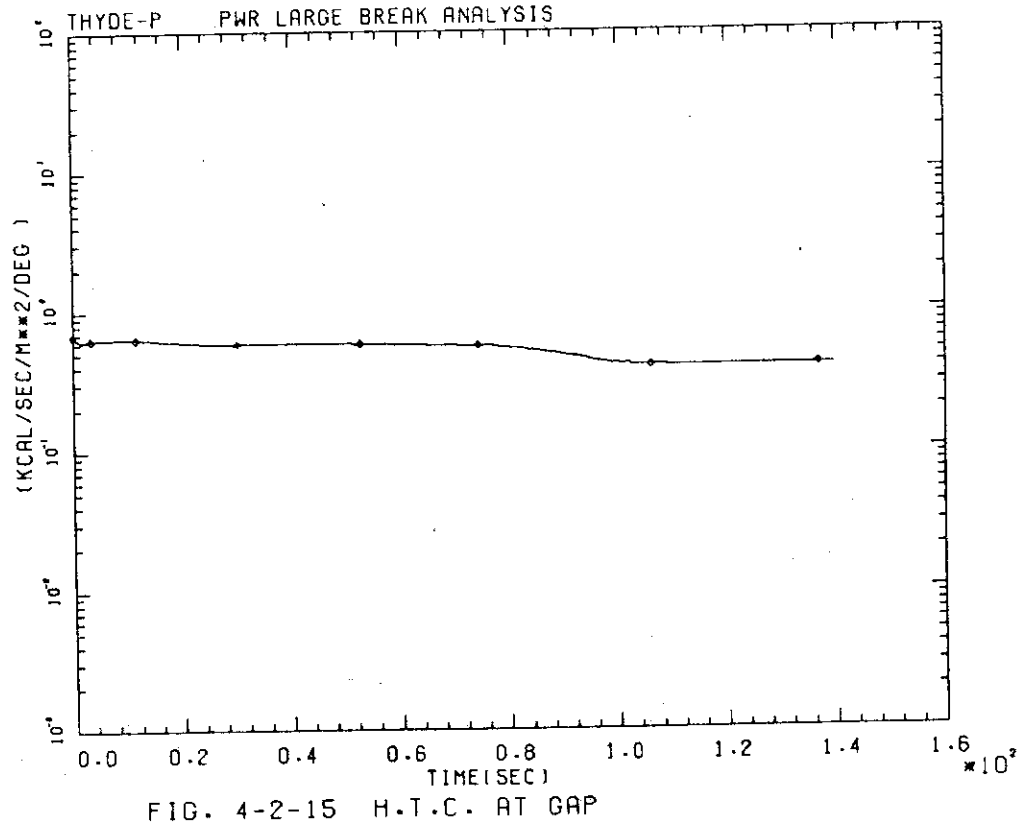

FIG. 4-2-15 H.T.C. AT GAP

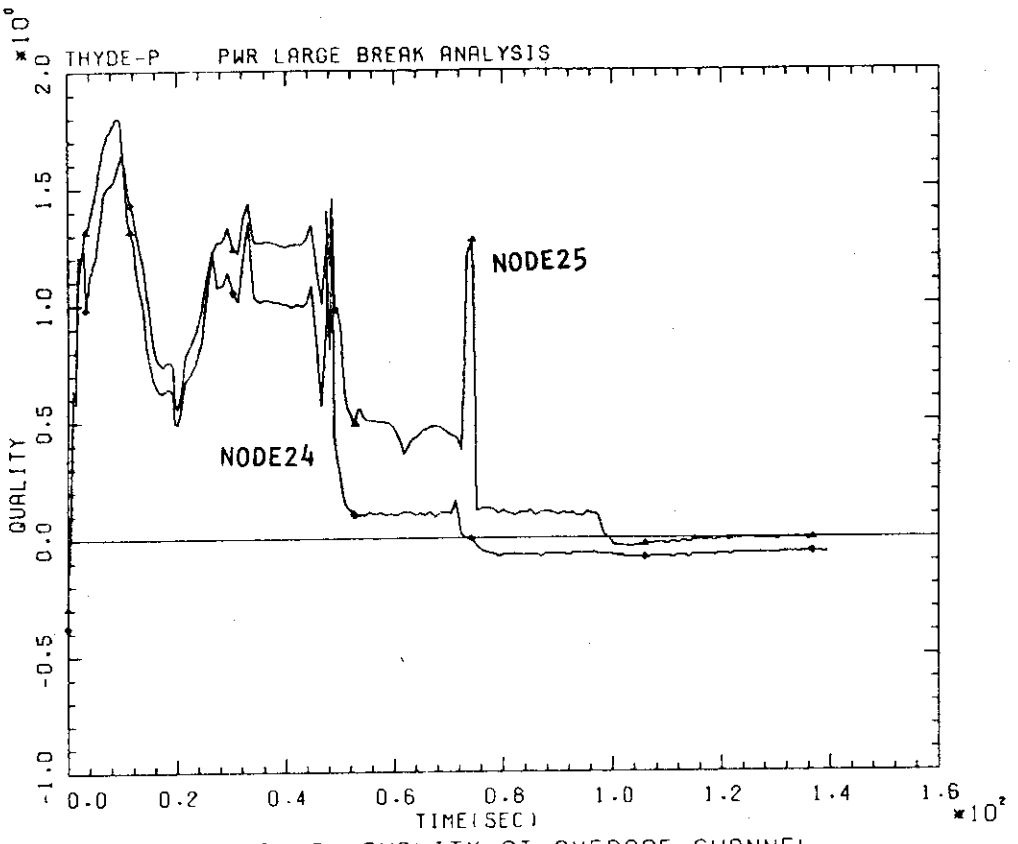

FIG. 4-2-16 QUALITY AT AVERAGE CHANNEL

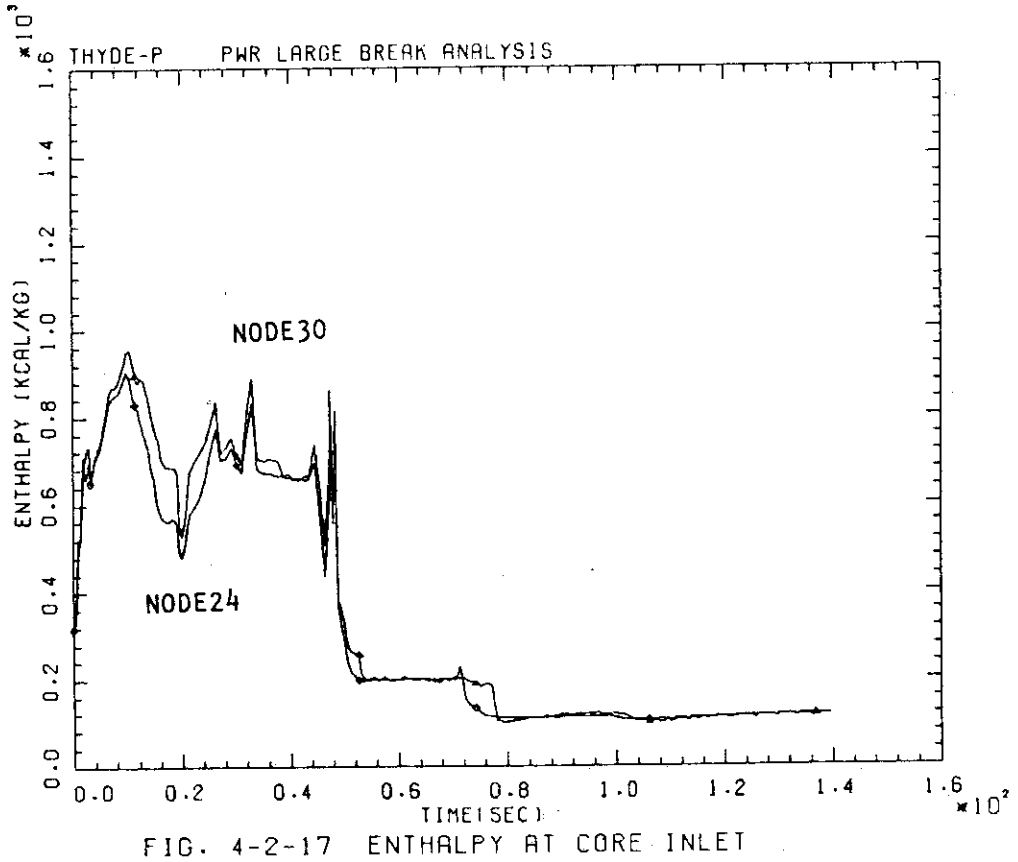

FIG. 4-2-17 ENTHALPY AT CORE INLET

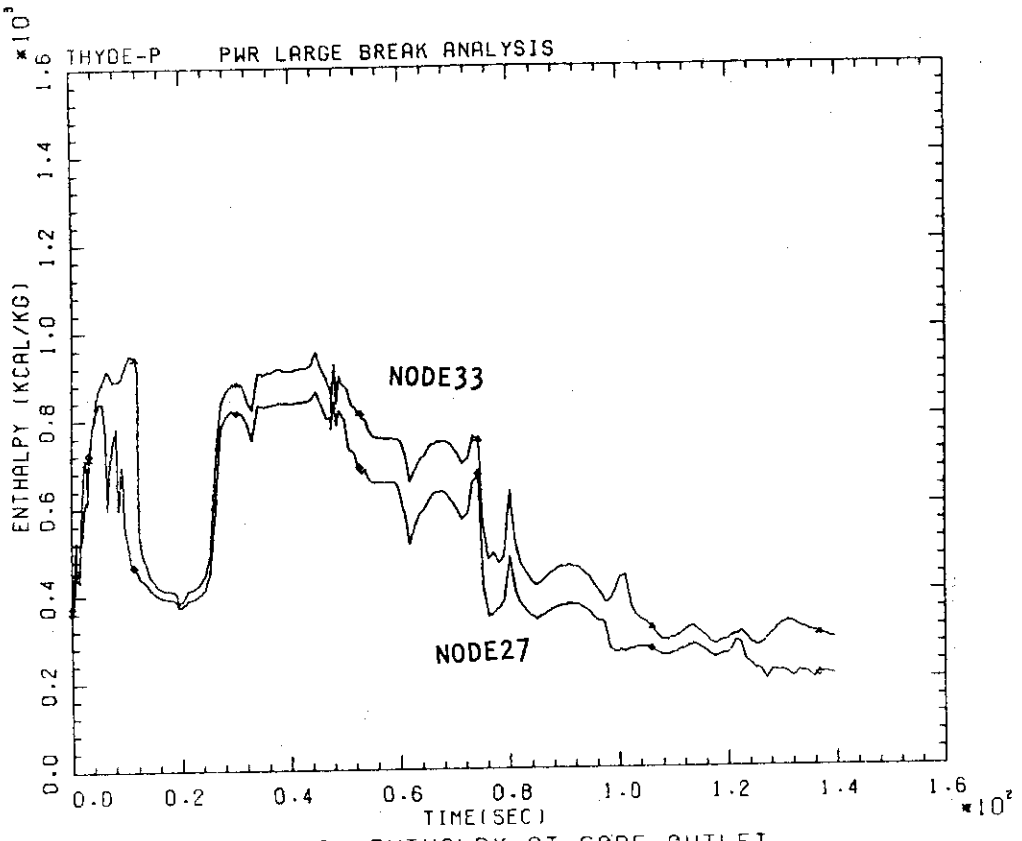

FIG. 4-2-18 ENTHALPY AT CORE OUTLET

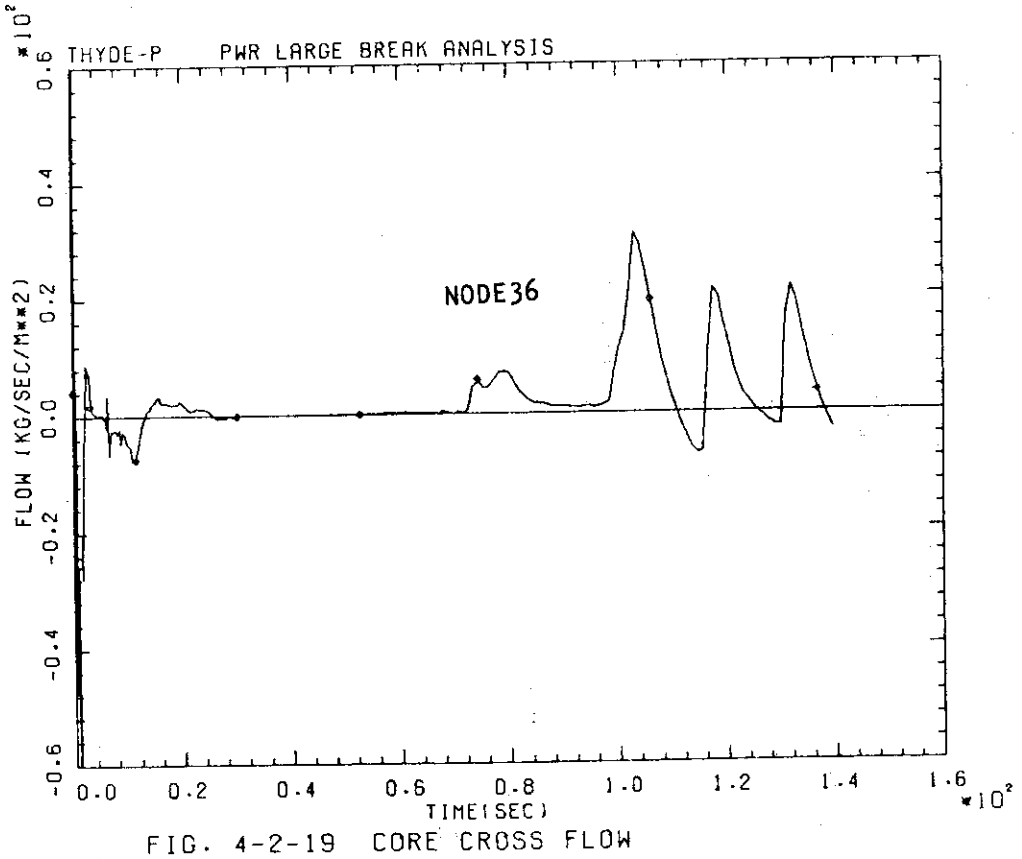

FIG. 4-2-19 CORE CROSS FLOW

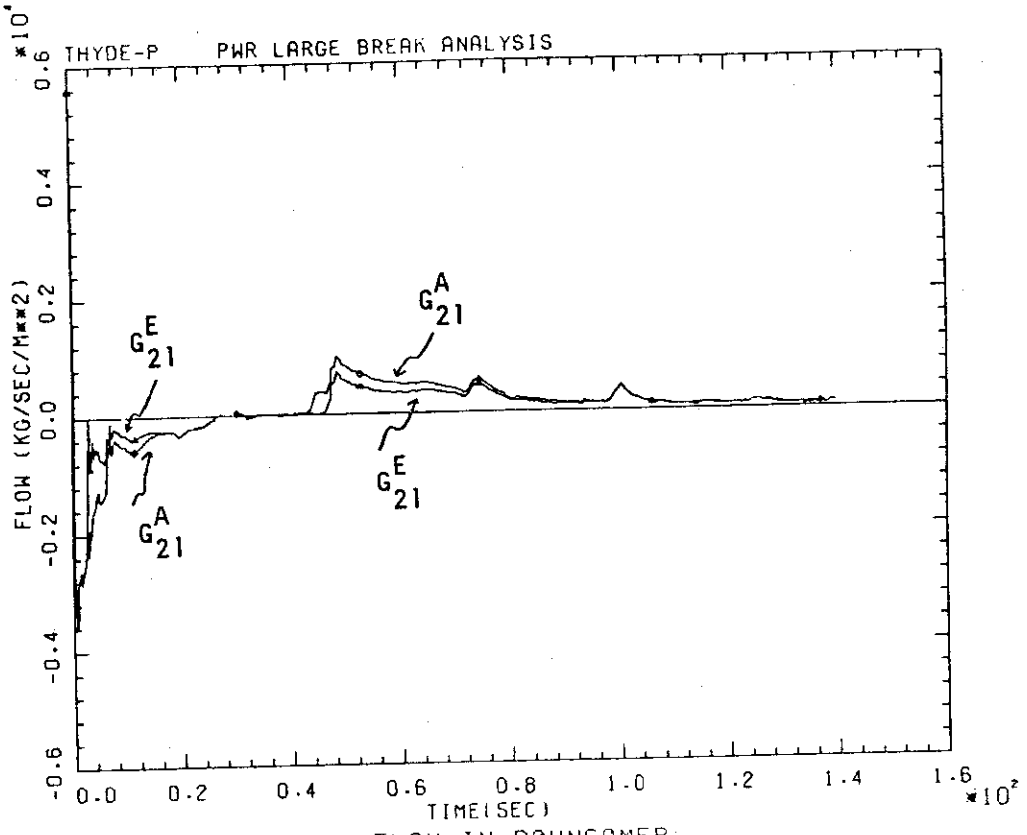

FIG. 4-3-1 FLOW IN DOWNCOMER

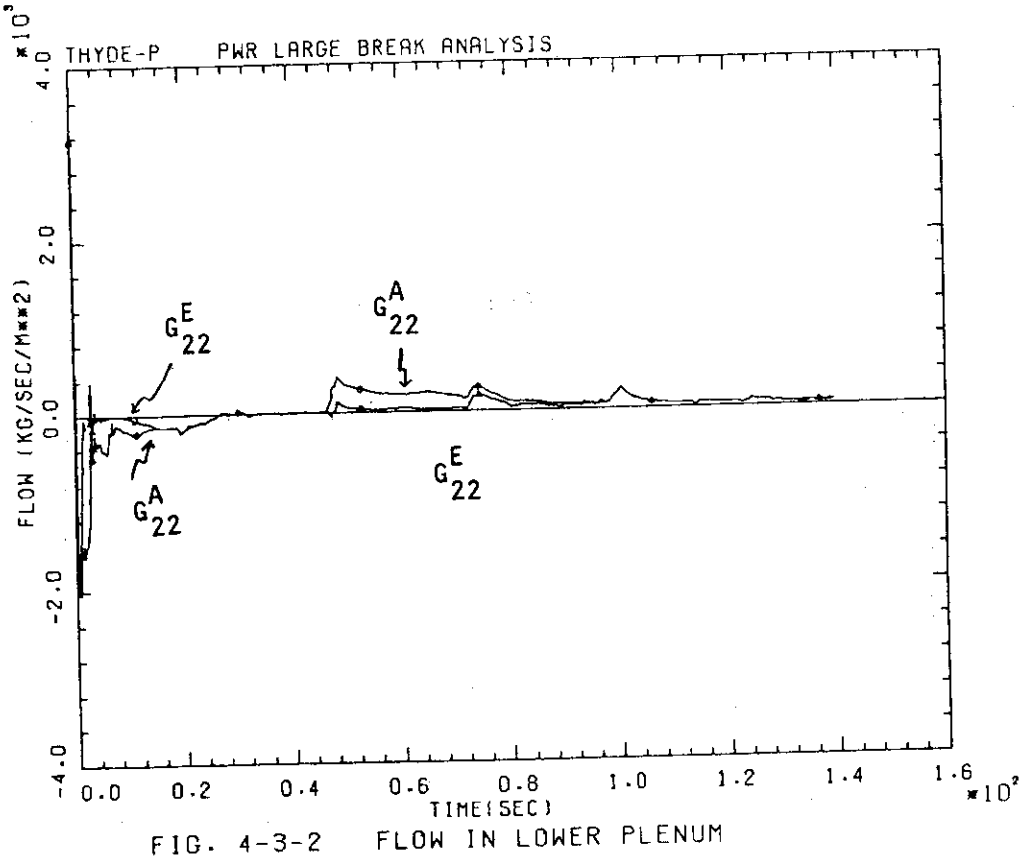

FIG. 4-3-2 FLOW IN LOWER PLENUM

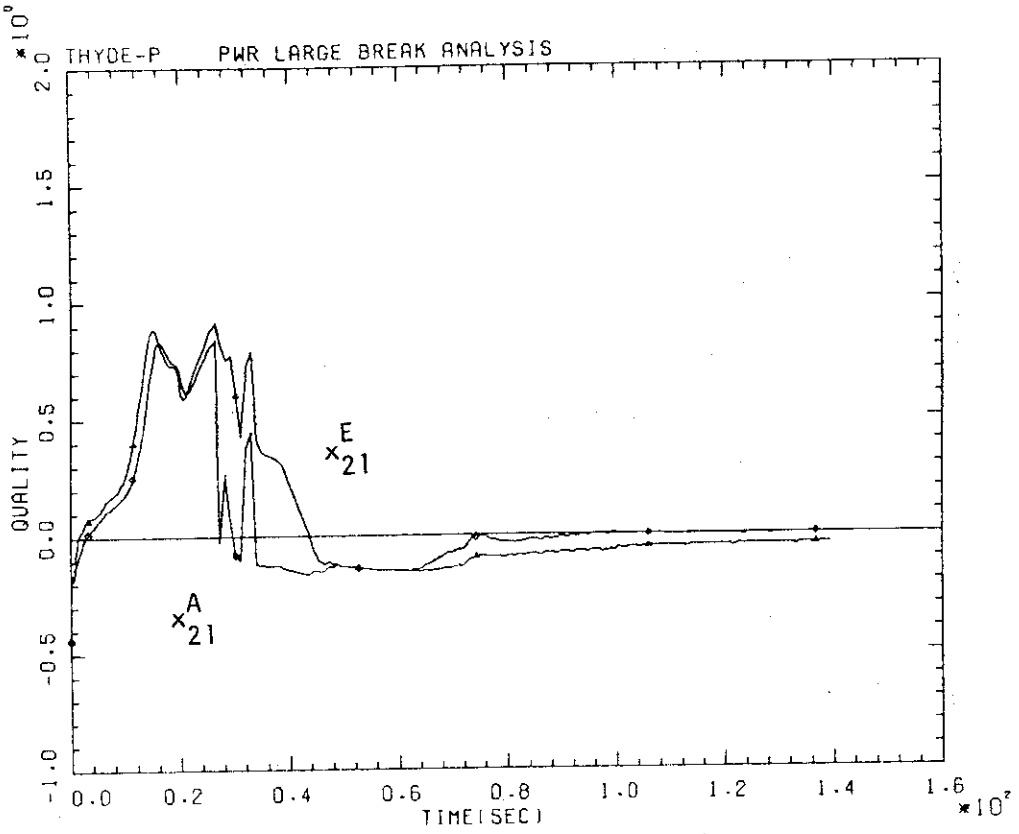

FIG. 4-3-3 QUALITY IN DOWNCOMER

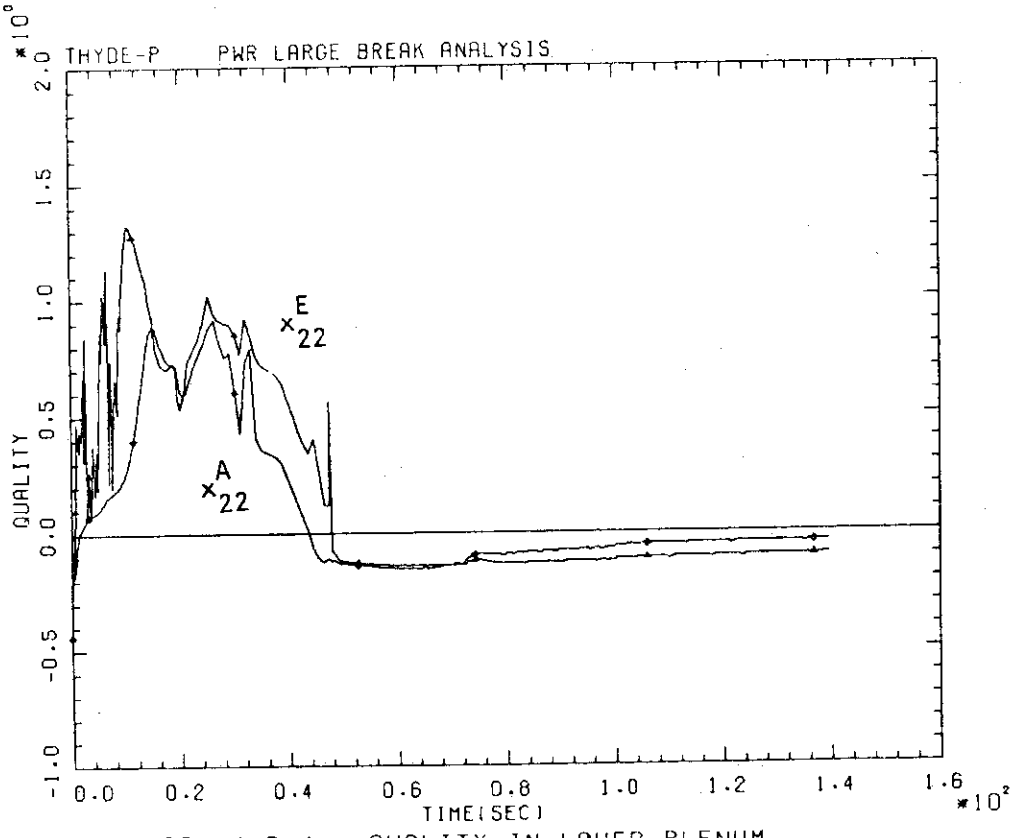

FIG. 4-3-4 QUALITY IN LOWER PLENUM

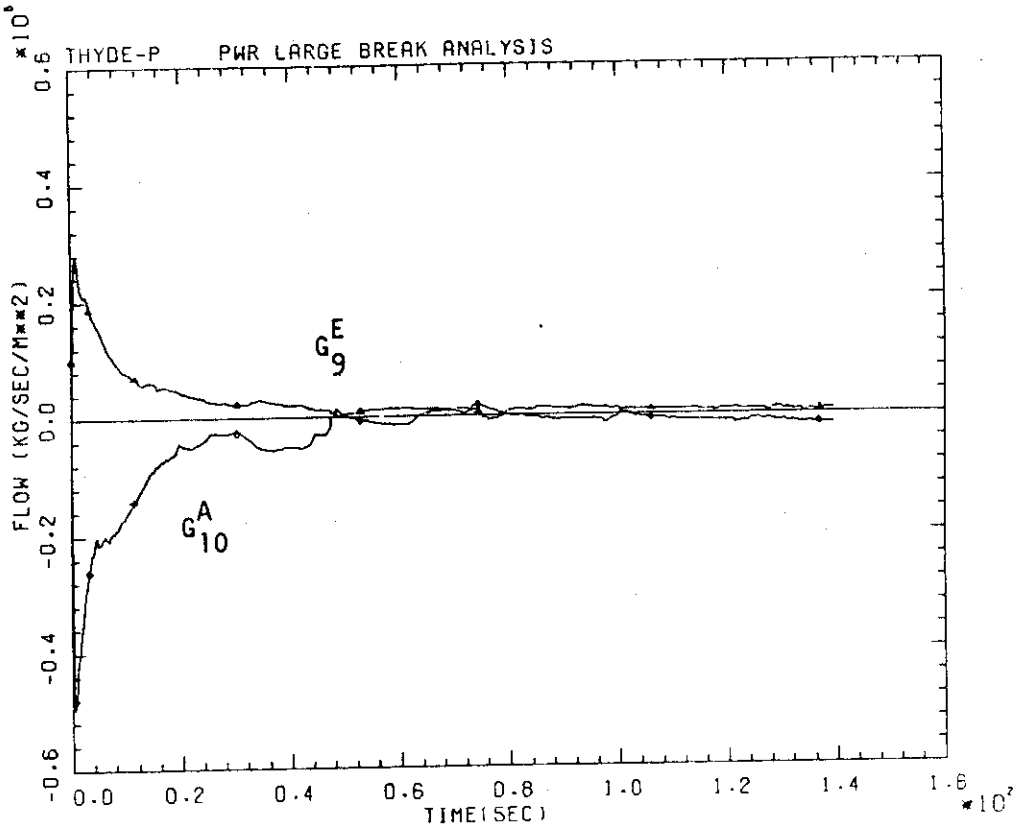

FIG. 4-4-1 BREAK FLOW

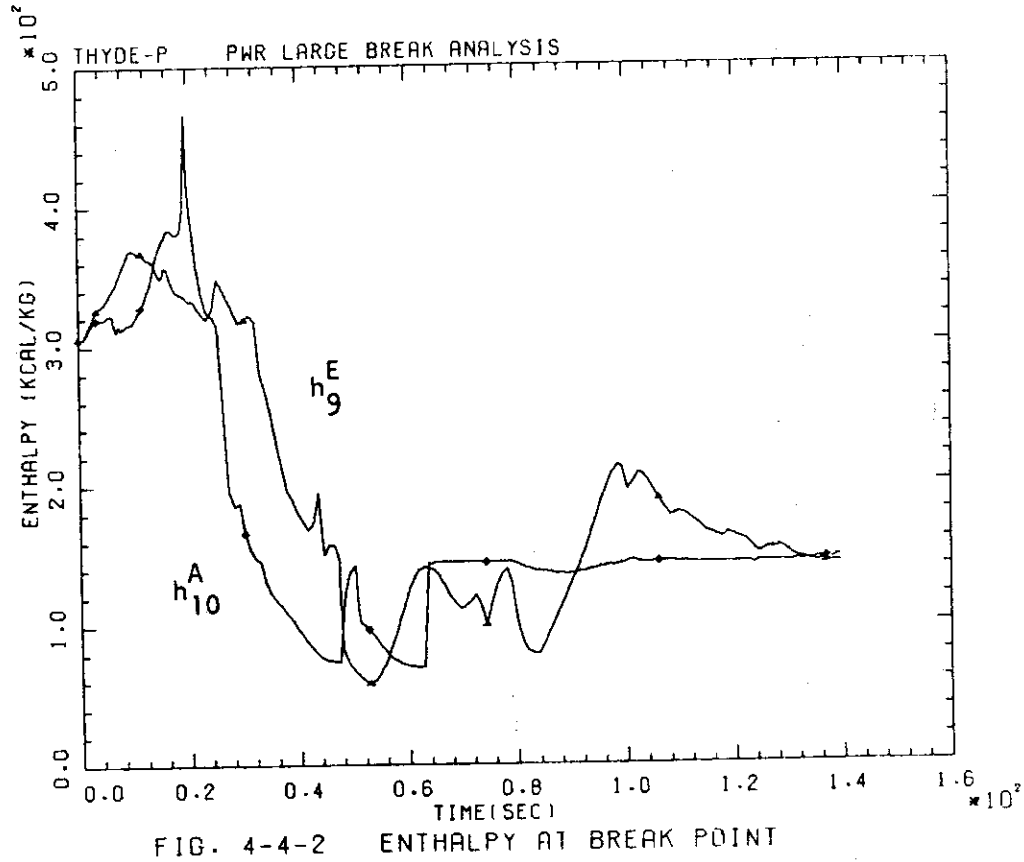

FIG. 4-4-2 ENTHALPY AT BREAK POINT

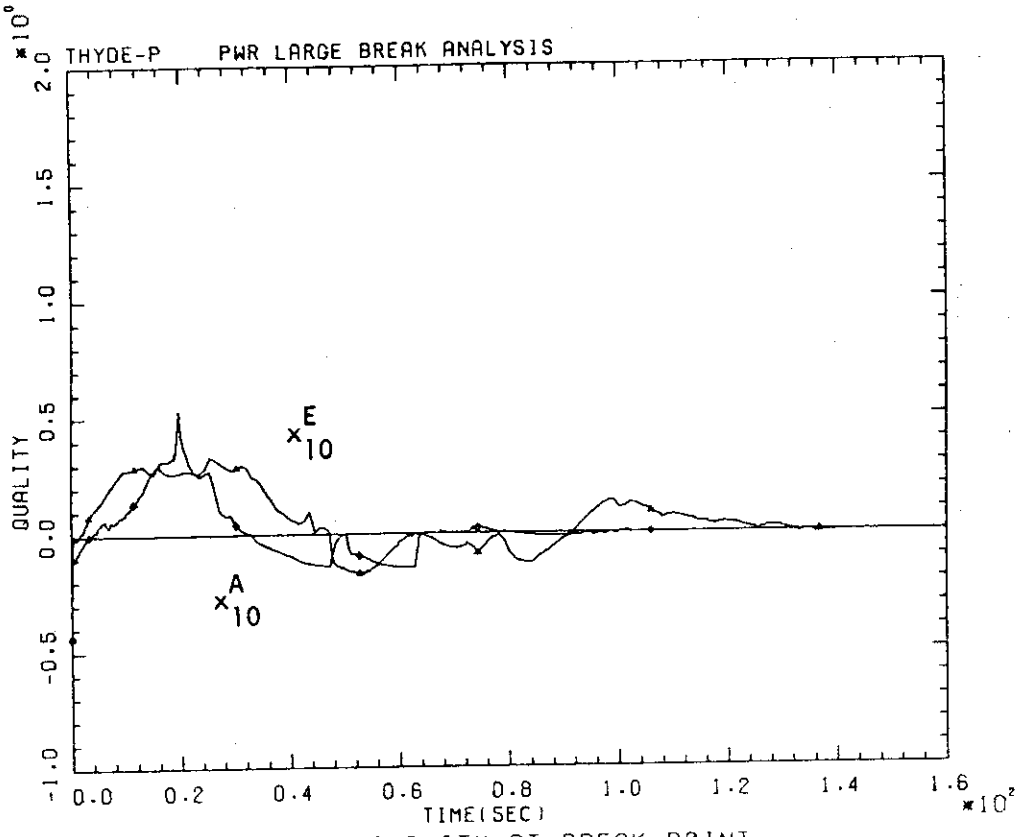

FIG. 4-4-3 QUALITY AT BREAK POINT

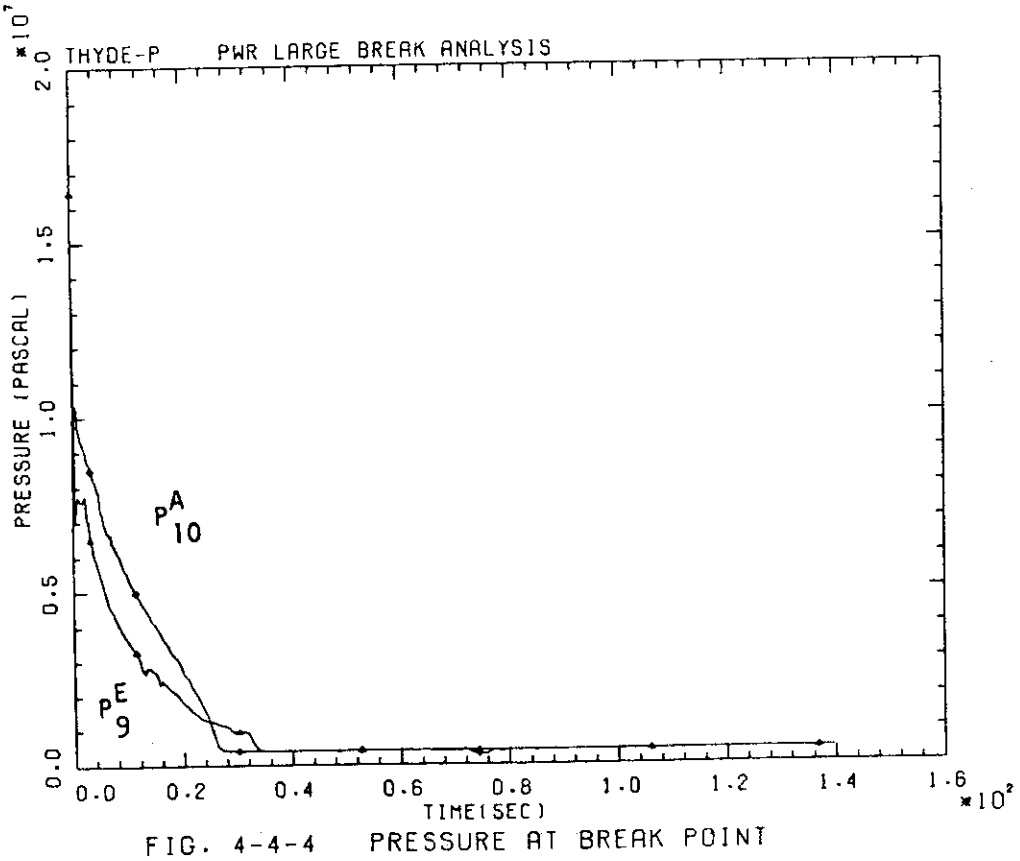

FIG. 4-4-4 PRESSURE AT BREAK POINT

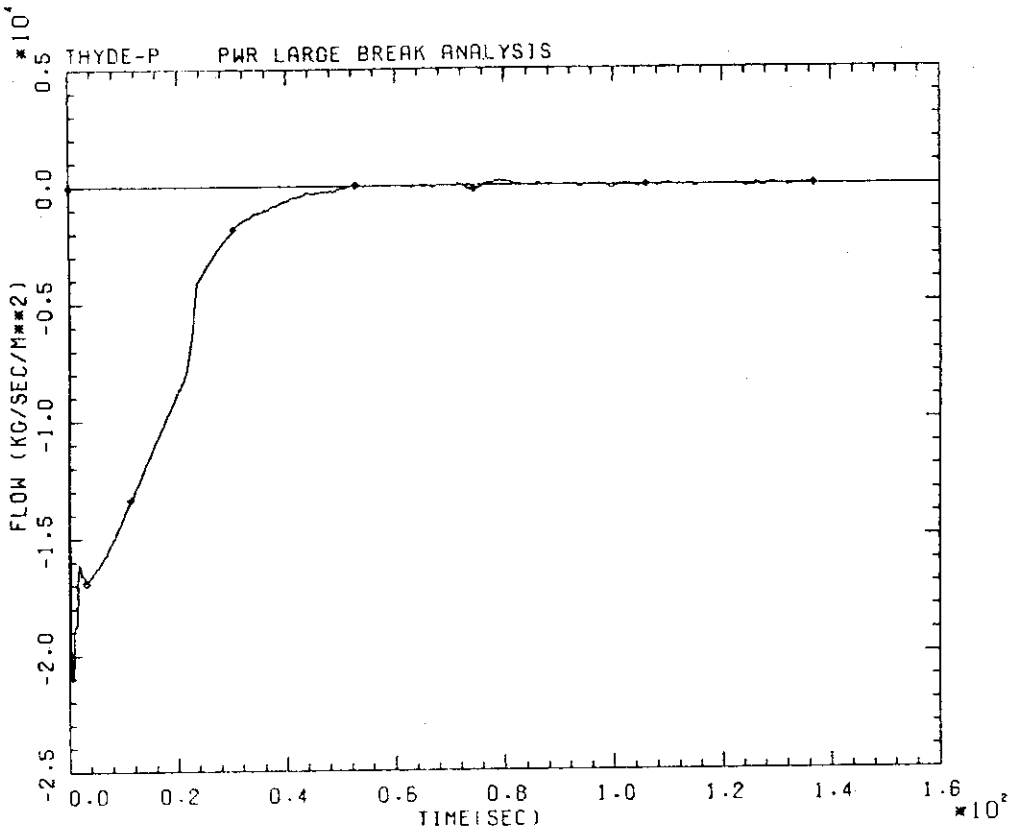

FIG. 4-5-1 PRESSURIZER SURGE FLOW

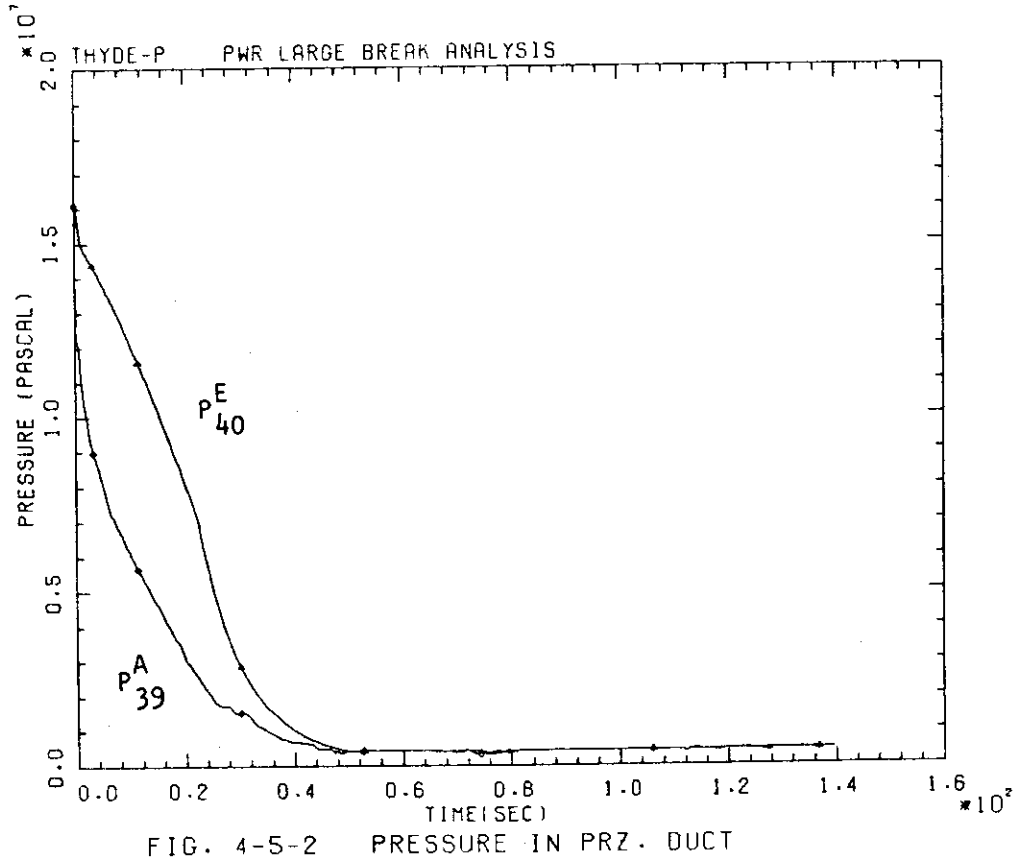

FIG. 4-5-2 PRESSURE IN PRZ. DUCT

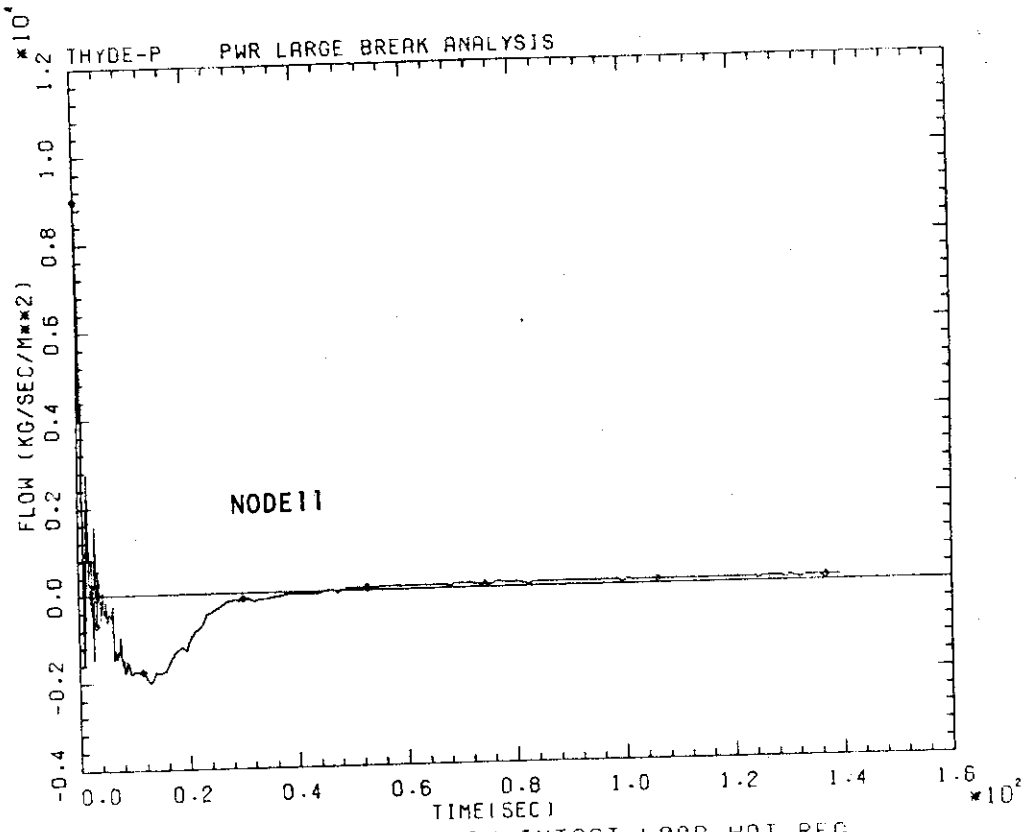

FIG. 4-5-3 FLOW IN INTACT LOOP HOT REG

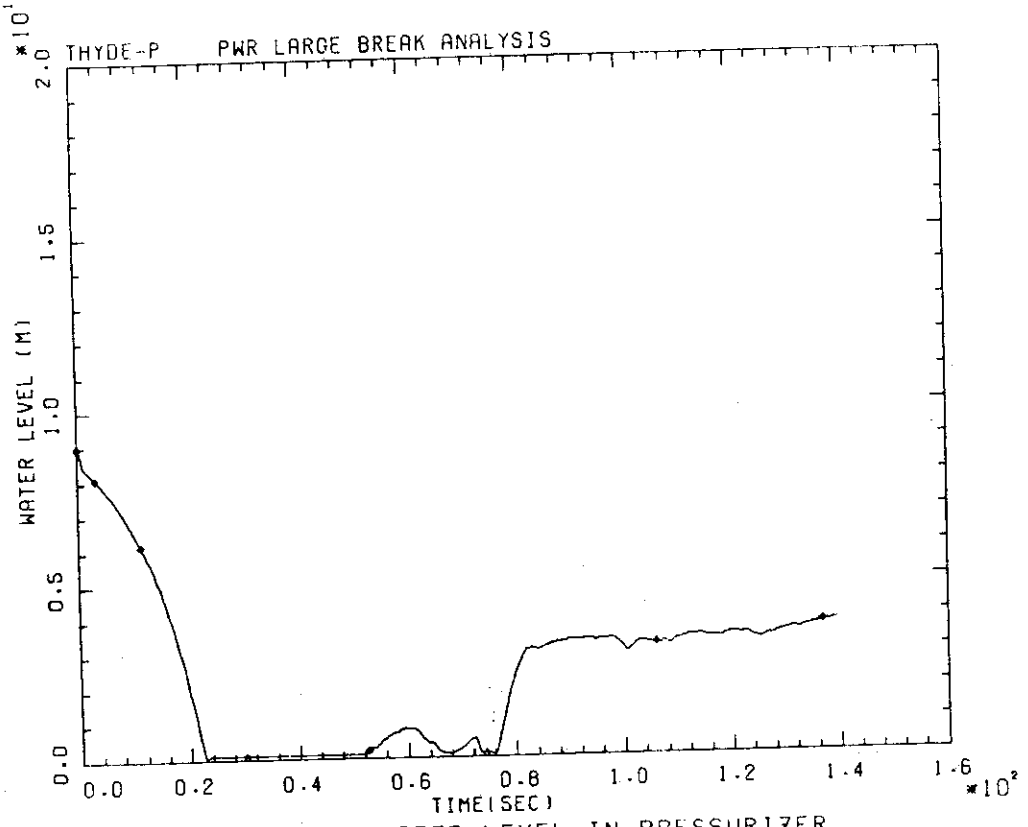

FIG. 4-5-4 WATER LEVEL IN PRESSURIZER

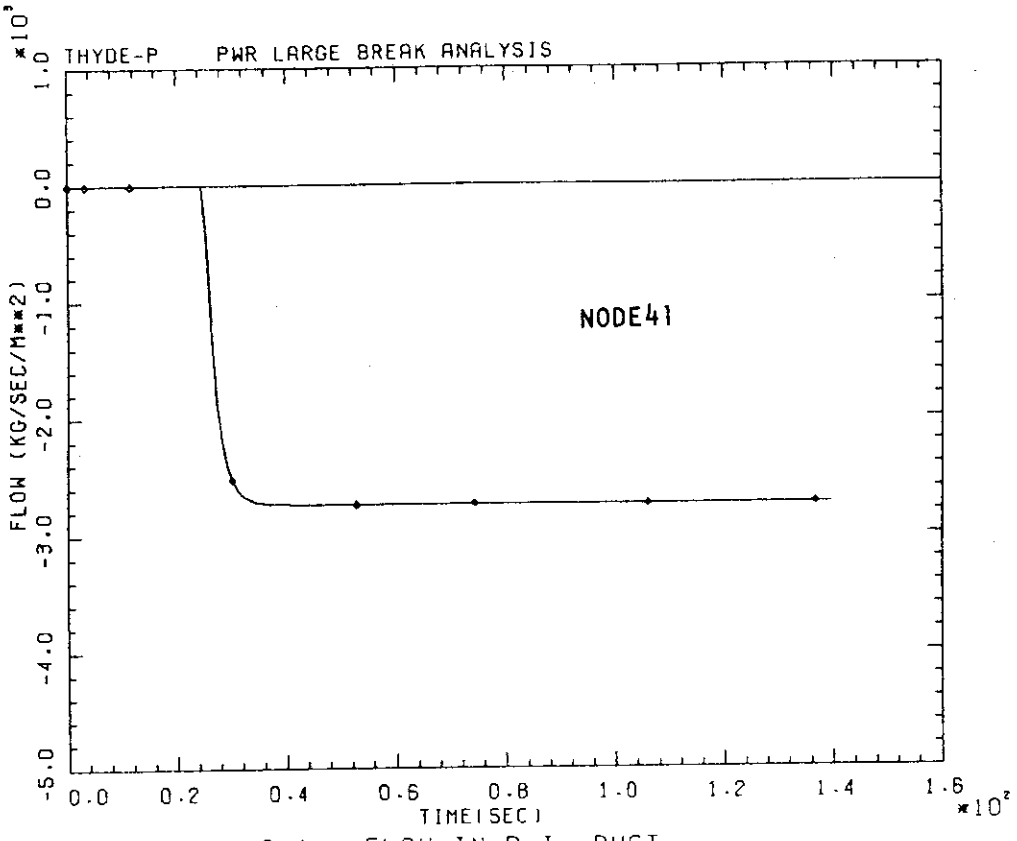

FIG. 4-6-1 FLOW IN P.I. DUCT

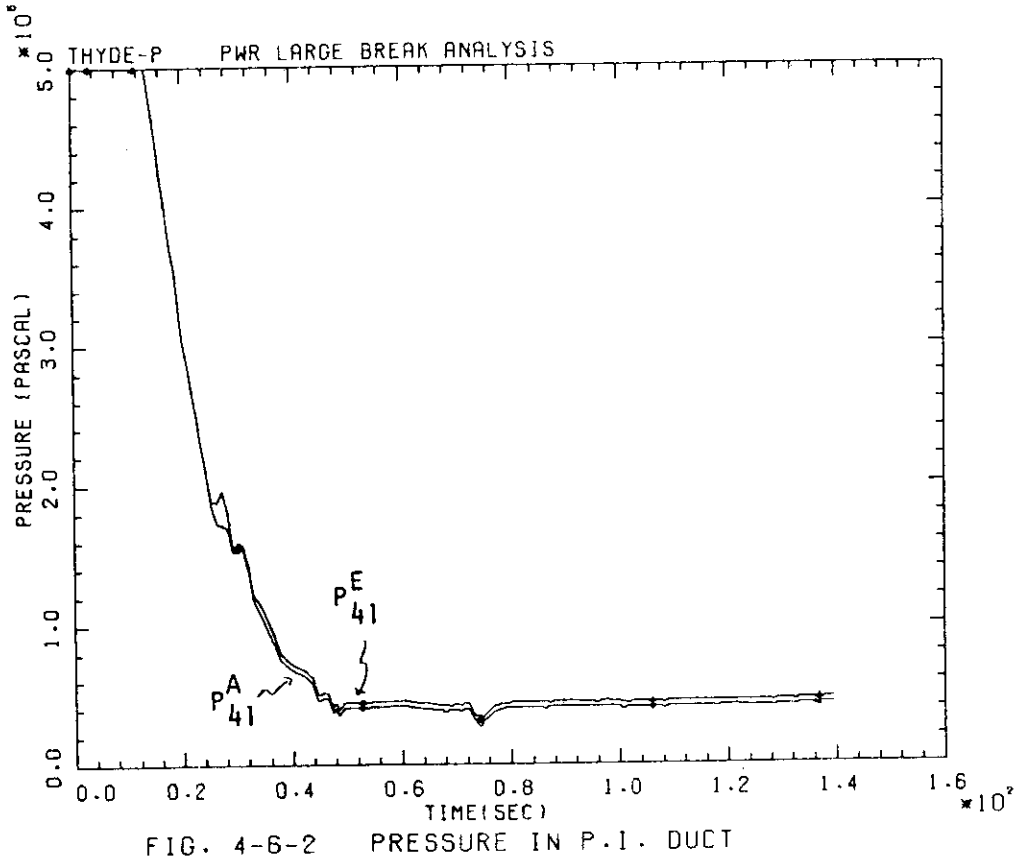

FIG. 4-6-2 PRESSURE IN P.I. DUCT

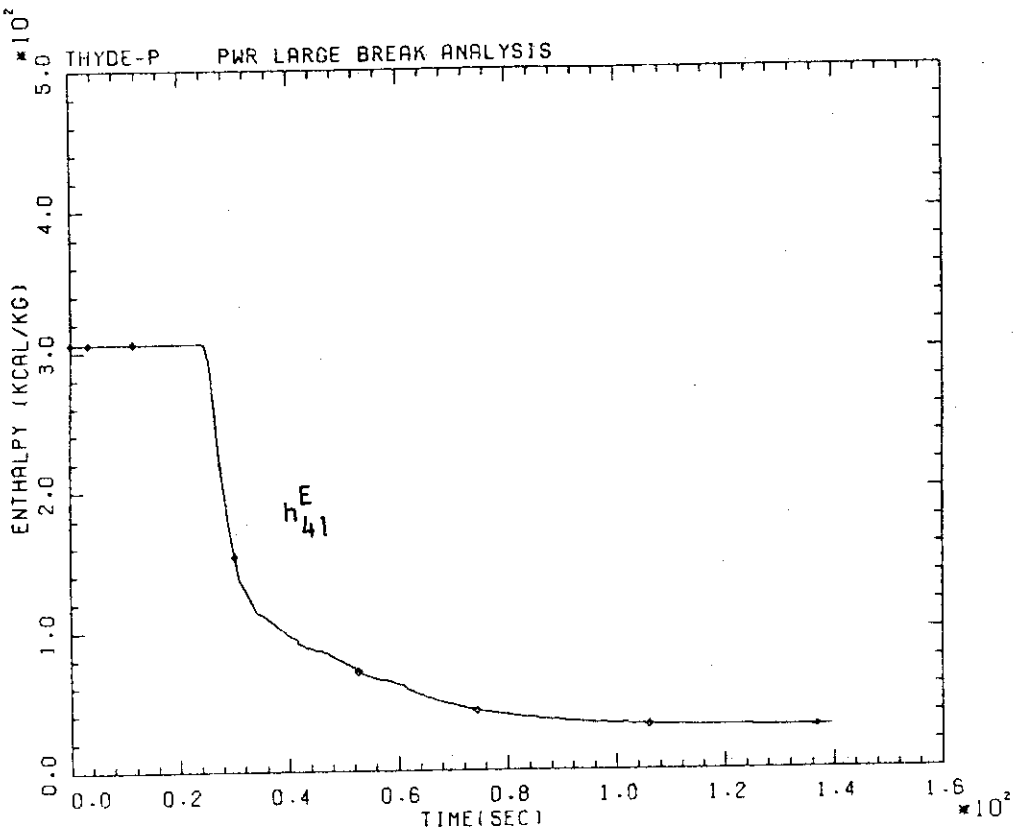

FIG. 4-6-3 ENTHALPY IN P.I. DUCT

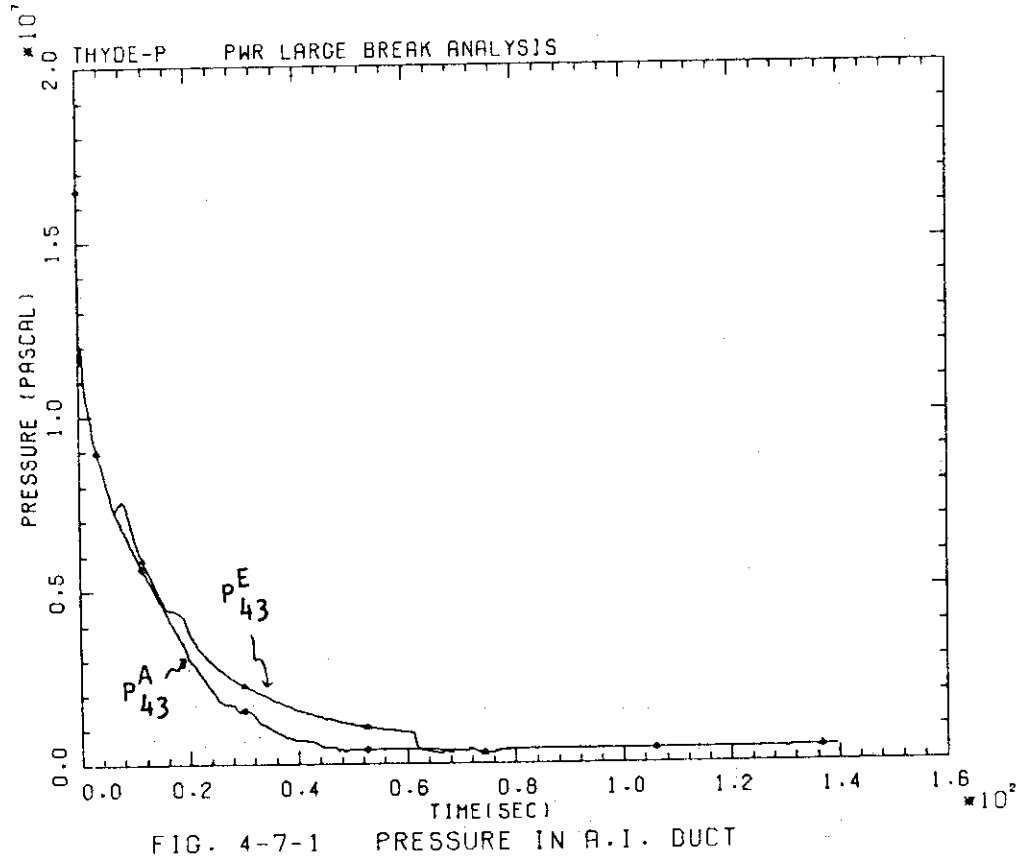

FIG. 4-7-1 PRESSURE IN A.I. DUCT

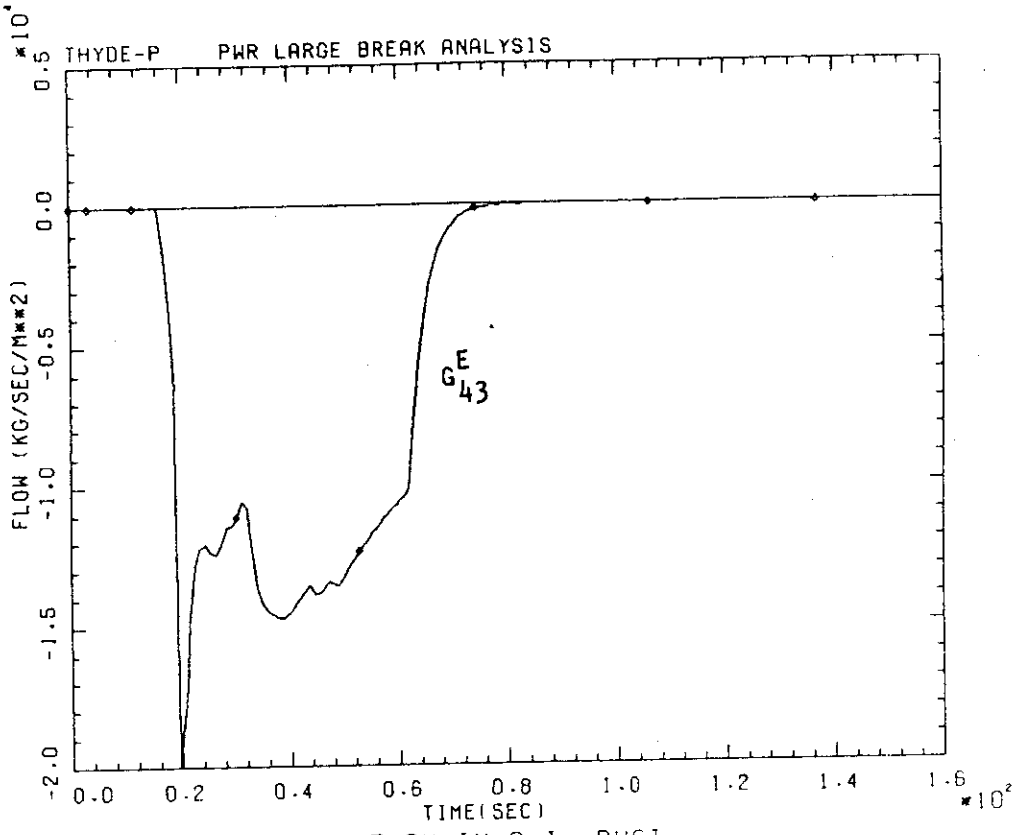

FIG. 4-7-2 FLOW IN A.I. DUCT

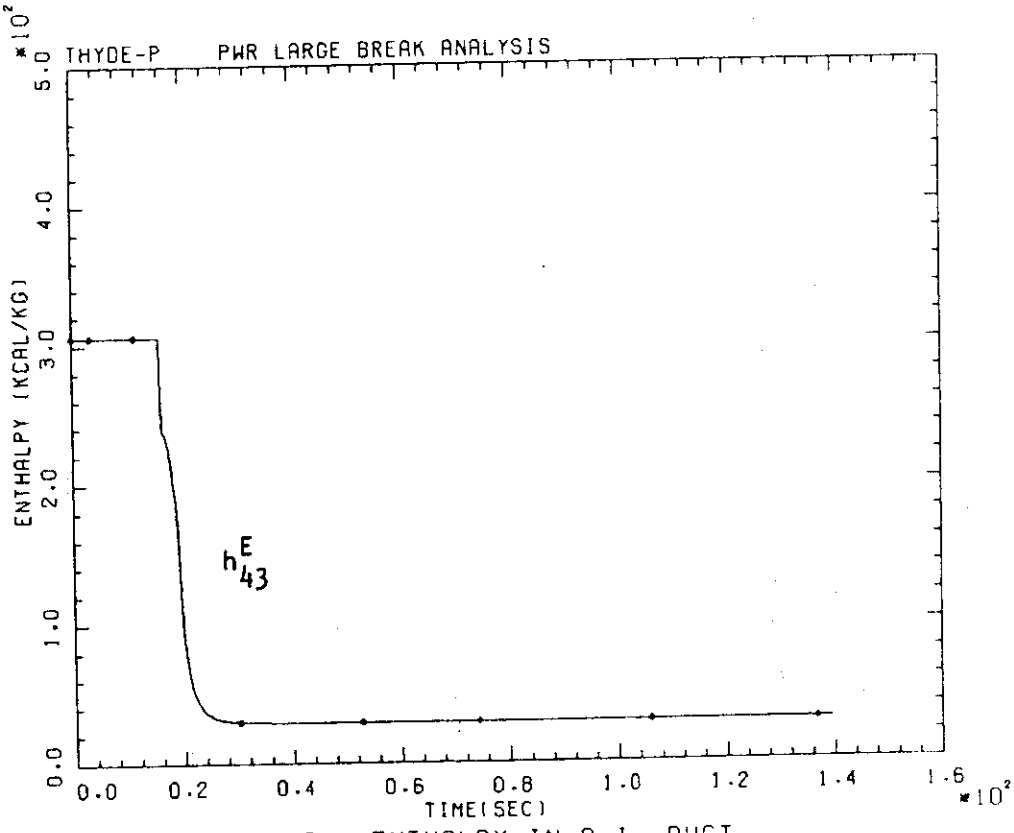

FIG. 4-7-3 ENTHALPY IN A.I. DUCT

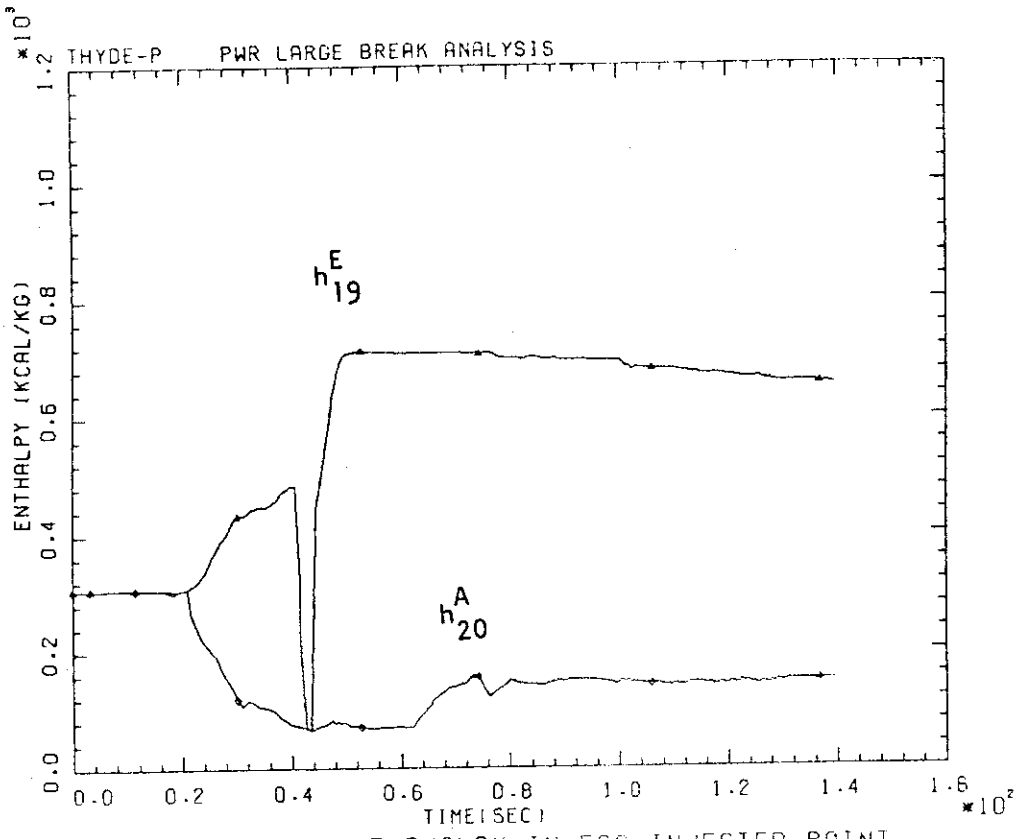

FIG. 4-7-4 ENTHALPY IN ECC INJECTED POINT

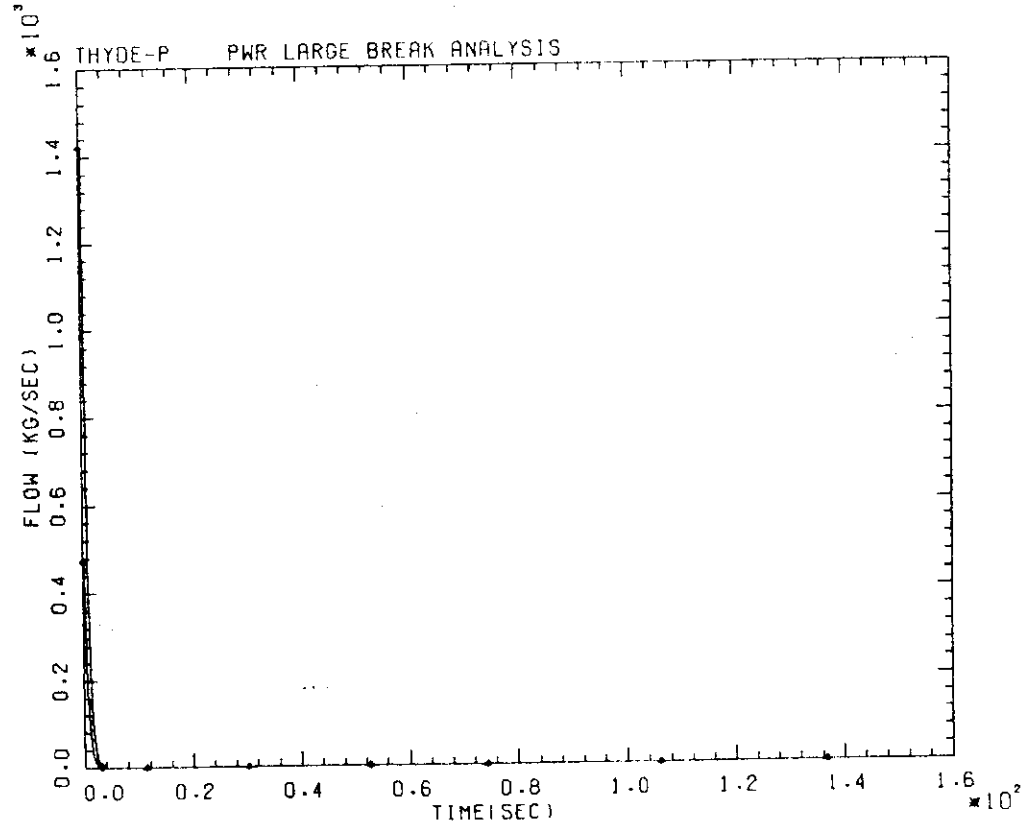

FIG. 4-8-1 S.G. FEED WATER

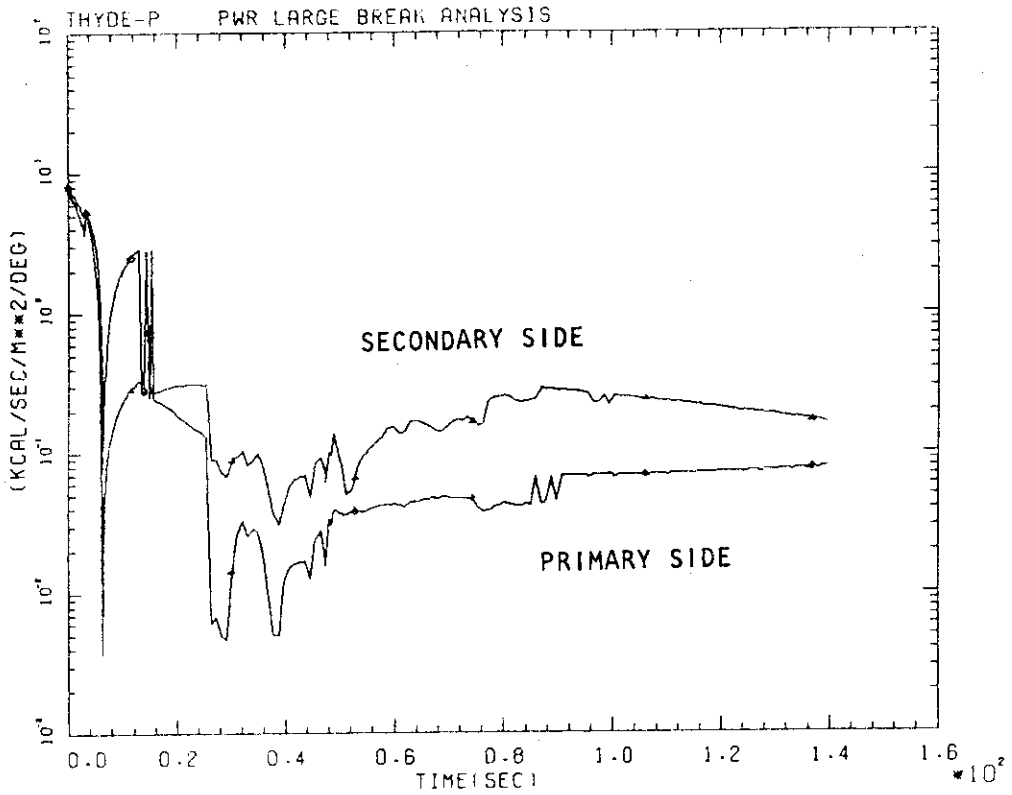

FIG. 4-8-2 H.T.C. IN INTACT LOOP S.G.

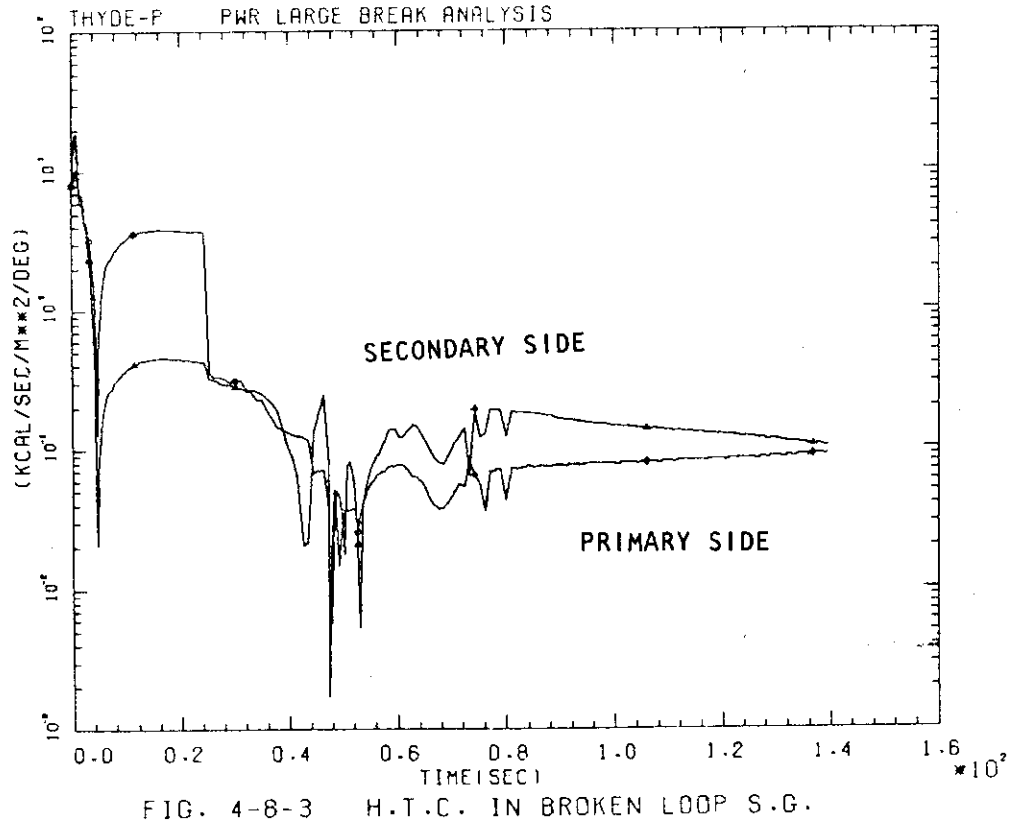

FIG. 4-8-3 H.T.C. IN BROKEN LOOP S.G.

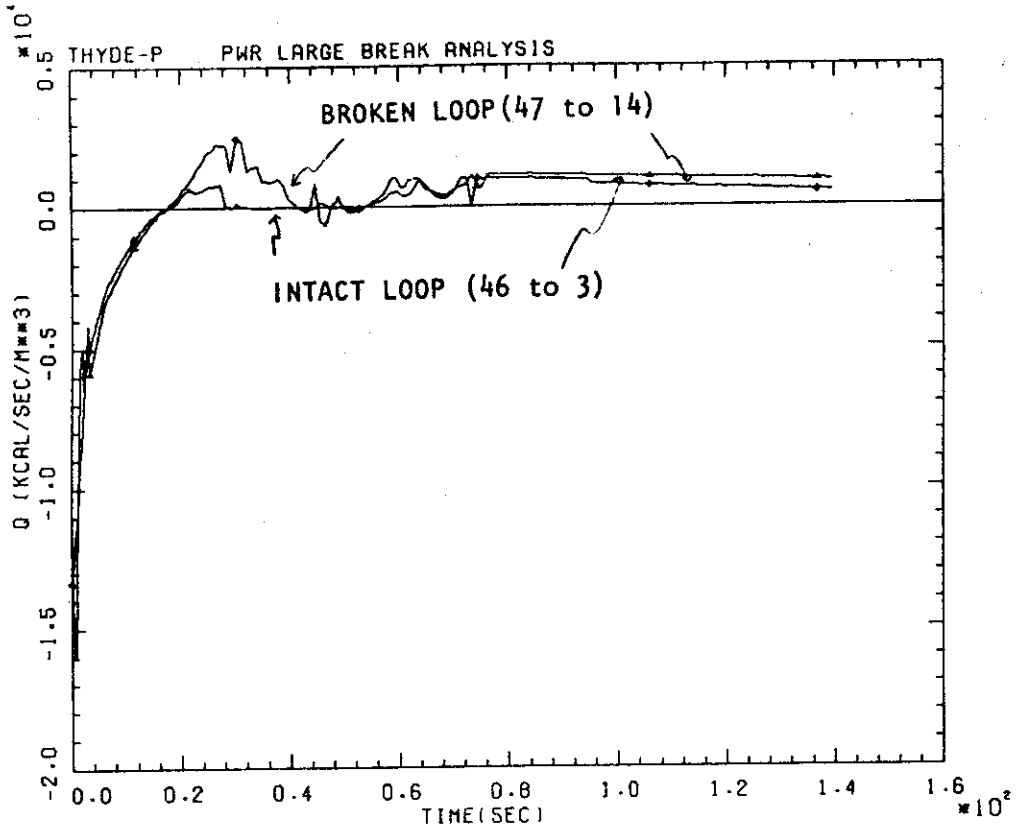

FIG. 4-8-4 HEAT FLOW IN S.G.

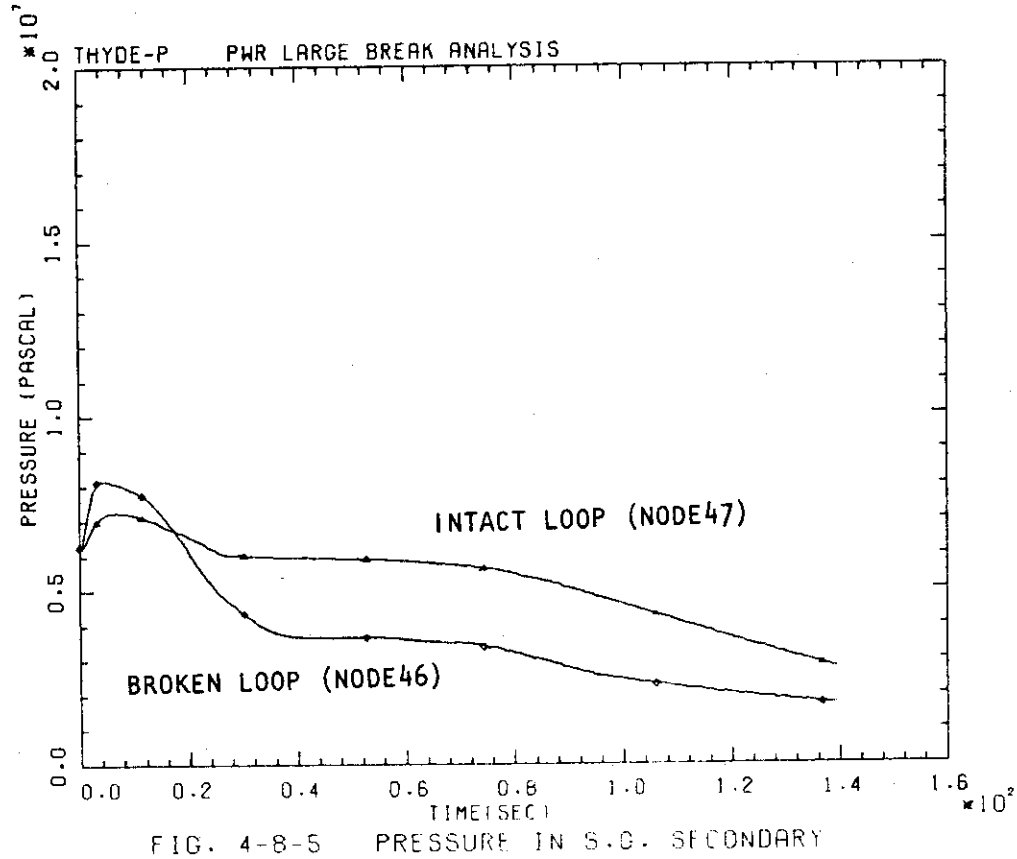

FIG. 4-8-5 PRESSURE IN S.G. SECONDARY

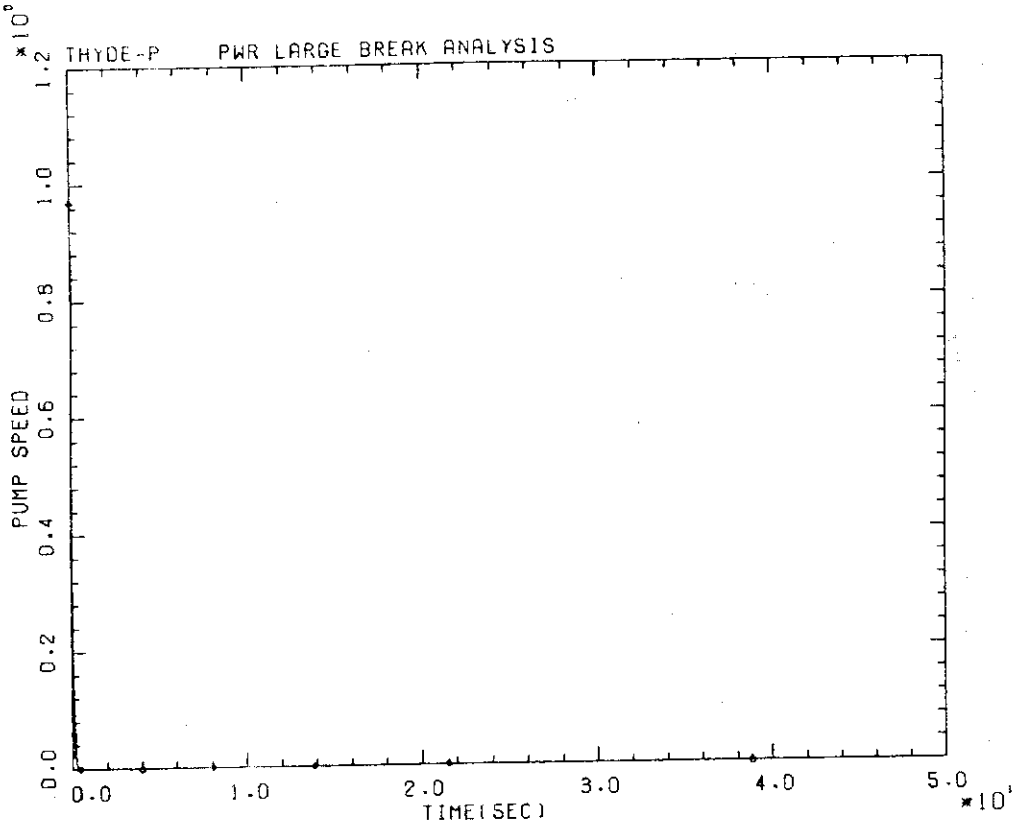

FIG. 4-9-1 PUMP SPEED

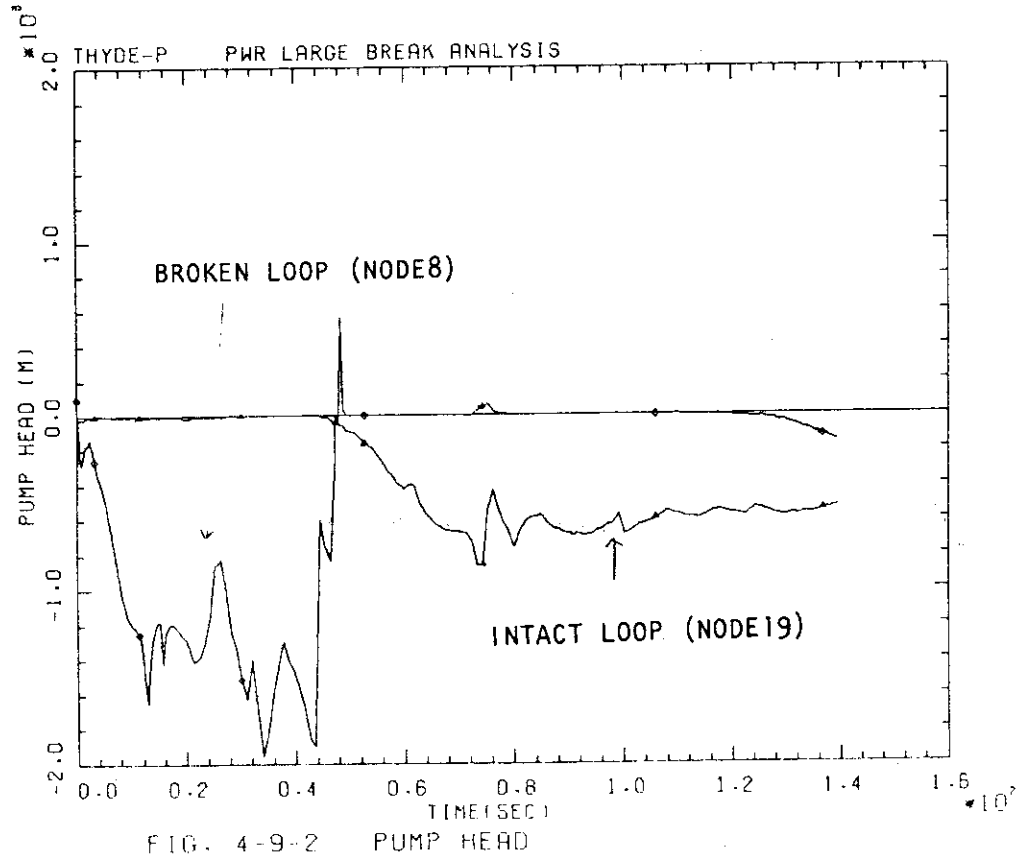

FIG. 4-9-2 PUMP HEAD

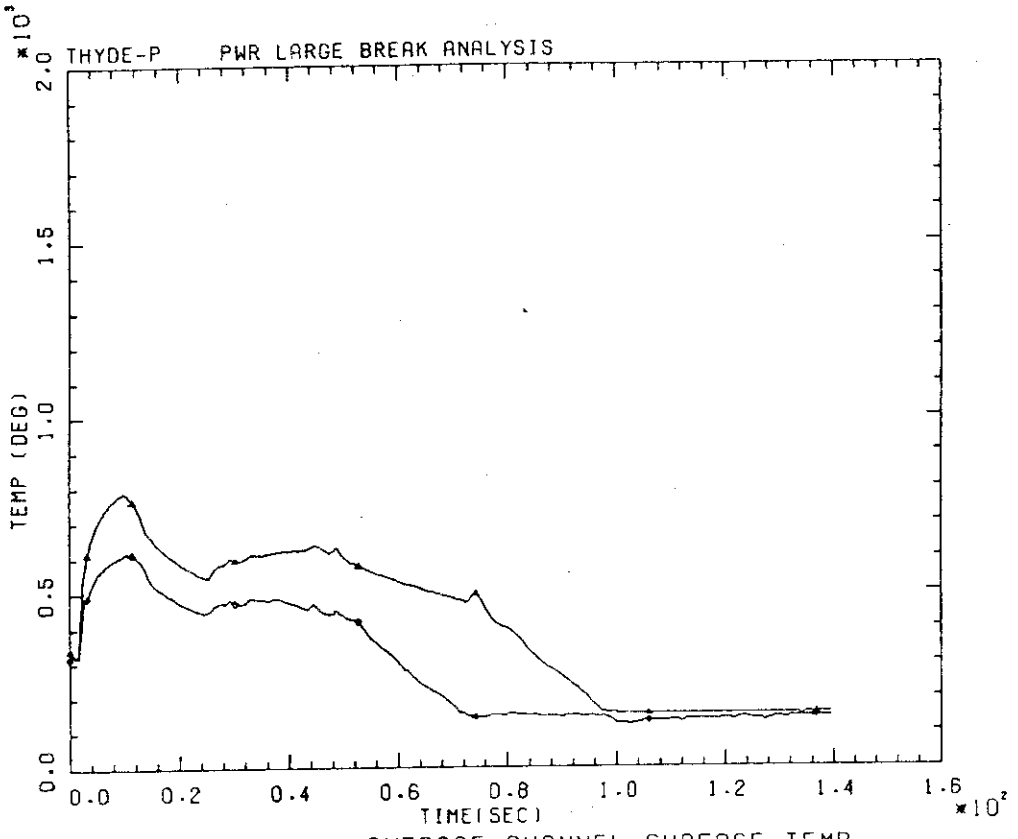

FIG. 4-10-1 AVERAGE CHANNEL SURFACE TEMP.

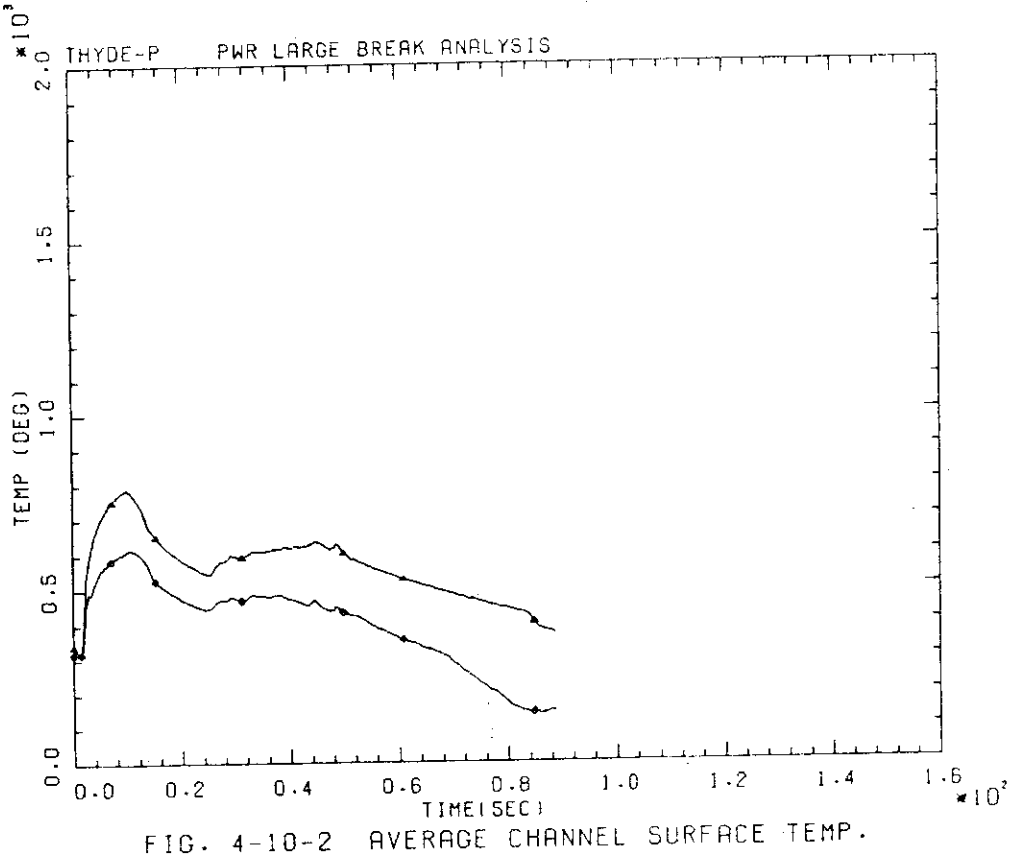

FIG. 4-10-2 AVERAGE CHANNEL SURFACE TEMP.

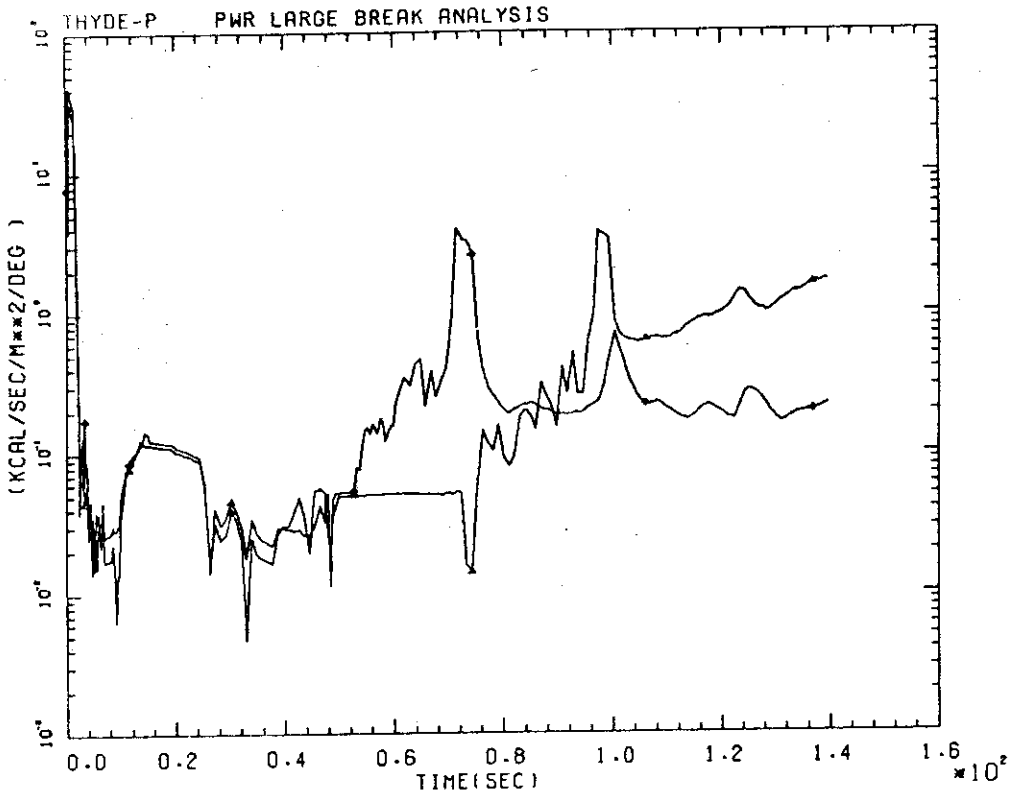

FIG. 4-10-3 H.T.C. IN AVERAGE CHANNEL

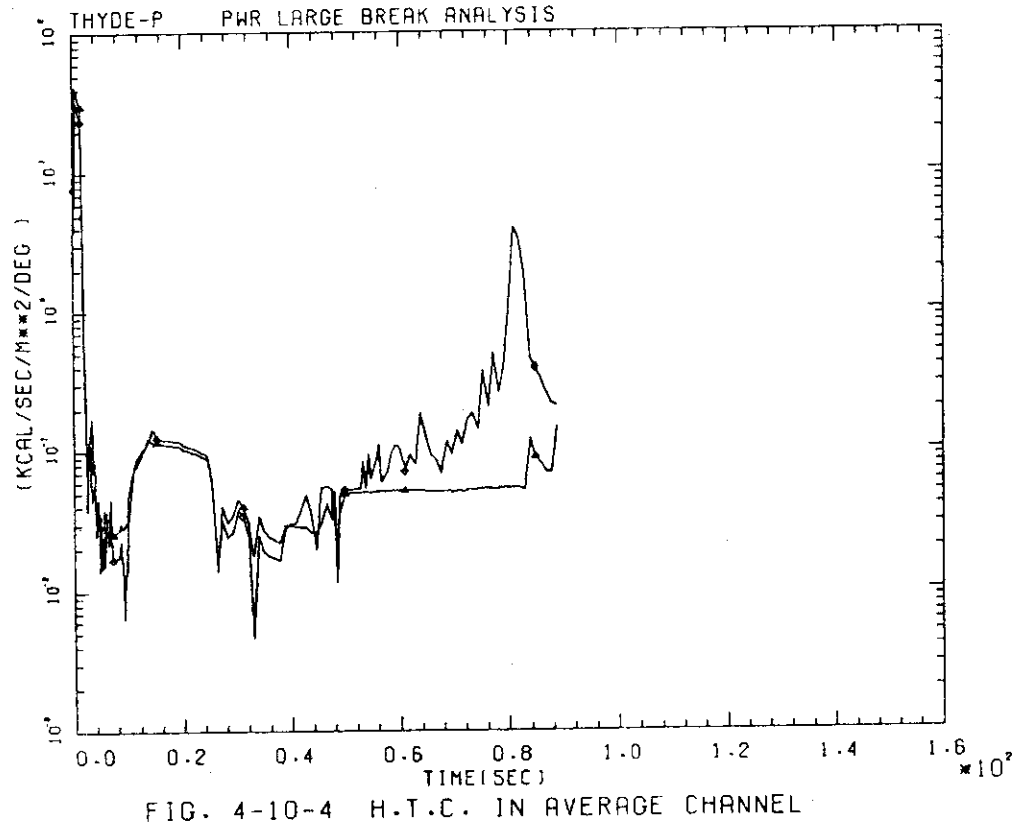

FIG. 4-10-4 H.T.C. IN AVERAGE CHANNEL

5. Conluding Remarks

This work was a through LOCA calculation for a commercial 1,100 MWe class PWR plant from the occurence of a double-ended break till complete fuel quenching due to core reflood. Therefore, the calculated chronology of events discussed in section 4 is of great interest. The assumptions and conditions for Run 20 are shown in section 3. Their effects on the calculated results should be examined in comparison with other sample calculations by THYDE-P under different assumptions.

The discharge coefficient for critical flow at break points and the delay parameters for non-equilibrium effects have a big influence on the calculation of clad surface temperature and on the quenching time of the core.

It was shown in the present calculation that surge flow from the pressurizer, drift flux model during reflooding phase, pumped injection flow rate and its enthalpy play important roles on core cooling.

Acknowledgments

The authors would like to express thier thanks to Mr. K Sato, Chief of Reactor Safety Code Development Labolatory, for his valuable suggestions to this work.

The authors are also very grateful to the members of the labolatory for thier useful discussions.

References

(1) Y. Asahi, 'Description of the THYDE-P Code (Preliminary Report of Methods and Models)', JAERI-M7751, 1978.

(2) Y. Asahi and M. Hirano, 'Verification Study of LOCA Analysis Code THYDE-P (Sample Calculation Run 10)', JAERI-M8560, 1979.

(3) M. Hirano and Y. Asahi, 'Through Analysis of LOFT L2-2 by THYDE-P Code', JAERI-M9535, 1981.

(4) M. Hirano, 'Through Analysis of LOFT L2-3 by THYDE-P Code', to be published.

(5) T.R. Chalton, et al.,'RELAP4/MOD5 Users Manual Volume 3 (Checkout Applications)', ANCR-NUREG-1335 (Vol.3), 1976.

(6) K.R. Katsuma, et al., 'RELAP4/MOD5 Users Manual Volume 1 (RELAP4/MOD5 Description)', ANCR-NUREG-1335 (Vol.1), 1976.

5. Conluding Remarks

This work was a through LOCA calculation for a commercial 1,100 MWe class PWR plant from the occurence of a double-ended break till complete fuel quenching due to core reflood. Therefore, the calculated chronology of events discussed in section 4 is of great interest. The assumptions and conditions for Run 20 are shown in section 3. Their effects on the calculated results should be examined in comparison with other sample calculations by THYDE-P under different assumptions.

The discharge coefficient for critical flow at break points and the delay parameters for non-equilibrium effects have a big influence on the calculation of clad surface temperature and on the quenching time of the core.

It was shown in the present calculation that surge flow from the pressurizer, drift flux model during reflooding phase, pumped injection flow rate and its enthalpy play important roles on core cooling.

Acknowledgments

The authors would like to express thier thanks to Mr. K Sato, Chief of Reactor Safety Code Development Labolatory, for his valuable suggestions to this work.

The authors are also very grateful to the members of the labolatory for thier useful discussions.

References

(1) Y. Asahi, 'Description of the THYDE-P Code (Preliminary Report of Methods and Models)', JAERI-M7751, 1978.

(2) Y. Asahi and M. Hirano, 'Verification Study of LOCA Analysis Code THYDE-P (Sample Calculation Run 10)', JAERI-M8560, 1979.

(3) M. Hirano and Y. Asahi, 'Through Analysis of LOFT L2-2 by THYDE-P Code', JAERI-M9535, 1981.

(4) M. Hirano, 'Through Analysis of LOFT L2-3 by THYDE-P Code', to be published.

(5) T.R. Chalton, et al.,'RELAP4/MOD5 Users Manual Volume 3 (Checkout Applications)', ANCR-NUREG-1335 (Vol.3), 1976.

(6) K.R. Katsuma, et al., 'RELAP4/MOD5 Users Manual Volume 1 (RELAP4/MOD5 Description)', ANCR-NUREG-1335 (Vol.1), 1976.

5. Conluding Remarks

This work was a through LOCA calculation for a commercial 1,100 MWe class PWR plant from the occurence of a double-ended break till complete fuel quenching due to core reflood. Therefore, the calculated chronology of events discussed in section 4 is of great interest. The assumptions and conditions for Run 20 are shown in section 3. Their effects on the calculated results should be examined in comparison with other sample calculations by THYDE-P under different assumptions.

The discharge coefficient for critical flow at break points and the delay parameters for non-equilibrium effects have a big influence on the calculation of clad surface temperature and on the quenching time of the core.

It was shown in the present calculation that surge flow from the pressurizer, drift flux model during reflooding phase, pumped injection flow rate and its enthalpy play important roles on core cooling.

Acknowledgments

The authors would like to express thier thanks to Mr. K Sato, Chief of Reactor Safety Code Development Labolatory, for his valuable suggestions to this work.

The authors are also very grateful to the members of the labolatory for thier useful discussions.

References

(1) Y. Asahi, 'Description of the THYDE-P Code (Preliminary Report of Methods and Models)', JAERI-M7751, 1978.

(2) Y. Asahi and M. Hirano, 'Verification Study of LOCA Analysis Code THYDE-P (Sample Calculation Run 10)', JAERI-M8560, 1979.

(3) M. Hirano and Y. Asahi, 'Through Analysis of LOFT L2-2 by THYDE-P Code', JAERI-M9535, 1981.

(4) M. Hirano, 'Through Analysis of LOFT L2-3 by THYDE-P Code', to be published.

(5) T.R. Chalton, et al.,'RELAP4/MOD5 Users Manual Volume 3 (Checkout Applications)', ANCR-NUREG-1335 (Vol.3), 1976.

(6) K.R. Katsuma, et al., 'RELAP4/MOD5 Users Manual Volume 1 (RELAP4/MOD5 Description)', ANCR-NUREG-1335 (Vol.1), 1976.

Appendix A. Input Data List

```
 -- 1000 MWE PWR BLOWDOWN ANALYSIS ( WITH HOT CHANNEL) 81.05.13 --
/
/  **** DIMENSION DATA ****
BB01
  0  0  9  3  16  49  40  9 2  2  2  2  3  6  5  3 0 2
/
/  **** MINOR EDIT DATA ****
BB02
PRE-08  PRA-12  GLA-23  GLA-29  GLE-35  GLE-36  GLA-37  GLA-38  PRA-26
/
/  **** TIME STEP CONTROL DATA ****
BB03
SB0301
    0.2  0.2  100.
SB0304
    20  3  50   0  1.0E-3  1.0E-6  0.3  0.1
SB0305
    30  3  50   0  8.0E-3  1.0E-6  90.0  0.1
SB0308
    30  3  50   0  4.E-3  1.E-6  2000.0  0.1
/
/  **** TRIP CONTROLL DATA ****
BB04
SB0480
  1  0  1  0  1000.0       0.0
SB0481
  5 46  1  0     0.4       0.0
SB0482
  5 47  1  0     0.4       0.0
SB0483
  2  8  1  0     0.01      0.0
SB0484
 2  19  1  0     0.01      0.0
SB0485
  3  0  1  0     0.01      0.0
SB0486
  4  1  1  0    25.01      0.0
SB0487
 -4  1  1  0  1000.0       0.
SB0488
  4  2  1  0    25.01      0.0
SB0489
 -4  2  1  0  1000.0       0.
SB0492
  6  1 -3  1   240.0       0.005
SB0493
  6  2 -3  1   250.0       0.0
SB0494
  6  3 -3  1   360.0       0.0
SB0495
 -6  1  3  1   350.0       0.0
SB0496
 -6  2  3  1   305.0       0.0
SB0497
 -6  3  3  1   380.0       0.00
/
/  **** FLOW AJUST DATA ****
BB05
  1  9000.0  360.0
```

```
/                                                                        00000600
/  **** NODE DATA ****                                                   00000610
BB06                                                                     00000620
SB0601                                                                   00000630
 1   1 26  1   0  1     158.4538  0.737 0.  5.24   0.0                   00000640
                        0.043 0.084  0.0  0.0                           00000650
SB0602                                                                   00000660
 2   1  1  2   0  1     158.9708  1.92  0.  1.665 1.665                 00000670
                        3.73  1.97   0.0  0.0                           00000680
SB0603                                                                   00000690
 3   7  2  3   1 3265  158.7624  0.0197 0. 5.0    5.0                   00000700
                        0.033 0.048  0.0  0.0                          00000710
SB0604                                                                   00000720
 4   7  3  4   1 3265  158.1581   0.0197 0. 5.46  5.46                  00000730
                        0.0   0.0    0.0   0.0                          00000740
SB0605                                                                   00000750
 5   7  4  5   1 3265  157.4898  0.0197 0. 10.46 -10.46                 00000760
                        0.0   0.0  0.033   0.048                        00000770
SB0606                                                                   00000780
 6   1  5  6   0  1     157.7862  1.92  0.  1.665 -1.665                 00000790
                        0.0   0.0   3.73   1.97                         00000800
SB0607                                                                   00000810
 7   1  6  7   0  1     157.4466  0.787 0.  7.34 -3.54                   00000820
                        0.042 0.077   -1.   -1.                         00000830
SB0608                                                                   00000840
 8   8  7 34   0  1     154.7227  0.494 0.  12.4117  3.54                00000850
                        -1.   -1.   0.2029  0.2027                      00000860
SB0609                                                                   00000870
 9   1 34  8   0  1     162.0607  0.699 0.  2.825  0.0                   00000880
                        0.0   0.0   0.0   0.0                          00000890
SB0610                                                                   00000900
10   1  8 29   0 1      162.0332   0.699 0.  3.13  0.0                  00000910
                        0.0   0.0   0.0   0.0                          00000920
SB0611                                                                   00000930
11   1 26 27   0 3      158.4538  0.737  0.  2.0 0.                     00000940
                        0.043 0.083  0.0   0.0                          00000950
SB0612                                                                   00000960
12   1 27  9   0 3      158.4334   0.737  0.  3.24 0.                   00000970
                        0.0   0.0   0.0   0.0                          00000980
SB0613                                                                   00000990
13   1  9 10   0 3      158.9528  1.92  0.  1.665  1.665                00001000
                        3.73  1.97  0.0   0.0                          00001010
SB0614                                                                   00001020
14   7 10 11   1 9795   158.7445  0.0197 0. 5.0  5.0                    00001030
                        0.033 0.048  0.0   0.0                         00001040
SB0615                                                                   00001050
15   7 11 12   1 9795   158.1387   0.0197 0. 5.46 5.46                  00001060
                        0.0   0.0   0.0   0.0                          00001070
SB0616                                                                   00001080
16   7 12 13   1 9795   157.4691  0.0197 0. 10.46 -10.46                00001090
                        0.0   0.0  0.033  0.048                        00001100
SB0617                                                                   00001110
17   1 13 14   0  3     157.7645   1.92  0.  1.665  -1.665              00001120
                        0.0   0.0   3.73  1.97                         00001130
SB0618                                                                   00001140
18   1 14 15   0  3     157.4249  0.787 0.  7.34 -3.54                   00001150
                        0.042  0.077  -1.   -1.                         00001160
SB0619                                                                   00001170
19   8 15 28   0  3     154.6997  0.494 0.  12.4117  3.54                00001180
                        -1.   -1.    0.2029  0.2027                     00001190
```

```
SB0620                                                                  00001200
20  1 28 29  0 3      162.0373  0.699 0. 5.955   0.                   00001210
                      0.0   0.0    0.0   0.0                           00001220
                                                                        00001230
SB0621                                                                  00001240
21  4 29 16  0 1      162.4638   1.869 0. 7.248 -7.248                  00001250
                      0.0   0.0    0.0   0.0                           00001260
SB0622                                                                  00001270
22  5 16 30  0 1      162.9140  2.487 0. 6.075 1.948                    00001280
                      0.0   0.0    0.0   0.0                           00001290
SB0623                                                                  00001300
23  2 30 17  0 39170 162.6047  1.0   0. 0.23  0.23                     00001310
                      0.74  0.74   0.0   0.0                           00001320
SB0624                                                                  00001330
24  2 17 18  1 39170 162.1173  1.0   0. 0.80  0.80                     00001340
                      0.0   0.0    0.0   0.0                           00001350
SB0625                                                                  00001360
25  2 18 31  1 39170 161.5410  1.0   0. 0.80  0.80                     00001370
                      0.0   0.0    0.0   0.0                           00001380
SB0626                                                                  00001390
26  2 31 19  1 39170 160.9517  1.0   0. 0.80  0.80                     00001400
                      0.0   0.0    0.0   0.0                           00001410
SB0627                                                                  00001420
27  2 19 20  1 39170 160.3296  1.0   0. 0.80  0.80                     00001430
                      0.0   0.0    0.0   0.0                           00001440
SB0628                                                                  00001450
28  2 20 33  0 39170 159.7062  1.0   0. 0.23  0.23                     00001460
                      0.0   0.0    0.0   0.0                           00001470
SB0629                                                                  00001480
29  2 30 21  0 200   162.6047  1.0   0. 0.23  0.23                     00001490
                      1.284  2.482  0.0   0.0                           00001500
SB0630                                                                  00001510
30  2 21 22  1 200   162.1173  1.0   0.  0.80  0.80                    00001520
                      0.0   0.0    0.0   0.0                           00001530
SB0631                                                                  00001540
31  2 22 32  1 200   161.5410  1.0   0.  0.80  0.80                    00001550
                      0.0   0.0    0.0   0.0                           00001560
SB0632                                                                  00001570
32  2 32 23  1 200   160.946155  1.0  0.  0.80  0.80                   00001580
                      0.0   0.0    0.0   0.0                           00001590
SB0633                                                                  00001600
33  2 23 24  1 200   160.3296  1.0   0.  0.80  0.80                    00001610
                      0.0   0.0    0.0   0.0                           00001620
SB0634                                                                  00001630
34  2 24 33  0 200   159.7062  1.0   0.  0.23  0.23                    00001640
                      0.76  0.34   0.0   0.0                           00001650
SB0635                                                                  00001660
35  3 30 33  0  1     162.6047  0.555 0.  3.66  3.66                    00001670
                      0.77  0.83   0.87  0.78                          00001680
SB0636                                                                  00001690
36  1 32 31  0 200   161.029550  0.034 0.  0.1   0.                    00001700
                      0.0   0.0    0.0   0.0                           00001710
SB0637                                                                  00001720
37  1 33 26  0  1     159.17209  3.44  0.  4.341  1.64                  00001730
                      0.0   0.0    0.0   0.0                           00001740
SB0638                                                                  00001750
38 13 26 40  0  1       5.0   2.216 0.  3.658  2.073                   00001760
                      1.491E4  1.491E4  0.0   0.0                      00001770
SB0639                                                                  00001780
39 13 27 25  0  1       5.0   0.29  0.  15.0   1.7                     00001790
                        0.41  0.87   0.0   0.0
```

```
SB0640                                                                  00001800
40 13 25 35  0  1      5.0    0.29  0.   14.3   1.6                     00001810
                       0.0    0.0    0.0   0.0                         00001820
                                                                        00001830
SB0641                                                                  00001840
41 13 28 37  0  3     10.0    0.305 0.    12.0   0.0                     00001850
                       0.0    0.0    0.0   0.0                         00001860
SB0642                                                                  00001870
42 13 34 38  0  1     10.0    0.305 0.    12.0   0.0                     00001880
                       0.0    0.0    0.0   0.0                         00001890
SB0643                                                                  00001900
43 13 28 36  0  3     10.0    0.222 0.   120.0   0.0                     00001910
                       0.109  0.049  0.0  0.0                          00001920
SB0644                                                                  00001930
44 13 34 39  0  1     10.0    0.222 0.   120.0   0.0                     00001940
                       0.109  0.049  0.0  0.0                          00001950
/                                                                       00001960
/  **** JUNCTION DATA ****                                             00001970
BB07                                                                    00001980
     1    1    0.0                                                     00001990
     2    1    0.0                                                     00002000
     3    1    0.0                                                     00002010
     4    1    0.0                                                     00002020
     5    1    0.0                                                     00002030
     6    1    0.0                                                     00002040
     7    1    0.0                                                     00002050
     8    1    0.0                                                     00002060
     9    1    0.0                                                     00002070
    10    1    0.0                                                     00002080
    11    1    0.                                                      00002090
    12    1    0.0                                                     00002100
    13    1    0.0                                                     00002110
    14    1    0.0                                                     00002120
    15    1    0.0                                                     00002130
    16    1    0.0                                                     00002140
    17    1    0.0                                                     00002150
    18    1    0.0                                                     00002160
    19    1    0.0                                                     00002170
    20    1    0.0                                                     00002180
    21    1    0.                                                      00002190
    22    1    0.                                                      00002200
    23    1    0.                                                      00002210
    24    1    0.                                                      00002220
    25    1    0.                                                      00002230
    26    2    1.027                                                   00002240
    27    4    0.049                                                   00002250
    28    4    0.351                                                   00002260
    29    3    0.531                                                   00002270
    30    4    0.1                                                     00002280
    31    4    0.01                                                    00002290
    32    4    0.01                                                    00002300
    33    4    0.05                                                    00002310
    34    4    0.117                                                   00002320
    35    6    0.                                                      00002330
    36    5    0.                                                      00002340
    37    7    0.                                                      00002350
    38    7    0.                                                      00002360
    39    5    0.                                                      00002370
    40    8    0.                                                      00002380
/                                                                       00002390
/  **** MIXING JUNCTION DATA ****
```

```
BB08                                                                    00002400
SB0801                                                                  00002410
   26   3    1  11  38   0   0.25    0.75     0.    0.                  00002420
SB0802                                                                  00002430
   27   2   12  39   0   0   1.0     0.0      0.    0.                  00002440
SB0803                                                                  00002450
   28   3   20  41  43   0   1.0     0.0      0.0   0.0                 00002460
SB0804                                                                  00002470
   29   1   21   0   0   0   1.0     0.0      0.0   0.0                 00002480
SB0805                                                                  00002490
   30   3   23  29  35   0   0.945   0.005    0.05  0.0                 00002500
SB0806                                                                  00002510
   31   1   26   0   0   0   1.0     0.0       0.    0.                 00002520
SB0807                                                                  00002530
   32   2   32  36   0   0   0.99    0.01     0.    0.                  00002540
SB0808                                                                  00002550
   33   1   37   0   0   0   1.0     0.0      0.0   0.0                 00002560
SB0809                                                                  00002570
   34   3    9  42  44   0   1.0     0.0      0.0   0.0                 00002580
/                                                                       00002590
/  **** PUMPED INJECTION DATA ****                                      00002600
BB09                                                                    00002610
SB0901                                                                  00002620
    1   37    30.0                                                      00002630
   2  1                                                                 00002640
   0.0   666.0  1000.0   666.0                                          00002650
SB0902                                                                  00002660
    2   38    30.0                                                      00002670
   2  1                                                                 00002680
   0.0   222.0  1000.0   222.0                                          00002690
/                                                                       00002700
/  **** PUMP DATA ****                                                  00002710
BB10                                                                    00002720
SB1001                                                                  00002730
   8  1 0 1185.0  5.58  4.33E4  105.0 749.0  1150.0  3460.0  0.5  0.0   00002740
   0.05                                                                 00002750
SB1002                                                                  00002760
  19 1 0 1185.0   5.58  4.33E4  105.0 749.0  1150.0  3460.0  0.5  0.0   00002770
   0.05                                                                 00002780
/                                                                       00002790
/  **** PUMP DATA TABLE ****                                           00002800
BB11                                                                    00002810
SB1101                                                                  00002820
 1                                                                      00002830
 14                                                                     00002840
 -1.0  1.56        -0.85 1.33        -0.80 1.28        -0.72 1.30       00002850
 -0.62 1.35        -0.50 1.36       -0.34 1.34        -0.21 1.29       00002860
 -0.11 1.23         0.0  1.22         0.25 1.16         0.50 1.13       00002870
  0.75 1.07         1.0  0.98                                           00002880
 14                                                                     00002890
 -1.0        0.18  -0.85       0.34  -0.80       0.40  -0.72       0.48 00002900
 -0.62       0.556 -0.50       0.67  -0.34       0.77  -0.21       0.84 00002910
 -0.11       0.89   0.0        0.95   0.25       1.16   0.50       1.35 00002920
  0.75       1.62   1.0        1.94                                    00002930
 11                                                                     00002940
 -1.0  0.18        -0.75 -0.13       -0.50 -0.32       -0.32 -0.40      00002950
 -0.16 -0.42        0.0  -0.39        0.16 -0.28        0.32  0.16      00002960
  0.50  0.01        0.75 0.40         1.0   0.98                       00002970
 11                                                                     00002980
 -1.0        1.56  -0.75       1.12  -0.50       0.90  -0.32       0.82 00002990
```

```
 -0.16        0.76    0.0          0.71    0.16         0.71    0.32         0.76 00003000
  0.50        0.90    0.75         1.33    1.0          1.94                      00003010
                                                                                 00003020
 14                                                                              00003030
 -1.0  0.70          -0.90 0.70          -0.80 0.68          -0.70 0.63         00003040
 -0.60 0.53          -0.50 0.47          -0.40 0.46          -0.30 0.45         00003050
 -0.20 0.45           0.0  0.48           0.25 0.55           0.50 0.66         00003060
  0.75 0.83           1.0  1.02                                                  00003070
 14                                                                              00003080
 -1.0        -1.42   -0.90        -1.32   -0.80        -1.23   -0.70        -1.14 00003090
 -0.60       -1.07   -0.50        -0.99   -0.40        -0.91   -0.30        -0.84 00003100
 -0.20       -0.77    0.0         -0.64    0.25        -0.49    0.50        -0.34 00003110
  0.75       -0.20    1.0         -1.10                                          00003120
   13                                                                            00003130
 -1.0 -1.42        -0.8 -1.12       -0.6 -0.82       -0.5 -0.68                 00003140
 -0.4 -0.55        -0.2 -0.28        0.0 -0.08        0.11 0.0                  00003150
  0.25 0.12         0.50 0.33        0.75 0.61        0.92 0.82                 00003160
  1.0  1.02                                                                    00003170
   13                                                                          00003180
 -1.0         0.70 -0.8         0.5 -0.6         0.4 -0.5         0.39         00003190
 -0.4         0.38 -0.2         0.33 0.0         0.28 0.11        0.25         00003200
  0.25        0.22  0.50        0.14 0.75        0.03 0.92        0.01         00003210
  1.0        -0.10                                                            00003220
/  2                                                                          00003230
/ 0.0 1.0  1000.0  0.5                                                        00003240
/ 2                                                                          00003250
/ -1.0  -50.0  1.0  50.0                                                     00003260
  12                                                                         00003270
  -1.0    -1.15        -0.9  -1.24        -0.6   -2.8        -0.5  -2.9      00003280
  -0.4    -2.7          0.0   0.0          0.12   0.85        0.2   1.1      00003290
  0.5      1.02         0.7   1.0          0.9    0.95        1.0   1.0      00003300
  4                                                                          00003310
  -1.0     0.0          0.0   0.0          0.5   -0.8         1.0  -1.46     00003320
  7                                                                          00003330
  -1.0     0.0          0.0   0.0          0.1   -0.02        0.2   0.0      00003340
   0.3     0.1          0.9   0.78         1.0    1.0                       00003350
  12                                                                         00003360
  -1.0    -1.15        -0.8  -0.5         -0.6   -0.2        -0.4   0.03     00003370
  -0.2     0.04         0.0   0.1          0.2    0.15        0.4   0.12     00003380
   0.6     0.05         0.8  -0.5          0.9   -0.9         1.0  -1.46     00003390
  0                                                                          00003400
  0                                                                          00003410
  0                                                                          00003420
  0                                                                          00003430
 13                                                                          00003440
  0.0  0.0     0.05 0.0       0.1  0.025       0.15  0.075    0.2  0.18      00003450
  0.3     0.475       0.4     0.625       0.5     0.74         0.6     0.82  00003460
  0.7     0.87        0.8     0.84        0.9     0.72         1.0     0.08  00003470
 11                                                                          00003480
  0.0     0.0         0.1     0.0         0.20    0.13         0.3     0.24  00003490
  0.4     0.31        0.5     0.33        0.6     0.3          0.7     0.23  00003500
  0.8     0.16        0.9     0.08        1.0     0.0                        00003510
  6  6                                                                       00003520
    0.0   0.2   0.4   0.6   0.8   1.0                                        00003530
  0.0   0.0   0.0   0.0   0.0   0.0   0.0                                    00003540
   0.2  0.0   3.065E-5  7.7239E-5  1.3263E-4  1.946E-4   2.6207E-4           00003550
  0.4   0.0   4.866E-5  1.2261E-4  2.1053E-4  3.0996E-4  4.1602E-4           00003560
  0.6   0.0   6.376E-5  1.6066E-4  2.7587E-4  4.0485E-4  5.4514E-4           00003570
  0.8   0.0   7.7239E-5  1.9463E-4  3.3419E-4  4.9044E-4  6.6037E-4          00003580
  1.0   0.0   8.9628E-5  2.2585E-4  3.878E-4   5.691E-4   7.6631E-4          00003590
/
```

```
/  **** ACCUMLATOR DATA ****                                                    00003600
BB12                                                                          00003610
SB1201                                                                        00003620
   48   36   70.   30.   30.0   44.                                           00003630
  0.9  3.0                                                                    00003640
SB1202                                                                        00003650
   49   39   23.3  10.   30.0   44.                                           00003660
  0.9  1.0                                                                    00003670
/                                                                             00003680
/  **** BREAK POINT DATA ****                                                 00003690
BB13                                                                          00003700
   8  0.01  0.4  0.8  0.6  0.6  0.8  0.6  0.6                                 00003710
   6                                                                          00003720
  0.0 1.0  7.5  2.7  15.  4.0  30.  4.0  60.  4.0  1000. 4.0                  00003730
/                                                                             00003740
/  **** PRESSURIZER DATA ****                                                 00003750
BB14                                                                          00003760
   45   35   11  3.58  15.56  9.0  0.99  0.1                                 00003770
        1.7  385.0                                                           00003780
   50.0  1.0  0.1  0.0  0.0                                                   00003790
   0.915  0.915  0.915  1.525  3.05  4.58                                     00003800
   0.564  0.67  0.619                                                        00003810
      2                                                                       00003820
   0. 1.0  1.0  1.0  1000.  1.0  1.0  1.0                                     00003830
/                                                                             00003840
/  **** STEAM GENERATOR DATA ****                                             00003850
BB15                                                                          00003860
SB1501                                                                        00003870
 46 3265  3  5  3  1                                                         00003880
 5.5   18.9  0.7  0.5    3.0E-2  1.0E-2    10.4  4.0  222.1  474.5           00003890
 0.1  0.95  62.0                                                            00003900
       2.0  11.0                                                            00003910
 -40.  -30.  -25.                                                           00003920
      0.001    80.  0.5  0.5  0.5                                           00003930
   3                                                                          00003940
   0.0  1.0  1.0  1.0  1.0  1.0  1.0  1.0  1000.0  1.0  1.0  0.0             00003950
SB1502                                                                        00003960
  47   9795  14  16  3  1                                                   00003970
  16.5  18.9   2.1   0.5     3.0E-2  1.0E-2    10.4  4.0  222.1 1423.5      00003980
 0.1  0.95  62.0                                                            00003990
       2.0  11.0                                                            00004000
  -40.0  -30.0  -25.0                                                       00004010
      0.003    80.  0.5  0.5  0.5                                           00004020
   3                                                                          00004030
  0.0 1.0  1.0  1.0  1.0  1.0  1.0  1.0  1000.0  1.0  1.0  0.0               00004040
/                                                                             00004050
/  **** CORE DATA ****                                                        00004060
BB16                                                                          00004070
/    --- AVERAGE  CHANNEL -----                                               00004080
SB1601                                                                        00004090
  1                                                                           00004100
 39170  23  28  0  3  1  2  2                                                00004110
  9000.0  5.3658E-3  0.6187E-3   4.6573E-3   1.42E-2     0.6   1.0E-4        00004120
  0.0124  0.0212E-02  0.0305  0.1402E-02                                      00004130
  0.111  0.1254E-02  0.301  0.2529E-02                                       00004140
  1.13  0.0736E-02  3.00 0.0269E-02                                          00004150
  5.0   0.6  4.91E-04  3.41E-06  1.2  1.54E03                               00004160
  0.  156.  234.  234.  156.  0.                                            00004170
  1.6122E-07  6.42E-07  7.56E-07  7.56E-07  6.42E-07  1.622E-07             00004180
  1.6122E-07  6.42E-07  7.56E-07  7.56E-07  6.42E-07  1.622E-07             00004190
```

```
  1.6122E-07  6.42E-07  7.56E-07  7.56E-07  6.42E-07  1.622E-07          00004200
  1.6122E-07  6.42E-07  7.56E-07  7.56E-07  6.42E-07  1.622E-07          00004210
/       --- HOT CHANNEL ---                                             00004220
                                                                        00004230
SB1602                                                                  00004240
  2                                                                     00004250
  200    29  34  0  3  1  2  2                                          00004260
  9000.0  5.3665E-3  0.6187E-3   4.6682E-3   1.42E-2     0.6   1.0E-4   00004270
  0.  203.0  304.0  304.0  203.0  0.                                    00004280
  1.6122E-07  6.42E-07  7.56E-07  7.56E-07  6.42E-07  1.622E-07          00004290
  1.6122E-07  6.42E-07  7.56E-07  7.56E-07  6.42E-07  1.622E-07          00004300
  1.6122E-07  6.42E-07  7.56E-07  7.56E-07  6.42E-07  1.622E-07          00004310
  1.6122E-07  6.42E-07  7.56E-07  7.56E-07  6.42E-07  1.622E-07          00004320
/                                                                       00004330
/  **** REACTIVITY DATA ****                                            00004340
BB17                                                                    00004350
    3                                                                   00004360
  0.  0.  0.5  -5.  1.  -25.                                            00004370
    5                                                                   00004380
 20.  0.5  300.  0.  1500.  -0.5  2500.  -1.  4500.  -5.                00004390
    5                                                                   00004400
  0.0  0.0  1.0  -0.1  1.5  -0.2  2.0  -3.0  1000. -8.0                 00004410
/                                                                       00004420
/   ****METAL WATER REACTION DATA ****                                  00004430
BB18                                                                    00004440
    1.54E03 0.775E-04 2.29E04                                           00004450
/                                                                       00004460
/  **** FUEL GAP DATA ****                                              00004470
BB19                                                                    00004480
 0.0301  0.0  1.235E-5  0.0  0.0  0.0  0.0  0.6  0.6  0.0               00004490
 0.9495  0.0157  0.0028  0.0  0.032  0.0  0.0                           00004500
/                                                                       00004510
/  **** BURST DATA  ****                                                00004520
BB21                                                                    00004530
2  2  5.0E7  6.96E-08  2.87E4  2.86E-03  1.15E0  1.528E0                00004540
1.49E-07  2.0E-08  1.25E-16  1.85E-01  8.0E09  3.3E-03                   00004550
       0.1                                                              00004560
/                                                                       00004570
/  **** OTHER DATA ****                                                 00004580
BB22                                                                    00004590
   0. 1.4  1.4  0.                                                      00004600
BEND                                                                    00004610
5                                                                       00004620
 0  0  0  0  0  0.0                                                    00004630
  0. 1.0-7 0. 0. 0. 0.                                                  00004640
  0                                                                     00004650
  0  0.0                                                               00004660
  0  0.0
```